Mitigation of Microbially Induced Concrete Corrosion in Wastewater Infrastructure using Surface Treatments

by

Mostafa Nasr

Submitted in Partial Fulfillment of the Requirements

for the Degree of

Master of Science in Engineering

in the

Civil and Environmental Engineering Program

YOUNGSTOWN STATE UNIVERSITY

May 2021

Mitigation of Microbially Induced Concrete Corrosion in Wastewater Infrastructure using Surface Treatments

Mostafa Nasr

I hereby release this thesis to the public. I understand that this thesis will be made available from the OhioLINK ETD Center and the Maag Library Circulation Desk for public access. I also authorize the University or other individuals to make copies of this thesis as needed for scholarly research.

Signature:

Mostafa M. Nasr, Student	Date

Approvals:

Dr. Richard A. Deschenes, Thesis Advisor	Date
Dr. Holly Martin., Committee Member	Date
Dr. Byung-Wook Park, Committee Member	Date
Dr. Salvatore A. Sanders, Dean of Graduate Studies	Date

ABSTRACT

Microbial induced concrete corrosion (MICC) occurs in concrete wastewater infrastructure when sulfate reducing bacteria (SRB) produce hydrogen sulfide (H_2S) gas. The internal pH of fresh concrete is typically in the range of 12 to 13. Exposure to hydrogen sulfide gas may cause an acid-base reaction with carbon in the concrete, reducing the surface pH. As corrosion progresses and a biofilm develops on the concrete surface, sulfur oxidizing bacteria (SOB) react with hydrogen sulfide to produce sulfuric acid (H_2SO_4). This process reduces the pH within the concrete, potentially leading to the dissolution of the hydration products, such as calcium-silicate-hydrate (C-S-H), of the cement and deterioration of concrete. Corrosion rates as high as 1 cm/year have been measured in some concrete wet wells. Wastewater infrastructure in Mahoning County, Ohio face similar corrosion rates in sewers and wet wells with long retention times.

In the present study, methods for controlling MICC in wastewater infrastructure were evaluated through a combination of laboratory and field trials. Treatment methods were evaluated for one year to determine effective surface preparation techniques, application strategies, maintenance strategies, and best practices. Mitigation technologies considered herein include permeability reducing coatings and surface applied biocidal inhibitor to reduce bacteria growth and control hydrogen sulfide conversion to sulfuric acid.

The mitigation measures were evaluated in a controlled laboratory experiment, where MICC conditions were simulated, and the results were validated in a concrete wet well. The efficacy of each treatment was monitored for one year. However, validation of the data included herein will require an additional year of investigation. The data and results included herein revealed that some mitigation measures prove viable treatment options for inhibiting MICC.

DEDICATION

I dedicate this thesis to the memory of my mother, ***Mona F. Nasr***

You are gone but never forgotten

ACKNOWLEDGEMENTS

I would like to thank and express the most profound appreciation to my thesis advisor Dr. Richard Deschenes of the Civil & Environmental and Chemical Engineering at Youngstown State University, for his invaluable guidance and continuous support throughout this research program. Without Dr. Deschenes's guidance and persistent help, this thesis would not have been possible. His dynamism, vision, sincerity, and motivation have deeply inspired me. Thank you for everything; it was a great privilege and honor to work and study under your supervision.

I am also profoundly grateful to Dr. Holly Martin for her wonderful guidance and suggestions to accomplish this research. Whenever I needed help with instrumenting or measurements, Dr. Martin was always available and always made her schedule work. Thank you for the help, advice, and support which was much needed in completing this research project and thank you for being part of my defense committee.

I would also like to thank Dr. Byung-Wook Park for being part of my defense committee. I appreciate his valuable time and consideration in reviewing this report.

Additionally, I would like to acknowledge the sponsorship of this research by Ohio Water Development Authority (OWDA), and I would also like to thank the Mahoning County Sanitary Engineers Office (MCSE) for providing all the necessary tools, instruments, and professional manpower for this research.

My Special thanks go to my wife Enas Selim for her love, understanding, prayers, and continuing support to complete this research work. Also, I am extremely grateful to my parents for their love, prayers, caring and sacrifices for educating and preparing me for my future. Finally, I express my thanks to my father-in-law for his continuous support and valuable prayers.

TABLE OF CONTENTS

LIST OF FIGURES

LIST OF TABLES

LIST OF ABBREVIATIONS

MICC	Microbial Induced Concrete Corrosion
SRB	Sulfate Reducing Bacteria
SOB	Sulfur Oxidizing Bacteria
C-S-H	Calcium- Silicate- Hydrate
NSOB	Neutrophilic Sulfur Oxidizing Bacteria
ASOB	Acidophil Sulfur Oxidizing Bacteria
RH	Relative Humidity
WW	Wastewater
H_2S gas	Hydrogen Sulfide Gas
H_2SO_4	Sulfuric Acid
SUR	Sulfide Uptake Rate

1. Chapter 1 Introduction

Constructing and maintaining a resilient, efficient, and durable infrastructure is the aspiration of modern societies. Subsurface infrastructure is the portion embedded below the ground surface, which plays a crucial role in this goal. Underground wastewater networks are one such system that must be resilient and sustainable. Although building an effective sewer system is achievable, maintaining this system has proven a challenge.

1.1. Background

Microbial induced concrete corrosion (MICC) is a chronic issue affecting sewer systems worldwide. The continuous deterioration and degradation of the wastewater system through the effect of MICC results in a continuous loss of existing vital infrastructure, which increases the necessity for sustainable mitigation measures. The damage caused by MICC is not only leading to substantial economic loss, but also severe environmental and health-related problems due to the accompanied generation of hazardous gases (Grengg et al., 2017; Islander et al., 1991) The corrosion rate in some severely affected concrete manholes were recorded by Grengg et al., 2017, with loss of concrete exceeding 1 cm/ year, which shortened the service life of the structure to only ten years. Furthermore, the release of harmful gases such as hydrogen sulfide (H_2S), carbon dioxide (CO_2), ammonia (NH_3), methane (CH_4), and other volatile organic compounds (VOCs) represents a serious health risk for both the wastewater system operators and surrounding neighborhood residents (Grengg et al., 2018).

Infrastructure maintenance costs in Germany and England were estimated to spend over $533 & $95 million each year, respectively (Berger et al., 2016). Similarly, the United States national rehabilitation cost exceeded $3.3 billion in 2009 and was expected to increase by more than $390 billion over the next 20 years (Sun et al., 2015; US EPA, 2010;

Gutiérrez-Padilla et al., 2010). Nevertheless, to date, no viable concrete or admixture has been developed to efficiently withstand aggressive MICC conditions over its service life (Grengg et al., 2018). Therefore, proactive measures and new technologies are much needed for managing MICC in sewer systems.

1.2. Objective

The primary objective of the research herein was to extend the service life of wastewater infrastructure by identifying mitigation strategies to control and inhibit MICC in concrete wastewater infrastructure. The objective was accomplished through the following strategies:

- Investigate the chemical and biological controlling factors of MICC through monitoring different corrosion stages, both on site and by experimental simulation.
- Investigate the chemical and biogenic concrete corrosion mechanism.
- Evaluate the applicability, functionality, cost, and service life of different mitigation treatments, including biocidal and permeability reducer surface treatments.

1.3. Scope

The scope of this research was to determine the efficacy of mitigation measures to slow or inhibit MICC through either permeability reducing surface treatments or surface applied biocidal treatments. The mitigation measures were evaluated in a controlled laboratory experiment, where MICC conditions were simulated, and the results were validated in a concrete wet well. Validation of the data included herein will require two or more years of investigation. As one year of data has been collected and analyzed, the results and conclusions presented herein are preliminary.

1.4. Thesis Organization

This thesis is organized into six chapters, beginning with a brief introduction in Chapter 1 Introduction, followed by an exhaustive literature review in Chapter 2 Literature Review. Next, the experimental methods are summarized in Chapter 3 Materials and Methods, with the results and discussion presented in Chapter 4 Results and Discussion. The conclusions and recommendations are provided in Chapter 5 Conclusions and Recommendations, followed by an alphabetized bibliography included in References. Lastly, an appendix is included with additional tables and figures of testing data.

2. Chapter 2 Literature Review

Over the past 30 years, several research studies have been conducted to investigate the MICC mechanism in sewer systems. Despite these efforts, limited literature is available to develop an efficient, long-lasting mitigation methodology. This chapter provides an inclusive review of the previous experimental studies on MICC, particularly the deterioration mechanism and the controlling factors. The discussions herein also include several previously studied mitigation technologies and testing measures to evaluate the performance of these mitigation treatments.

2.1. Mechanism

Proper MICC investigation requires a full understanding of the chemical and biological mechanisms responsible for the corrosion rates observed within sewer systems. Grengg et al. (2018) summarized the MICC mechanism as follows. MICC is a complex interlocking process that occurs as a sequence of biogenic sulfate reduction and re-oxidation reactions. "To efficiently study MICC, an interdisciplinary approach that brings together the fields of civil and chemical engineering (material scientists), microbiology, mineralogy, hydro(geo)chemistry, as well as environmental sciences, is desired" (Grengg et al., 2018).

The MICC process starts when anaerobic sediment layers accumulate in manholes and slow-flowing sewer pipes due to long retention times, exceeding 12 hours (Grengg et al., 2018; Alexander et al., 2013). Subsequently, complex organic molecules (COM) are transformed to low molecule organics (LMO) during the initial fermentation processes, accompanied by CO_2 generation. Thereafter, sulfate-reducing bacteria (SRB) consume the resultant LMO during sulfate respiration, leading to the production of hydrogen sulfide

(H_2S) accompanied by some other gaseous compounds (Herisson et al., 2013; Grengg et al. 2018; Alexander et al., 2013).

After being liberated into the concrete pipes and manholes' confined atmosphere, these gaseous compounds accumulate and diffuse into the moist concrete pore structure (Yuan et al., 2015; Grengg et al., 2017). Along the surface and inside concrete pores, colonized sulfur-oxidizing bacteria (SOB) re-oxidize the H_2S producing biogenic sulfuric acid (H_2SO_4). Acidophilic (SOB), mainly A. Thiooxidans and A. Ferrooxidans, are thought to be the key players in this process with an optimum growth occurring around pH ~2. The generated sulfuric acid H_2SO_4 will react with the cement compounds, mainly calcium and aluminum minerals, forming expansive minerals like ettringite and gypsum. Eventually, the continuous H_2SO_4-production process and resultant biogenic acidic attack, lead to pH reduction and subsequent concrete deterioration (Grengg et al., 2017; Alexander et al., 2013; De Belie et al., 2004; Sun et al., 2014; Zivica and Bajza, 2001).

2.2. Deterioration Mechanism

The fundamental deterioration processes that occur due to the aerobic progression of MICC were initially summarized by Islander et al. (1991). Starting from the strongly alkaline initial stage of concrete with a pH of ~13, Islander proposed the detailed corrosion model which has been adapted later by Grengg et al. (2018). The model breaks the entire sewer corrosion process into three distinct corrosion phases as follows. The initial stage accompanies a surface pH drop from approximately 13 down to 9 due to chemical oxidation of CO_2 within the concrete and H_2S gas. This phase is controlled by the abiotic acid-base reaction, the initial stage of corrosion results in carbonation weak acids (e.g., thiosulfuric or polythionic). The microbial growth within this stage is commonly thought to be limited by the alkaline conditions typical of fresh concrete (Joseph et al., 2012).

Limited material loss occurs during this stage. However, leaching of calcium based hydroxides (e.g., CH, C-S-H) occurs when sulfate fluids disperse into the pores. Furthermore, concurrent precipitation of expansive sulfate salts is typically observed within the interstitial transition zone (ITZ) between the bulk cement and aggregates. This leads to an increase in pore pressure that may cause a loss of structural stability and initial formation of microcracking (Grengg et al., 2015; Grengg et al., 2018). This phase is analogous to passivation of the high concrete surface pH, which typically would inhibit the growth of sulfate oxidizing bacteria.

The subsequent stage begins with the colonization of neutrophilic sulfur-oxidizing bacteria (NSOB), which initiates when conducive conditions are established, primarily a surface pH ~9 (Islander et al., 1991; Grengg et al., 2018; Joseph et al., 2012; Satoh et al., 2009; Vincke et al., 2000). With the decreasing surface pH, at least four successive phylotypes of NSOB have been observed. Under moist conditions, SOBs oxidize distinct sulfur compounds to generate sulfuric acid (H_2SO_4) (Gomez-Alvarez et al., 2012; Okabe et al., 2007; Grengg et al., 2018). The continued production of biogenic H_2SO_4 depresses the pH over time from ~9 to ~4, leading to sulfate salts formation and elementary cementitious (CH) matrix degradation. No appreciable mass loss of cementitious material typically occurs during this phase (Joseph et al. 2010; Islander et al., 1991). However, the formation of secondary ettringite, observed at the gradient between the healthy (non-corroded) and severely corroded concrete, which triggers additional cracks and furthers concrete degradation (Jiang et al., 2015; Peyre Lavigne et al., 2016, 2015a,b).

Once the pH decreases below 4, the final corrosion stage begins. Acidophil sulfur-oxidizing bacteria (ASOB), commonly A. Thiooxidans and A. Ferooxidans, start dominating the biofilm (Grengg et al., 2018; Jiang et al., 2016; Li et al., 2017; Okabe et al., 2007; Satoh et al., 2009). Subsequently, rapid pH reduction prevails, leading to the dissolution of the calcium-silicate-hydrate (C-S-H) structure of the cement and deterioration of the concrete. A rapid loss of concrete material occurs in this final stage of MICC. For instance, significant corrosion rates of over 1 cm /year were reported (Grengg et al., 2015; Mori et al., 1992).

The appearance and dominance of both NSOB and ASOB throughout the biotic phase of MICC is mainly influenced by pH, trophic (nutrient) availability, and the utilization of different sulfur compounds like H_2S, S^0, S_2O_3 (Islander et al., 1991; Li et al., 2017). Although SOB are more prevalent, heterotrophic bacteria and fungi were also observed in the biofilm of several deteriorated wastewater systems (Grengg et al., 2018). Detailed knowledge of these microorganisms' metabolic interaction is vital to interpret the reactions of biofilms with different cementitious materials. Accordingly, the existing gaps in current understanding of the biogenic and chemical corrosion need to be further investigated to produce materials durable in aggressive environments and to develop effective strategies to control MICC (Gomez-Alvarez et al., 2012; Okabe et al., 2007; Satoh et al., 2009; Grengg et al., 2018).

2.3. Controlling Factors

To efficiently mitigate MICC in sewer systems, it is central to understand the main factors governing the corrosion rates and then investigate the possible measures to increase the service life of these sewers. The following sections detail the key controlling factors as identified in the literature. Although there are likely factors that are not well known or

documented at this point, a sturdy knowledge of the known factors is essential to proceed in experimental studies while maintaining precise control over the environmental conditions that simulate the sewer environment (Joseph et al. 2010). Moreover, constant monitoring and further studies must be performed to understand the interlocking relationships between these ruling factors and their disparity over time.

2.3.1. H_2S Gas Concentration

Undoubtedly, the H_2S concentration in the gas phase is the primary factor influencing the entire MICC process. The average level of H_2S released by SRB in the sewer system directly affects the acid production rate on the surface of the concrete (Joseph et al. 2010). H_2S gas density is controlled by the sulfide concentration of the wastewater, in addition to pH, turbulence, and temperature (Sun et al., 2014; Wiener et al., 2006; Yongsiri et al., 2004a, 2004b, 2005).

2.3.2. H_2S Oxidation Rate

The chemical and biological oxidation rate of H_2S represents a crucial factor in microbial concrete corrosion (Joseph et al., 2010; Parker and Prisk, 1953). SOBs are believed the key player in re-oxidizing the H_2S producing biogenic sulfuric acid (H_2SO_4) and stimulating corrosion products. The oxidation rate is mainly ruled by the SOB population, biofilm adhesion, and the biofilm development rate on the concrete surface, which subsequently deteriorate the concrete.

2.3.3. Concrete Porosity and Permeability

Likewise, concrete porosity plays a vital role in determining the corrosion rate in sewers. "Concrete is a moderately porous mixture of inorganic precipitates and mineral aggregate" (Islander et al. 1991). Although only a small fraction of fresh concrete pores are large enough to be penetrated by microorganisms, the existing gel-void network allows

dissolved sulfide diffusion. The penetrating acid gradually deteriorates the calcium hydroxide structure, enlarging the pores and increasing the concrete's permeability. Later, the resulting porous outer surface slowly permits the gradual penetration of microorganisms. Over time, a gradient of deteriorated concrete forms and the interface between deteriorated and sound concrete penetrates further into the concrete, sustained by microbial transport deeper into the concrete (Berndt, 2011; Nielsen et al., 2008; Zivica and Bajza, 2001; Islander et al., 1991).

2.3.4. Relative Humidity

Another critical factor affecting corrosion rates is relative humidity (RH). A direct relation was observed between moisture content on the walls of sewer pipes and the biological activity. Higher RH enhances biological activity, leading to a higher corrosion rate (Joseph et al., 2010; Mori et al., 1992). In some experiments, the sulfate levels attained were 5-6 times higher on pre-corroded coupons exposed to 100% RH than those obtained at 90%RH (Joseph et al., 2010).

2.3.5. Temperature

Temperature is the final of the well documented factors affecting MICC rates. Temperature impacts the H_2S generation rate from the liquid to gas phase and governs the kinetics of various abiotic and biotic reaction rates fundamental for corrosion (Yongsiri et al., 2004; Joseph et al., 2010). "The temperature would also influence corrosion rates [chemical reaction between calcium and sulfuric acid]; however, this is yet to be proven" (Joseph et al., 2010).

2.4. Mitigation Measures

Grengg et al. (2018) reported, after a comprehensive review of the literature, that "no commercially available concrete can satisfactorily withstand the adverse conditions in such

aggressive environments over its projected operating life". Therefore, research into mitigation measures for concrete exposed to MICC is a topic of great interest to the wastewater industry. MICC mitigation requires identifying or developing practical treatment methods to alleviate the influence of controlling factors on the corrosion process. However, only three out of the five MICC's controlling factors mentioned in section 2.3 can be mitigated. Controlling the relative humidity and temperature inside the sewer system is infeasible in most conditions. Accordingly, the MICC mitigation strategy could be categorized into three methods. The first involves reducing the rate of H_2S gas formation by inhibiting SRB activity. The second method targets impeding the biological oxidation of H_2S by deactivating SOB. The third method involves chemical and/or physical alteration of the concrete properties, mainly reducing the concrete porosity and/or permeability.

2.4.1. Reducing Sulfide Formation Rates

The first category of methods to control MICC is to suppress the continuous production of H_2S in the liquid phase. Dosing wastewater with chemicals is typically used to inhibit SRB activities through pH shock or other mechanisms (Ganigue et al., 2011; Sun et al., 2015). Magnesium or sodium hydroxide can be used to control H_2S transfer from liquid to air by increasing the pH, since the formation of H_2S gas decreases exponentially with increasing pH of the solution and is nearly zero when the pH is above 10 (Gutierrez et al., 2009; Rees et al., 2003). Iron based salts can be used to remove sulfides through precipitation of insoluble salt phases (Firer et al., 2008; Zhang et al., 2009a), while nitrate and oxygen are also used for sulfide removal by oxidation (Gutierrez et al., 2008; Mohanakrishnan et al., 2009). Inhibitors and biocides like caustic and molybdate indicates significant efficacy in inhibiting SRB activities by disrupting the sulfide biofilm's generating capacity. (Predicala et al., 2008; Gutierrez et al., 2014; Zhang et al., 2009b).

The limitation of these methods includes cost, wastewater contamination, and limited efficacy (Gutierrez et al., 2014; Jiang et al., 2013; Zhang et al., 2009b; Sun et al., 2015). For instance, in high-volume wastewater networks, the continuous dosing of vast amounts of chemicals is costly and produces unwanted residues (Sun et al., 2015; Jiang et al., 2011a).

2.4.2. Reducing Sulfide Oxidation Rates

The second mitigation method works by hindering the biological sulfide oxidizing activity rate through SOB disruption. Several research studies have developed proprietary biocide and surface treatment methods. These treatment methods involve a chemical or antibacterial additive, which inactivates the Thiobacillus SOB and prevents biofilm formation. This process typically starts by removing the pre-existed corrosion layer through high-pressure washing (Islander et al., 1991; Nielsen et al., 2008; Sun et al., 2015). After washing, the surface pH is increases and the SOB inactivated by applying biocides or inhibitors on the concrete (Negishi et al., 2005; Yamanaka et al., 2002; Sun et al., 2015).

Nitrous Acid (HNO_2) from nitrite in acidic conditions was used as a biocide to effectively control anaerobic sewer biofilms (Jiang et al., 2010; Mohanakrishnan et al., 2008; Jiang et al., 2011b). Addition of FNA with a concentration of 0.2-0.3 mg HNO_2-N/L and exposure times of 6 to 24 hours, was shown to diminish sewer biofilm activity from 80% down below 15% (Jiang et al., 2011b). Combining hydrogen peroxide (H_2O_2) at 30 mg/L, or above, with FNA was observed to increase microbe inactivation by approximately 1-log (Jiang and Yuan, 2013). Whereas FNA is considered the primary inactivation agent, H_2O_2 was identified as an effective catalyzing agent (Jiang et al., 2013). Although FNA and H_2O_2 dosing combination is seen as a viable avenue for MICC mitigation. However, the effect of frequent treatment on biofilm activities has yet to be evaluated long-term. "It

is possible that sewer biofilms develop resistance to FNA during repetitive dosing" Jiang et al., 2013.

2.4.3. Reducing Concrete Permeability

The last category of MICC mitigation methods concentrates on modifying the concrete parameters to impede the biofilm's progression and penetration efficacy. These methods include physical or chemical treatments of the exposed concrete surface. Resembling the methods described in Section 2.4.2, this process involves pressure washing followed by adding a corrosion-resistant surface coating or mortar with admixtures to inhibit biofilm adhesion, composition, diffusion, and development (Grengg et al., 2018; Berndit et al., 2011; De Muynck et al., 2009; Haile and Nakhla, 2010; Page and Page, 2007; Sun et al., 2015). Polyurea linings and antimicrobial coatings like silver-bearing zeolite, epoxies, and polymer fiber demonstrated the most promising results to obtain an impermeable corrosion-resistant surface (Grengg et al., 2018; Berndt, 2011; De Muynck et al., 2009; Haile and Nakhla, 2010). However, the practical application of some of these methods is limited. Preparing the concrete surface for coating when in a damped condition is the main constraint in the treatments that can be applied. Coatings may not bond to the existing concrete structure unless the corroded concrete is entirely removed by pressure washing. Additionally, the use of environmentally hazardous chemicals and the high cost of these chemicals are considered significant disadvantages (Sun et al., 2015; Nielsen et al., 2008; Matthews et al., 2014).

2.5. Test Methods

Accurate testing methods are essential to determining the effectiveness of any applied mitigation measures. Several approaches have been developed to monitor and analyze the corrosion rates of concrete in sewers. These include measuring the thickness of the

corrosion layer, a microstructural and chemical analysis of the corrosion products, and characterization of the microbes within the corrosion layer (Cayford et al., 2012; Joseph et al., 2012; Satoh et al., 2007; Sun et al., 2014). However, these methods were considered arduous, costly, slow, or destructive measurements (Sun et al., 2015). To overcome these limitations, rapid and non-invasive methodologies were later developed to monitor MICC at various stages.

2.5.1. Surface pH Measurement

Maintenance of a high (>10) surface pH is a fundamental indicator for any successful MICC mitigation treatment. The continuous production of biogenic sulfuric acid (H_2SO_4) by SOB is strongly associated with decreasing surface pH of the concrete. Simultaneously, the formation of expansive sulfate phases leads to microstructural damage of the cement matrix. This external acid attack, which progresses inward, is a decisive factor in the increasing MICC rates. Interstitial concrete solutions, taken from severely corroded concrete, showed pH levels between 0.7 and 3.1 with higher concentrations of dissolved ions, such as sulfate (Grengg et al., 2017). Accordingly, precise pH measurement is central for evaluating the degree of deterioration and the corresponding development of mitigation measures (Grengg et al., 2019). Surface pH is an indirect quantification of the MICC progression, which was shown to be a controlling factor in the MICC mechanism in concrete as summarized in Section 2.2. Additionally, surface pH can be rapidly and accurately measured, with reproducible results.

An accurate method for measuring surface pH was developed by (Joseph et al. 2010; Ashock M. Kakade 2014; and Sun et al., 2015) to precisely measure the surface pH with a flat pH electrode (PH150-C, ExStik™). The concrete surface is first cleaned to remove dirt, concrete sealers, or adhesive residues. To improve the accuracy and repeatability, the

surface is then wet with 1 mL of Milli-Q water using a pipet and then allowed to equilibrate. The pH electrode is then placed on the surface and allowed to obtain a steady reading. An average pH is later calculated from several individual measurements performed at three different locations on the surface.

This testing method is considered a precise, practical, and inexpensive technique for evaluating the progression of MICC, and as such can be used to quantify successful mitigation. Unlike other methods, surface pH measurement is also a non-destructive procedure. Continuous monitoring can be performed throughout the structure's service life without the corrosion biofilm being disturbed. As MICC progresses and a pH gradient forms, surface pH may stabilize around pH 3-4. The deteriorated concrete and WW spraying increase the alkalinity of the near surface layers causing partial neutralization of the acid production. However, the pH at the interstitial region will continue to decrease. Therefore, at these later stages of MICC, it is insufficient to monitor the induced concrete corrosion development through surface pH measurement only.

The practicality of surface pH measurements indicates such methods can be used to periodically monitor the MICC process to determine when surface treatments should be applied before stage 2 of MICC initiates. As such, reapplication of treatments can occur before deterioration progresses and the surface pH decreases below ~9.

2.5.2. Sulfide Uptake Rate (SUR) Measurement

Unequivocally, the overall MICC process is primarily driven by the chemical and biological sulfide oxidation to sulfuric acid. Severely corroded concrete coupons were observed to have higher sulfide uptake rates (SUR) as compared to the less corroded samples. The hypothesized explanation for this observation was the increased biological sulfide oxidation in the more corroded coupon (Sun et al., 2014). Accordingly, a direct

relationship between the H_2S uptake rate (SUR) and biofilm development on the concrete surface was concluded (Sun et al., 2014; Joseph et al., 2010; Parker and Prisk, 1953). Accordingly, H_2S oxidation and adsorption is a rapid process that directly impacts the corrosion reaction. Measuring the SUR is a useful method for monitoring MICC activity at various stages.

A rapid, non-invasive testing method was developed by (Sun et al. 2014) to monitor the MICC process by measuring the H_2S uptake rates of concrete at different corrosion phases. The procedure begins by placing the to-be-tested concrete sample in a gas-tight reactor. Temperature and humidity were controlled and then H_2S gas was injected into the chamber. After reaching a specified gaseous concentration, the H_2S concentration gradually decreases over time due to chemical and biological sulfide oxidation to sulfuric acid (H_2SO_4). The data recorded by an H_2S meter is then retrieved and plotted. Afterward, the background uptake rate is subtracted, and the corresponding SUR determined from the slope of the H_2S concentration with respect to time, using Equation 2-1 (Vollertsen et al., 2008). The background uptake rate occurs due to chemical adsorption or oxidation of H_2S by the confined moist air and/or the chamber materials (fan, sensor, and walls). Finally, the rate is converted into a surface specific H_2S uptake rate using Equation 2-2. Repeated tests on several concrete samples were carried out to assure the consistency of this method.

$$r_{H_2S} = -\frac{d[H_2S]}{dt} \qquad \textbf{Equation 2-1}$$

$$r_{H_2S} = -\frac{d[H_2S]}{dt} \times P_{atm.} \times \frac{MW_{sulfur}}{R \cdot T} \times \frac{V_{reactor}}{S_{area}} \qquad \textbf{Equation 2-2}$$

Where,

r_{H_2S} = Surface-Specific H_2S Uptake Rate (mg-S m^{-2} h^{-1})

$[H_2S]$ = H_2S Gas-Phase Concentration (ppm),
t = Time (h).
P_{atm} = Atmospheric Pressure (101.325 KPa)
MW_{sulfur} = Molecular Weight of Sulfur atom (32.065 gm mol^{-1})
R = Universal Gas Constant (8.3145 J K^{-1} mol^{-1})
T = The Absolute Temperature (K),
$V_{reactor}$ = Total Gas Volume in the Reactor (m^3)
S_{area} = Exposed Surface of Concrete (m^2)

2.5.3. Live/Dead Staining

Although the sulfide-induced corrosion process initiates with chemical oxidation, the sulfide biological adsorption has a significant influence on the subsequent stages (Islander et al., 1991). At preliminary stages, when the surface pH is greater than 6, the chemical oxidation of H_2S controls the reaction, but slows at later phases when the pH is less than 6 (Chen and Morris, 1972; Millero et al., 1987). Conversely, at pH ~4, acidophilic SOB present in larger numbers and become more active, thereby oxidizing larger amounts of sulfide to sulfuric acid (Roberts et al., 2002). The viability of these bacterial cells depends on the microbial growth conditions present in the biofilm and the treatment methods applied to the concrete. To evaluate the efficacy of treatment methods, Live/Dead staining (Viability/Cytotoxicity Assay Kit for Bacteria, Biotium) is used, especially in later corrosion stages, to quantify the amount of living and dead bacteria present in the biofilm.

This methodology involves staining the bacteria with a reagent and then incubating the bacteria. A small sample of the biofilm is collected by scraping, which is then mixed with pyro-phosphate solution. The mix is sonicated and then layered onto sucrose solution and centrifuged. The upper layer of sodium pyrophosphate (now with the microbial cells) is then transferred to a fresh tube and centrifuged a second time. The pellet is then decanted and re-suspending twice in NaCl solution. Finally, the pellet is re-suspended in NaCl solution and the staining reagent is added. The solution is next mixed and incubated before

being placed on microscope slides to be viewed with a fluorescence scanning microscope. This method was developed and documented by Jensen et al. (2011) and later by Sun et al. (2015).

2.6. Summary

A thorough review of the existing literature concerning mitigation of MICC reveals knowledge gaps concerning methods for reducing sulfide formation rates, reducing sulfide oxidation rates, and reducing concrete permeability and biofilm permeation. Therefore, the focus of the present study was to investigate a series of mitigation measures to specifically control sulfide oxidation rates and concrete permeability. The following section details the research methodology and experimental methods utilized in pursuit of this objective.

3. Chapter 3 Materials and Methods

The research program herein was divided into two major, concurrent phases. An outline of this program is summarized in Figure 3-1. The first phase involved a laboratory investigation of possible MICC treatment methods applied to concrete coupons. The second phase included field trials and validation of results in a sewer wet well. Both the concrete coupons and core samples collected from the wet well were assessed using similar methods (discussed below) to appraise the difference between laboratory and field trials. Results from the two research phases were compiled to evaluate the applicability, practicality, cost-effectiveness, and longevity of each treatment. Construction of the laboratory experiment, field trials, treatment application methods, and testing setups are also described in detail in the subsequent sections.

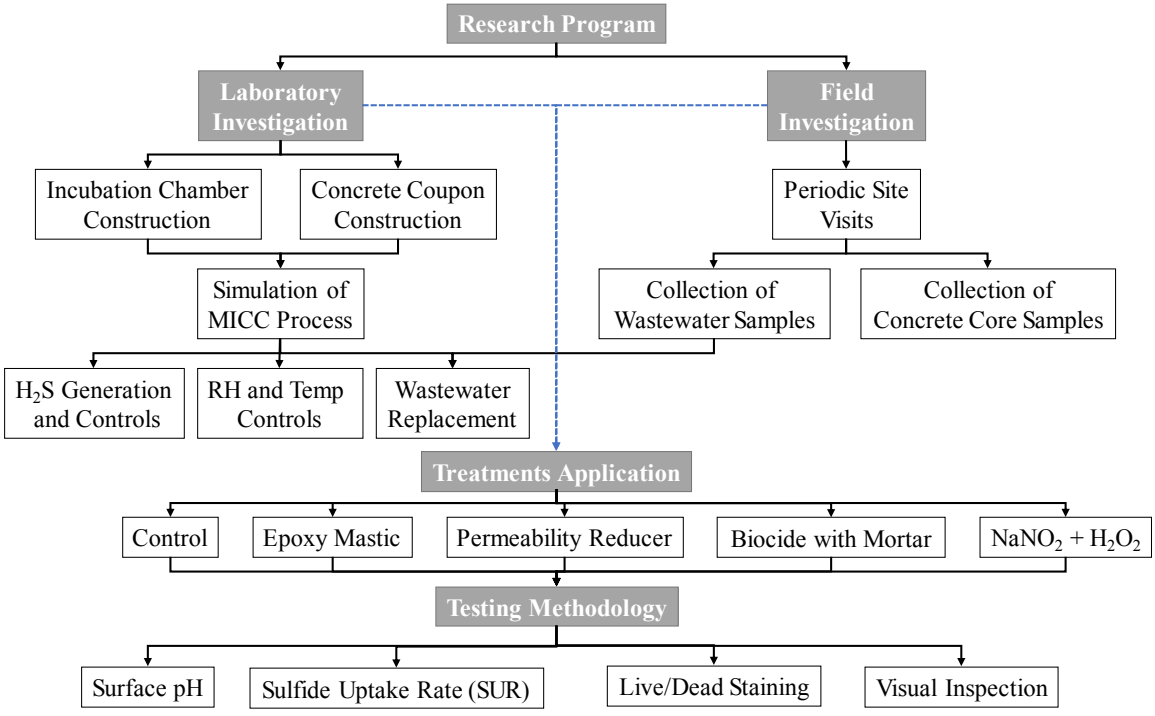

Figure 3-1, Flow chart for the Research Program

3.1. Lab Experiment

An experimental incubation chamber was designed and constructed to simulate and expedite the corrosion process that occurs in wastewater systems. Concrete coupons were cast and incubated in the chamber with a sequential generation of hydrogen sulfide gas (H_2S) and periodic addition of wastewater (WW). Several different surface treatments were then applied to subsets of the coupons, and the progression of MICC monitored was periodically. The experiment setup diagram is shown in Figure 3-2

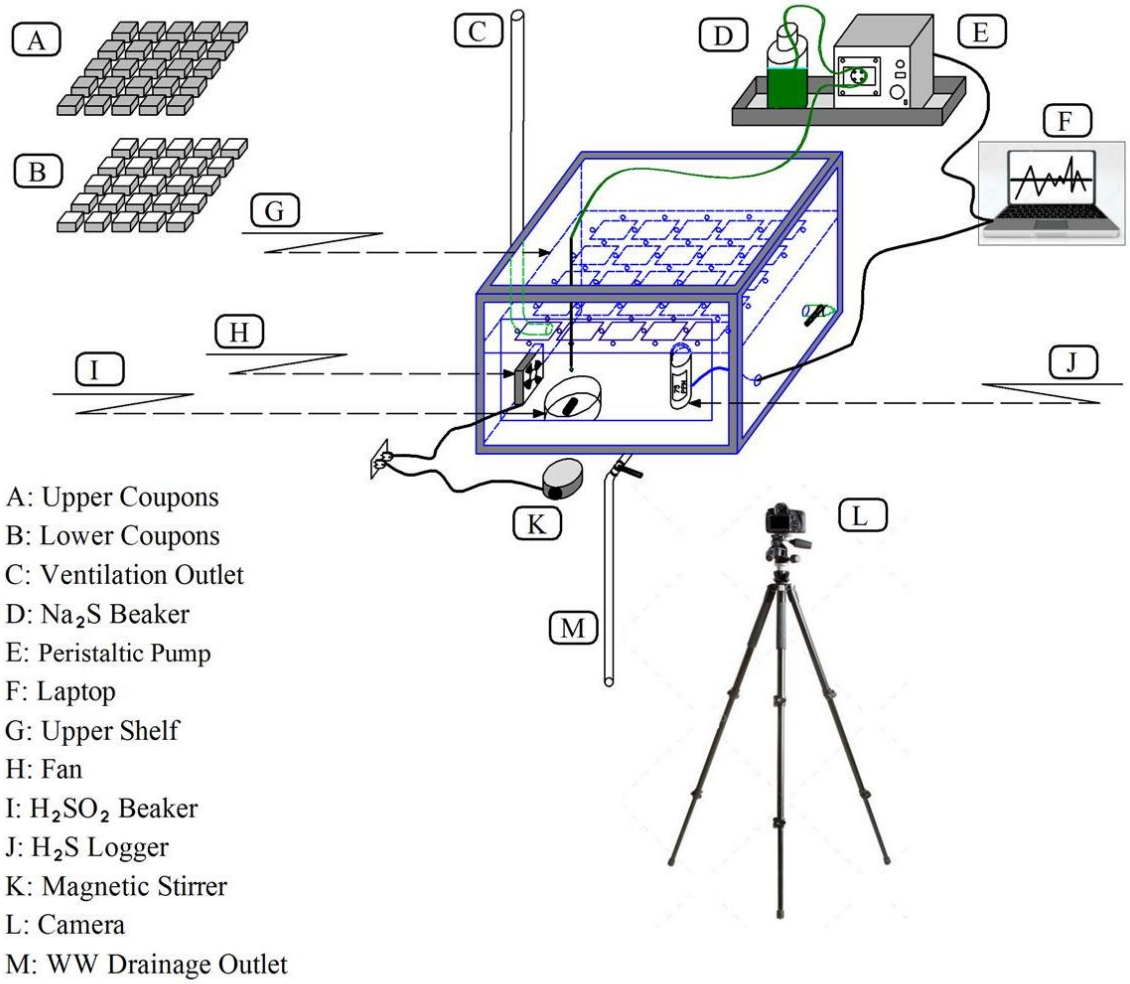

Figure 3-2, Experiment setup diagram

3.1.1. Construction of the Chamber

The incubation chamber was designed following the methods described by Joseph et al., 2010 and Joseph et al., 2012. The assembly process is documented in Figure 3-3. The chamber was constructed of transparent PVC sheets (0.25 in. thick) with dimensions of 31 in. (length) by 21 in. (width) by 19 in (height). PVC panels were precision cut by a machinist to the desired dimensions. The chamber's sides were assembled using PVC glue, which once cured will not react with the H_2S gas. One shelf, with 25 window openings (4 in. x 3 in. each), was mounted at the mid-height to carry the upper set of concrete coupons. For extra protection, PVC angles (1 in. x 1 in.) were also glued to the chamber's outer edges. PVC fittings and stainless-steel valves were attached to the inlet and outlet for gas ventilation and WW drainage purposes. Rubber (EPDM) gasket strips were placed around the perimeter of the door opening to prevent any gaseous leakage. Screws, washers, and nuts were later used to fix the access door cover tightly. Any remaining gaps were sealed by PVC cement and then covered by silicone. After construction and curing, the chamber was placed into a fume hood and tested for leaks under pressure. Detailed CAD drawings for the chamber are provided in the appendix of Section 7.1

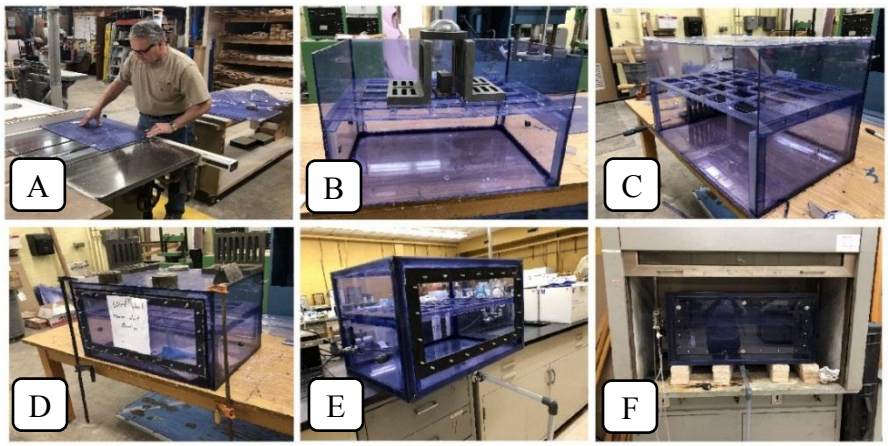

Figure 3-3, Chamber Construction, (A) cutting PVC sheets, (B) load testing the shelf, (C) assembling the chamber, (D) installing supports and door, (E)attaching PVC pipe fittings, and (F) leakage test under the fume hood. (pictures by Mostafa Nasr)

3.1.2. Concrete Coupons

Unlike several previous studies that utilized pre-corroded concrete coupons for MICC simulation, this research program used fresh concrete coupons for two reasons. Primarily, it was observed that deterioration in some visited wet well locations, as shown in Figure 3-4, has progressed to the point where surface treatment would be impossible without first rehabilitating the concrete surface. This rehabilitation process mainly involves cleaning the wet well with pressurized water and then coating the perimeter with shotcrete. Therefore, in the authors' opinion, the application of surface treatment methods will typically be onto the hardened shotcrete. Secondly, the three-step corrosion model mentioned in section 2.2 demonstrated that MICC initiates at the early age of fresh concrete in sewer structures. The elementary corrosion stage, dominated by abiotic acid-base reactions, begins with pH reduction of the fresh concrete's strongly alkaline surface. Thiosulfuric and polythionic acids, produced by chemical oxidation of H_2S, simultaneously attack the fresh concrete which is characterized by an initial pore solution of pH approximately 13, and a surface pH around 10-11) (Roberts et al., 2002). Accordingly, the authors determined to best investigate and fully understand the entire MICC process in the laboratory, it would be best to evaluate the treatment methods on fresh concrete rather than the pre-corroded concrete.

Figure 3-4, Severe deterioration of wet well at Meadowood Circle location , Poland, Ohio (pictures by Mostafa Nasr)

After the chamber was tested and the safety verified, fresh concrete coupons were cast to simulate the rehabilitation and treatment of wet well concrete in a controlled laboratory environment. A concrete mixture was developed to mimic the shotcrete mixtures used for wet well rehabilitation. This mixture was designed with a low slump and no coarse aggregates to allow vertical application and simulate the concrete spraying on site. The mix design for the concrete coupons is summarized in Table 3-1.

Table 3-1, Mixture design for concrete coupons.

	Weight lbs./yd^3	Volume ft^3	Ratio	S.G.	A.C.	Weight lbs.
Cement	1301	6.62	1.00	3.15	-	24.10
Fine Aggregate	1952	11.50	1.50	2.72	0.01	36.14
Water	520	8.34	0.40	1.00	-	9.64
Air	-	0.54	-	-	-	-

The concrete mixture was batched in the Concrete Materials Lab (CML) at Youngstown State University and then placed into a leveled plywood formwork (Figure 3-5, A). Three concrete slabs of 25 in (length) x 25 in (width) x 2 in (thick) dimensions were caste as shown in Figure 3-5 (B). Float troweling and edging were performed to obtain a consistent 2-inch thickness and a smooth top concrete surface (Figure 3-5, C). The next day, the formwork was removed, and concrete slabs were submerged into the water for 14 days at room temperature. Once the curing procedure was complete, the concrete slabs were cut using a water-cooled saw into 54 symmetrical concrete coupons, as shown in Figure 3-6. A coupon size of approximately 4 in. (length) x 3 in. (width) x 2 in. (thick) (100 x 75 x 50 mm) was selected to provide adequate surface area for testing and room for 50 coupons in a single incubation chamber. The two-inch thickness was also selected to secure

an adequate depth for future severe corrosion as microorganisms were detected throughout the entire corroded layer to a depth of around 1.5 inches (4 cm) by Grengg et al. (2017).

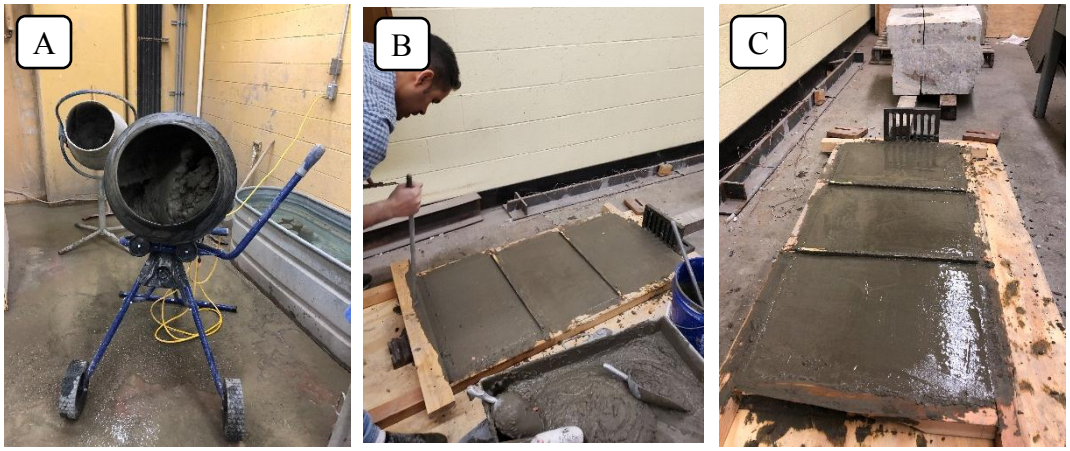

Figure 3-5, Concrete coupons casting, (A)Concrete patching, (B)Slabs casting, (C) Surface finishing (pictures by Mostafa Nasr).

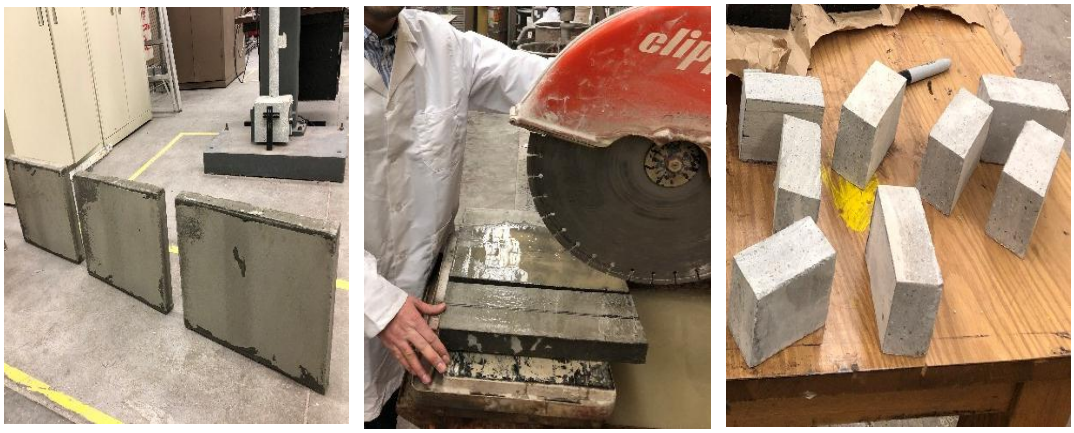

Figure 3-6, Concrete coupons cutting (pictures by Mostafa Nasr)

As the concrete in the wet well is only exposed to H_2S and corrosion on one face, coupons were coated with DTM epoxy mastic on all but the exposed face, as shown in Figure 3-7 (A). Coupons were divided into two sets of 25 coupons each and then numbered with epoxy paint, as shown in Figure 3-7 (B-C). Four extra coupons, two from each set, were left as fresh concrete control for further comparisons. Afterward, the initial surface pH was measured and recorded, as shown in Section 7.3 - Appendix C, Table A3. After 14 days, coupons were placed into the incubation chamber, as shown in Figure 3-7 (D).

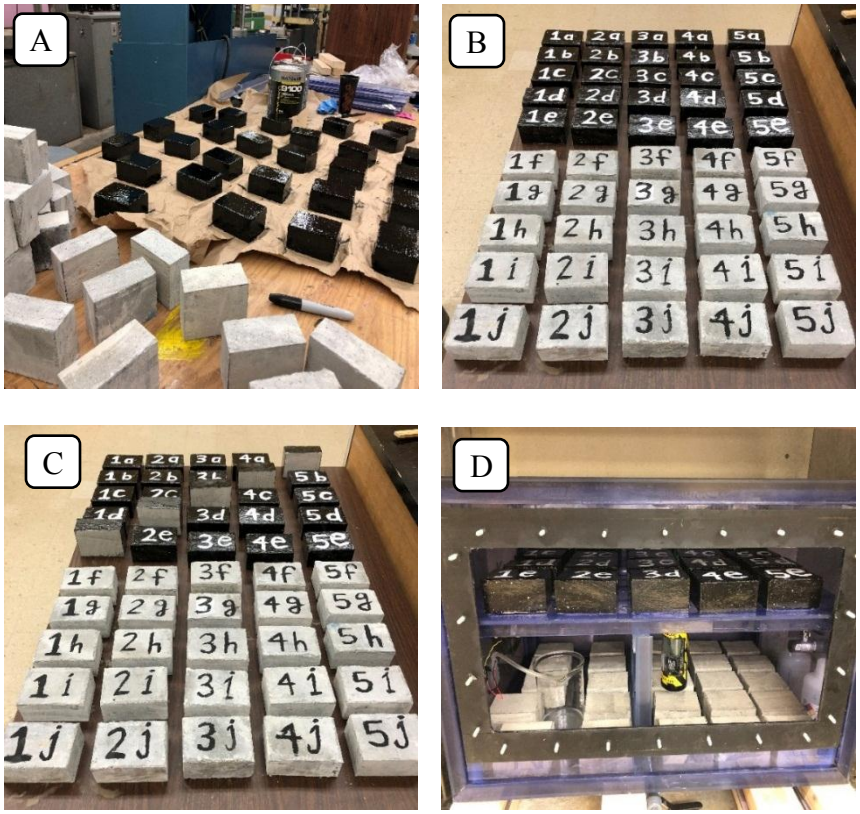

Figure 3-7, Epoxy coating and numbering of coupons (pictures by Mostafa Nasr)

3.1.3. Coupons Arrangement and Sewage Addition

Typically, the most active concrete corrosion was previously observed to occur at both the crown and the waterline of sewer pipes, manholes, and wet wells (US EPA, 1985; Mori et al., 1992, Vollertsen et al., 2008). Accordingly, the coupons were arranged to simulate two different exposure types where these severe corrosion conditions occur. One set of coupons was stored on the shelf, while the other set was laid on the chamber floor where four liters of sewage were added and periodically replaced every 7 days. Actual residential wastewater was sampled from a wet well in Ellsworth- Ohio (the same location used for the field experiment), was used to capture any yet undocumented effects of volatile components existing in real wastewater environment.

The first set of coupons was placed on the shelf, with all but one side coated with DTM epoxy mastic. The uncoated and exposed surface was placed facing downwards about 7 inches above the sewage surface. This arrangement allowed the exposed surface to contact only the gas phase, meant to simulate the sewer pipe crown, a region that suffers severe corrosion. Every other month, the coupons were soaked in wastewater for 30 seconds prior to placement on the shelf within the chamber to provide SRB and SOB on the concrete surface. This method was selected to simulate the periodic, direct exposure of the pipe crown to wastewater during high-flow events.

The remaining set of 25 companion, and uncoated, coupons were partially submerged in the wastewater with the designated exposed surface facing upwards. This set of coupons was exposed to both the gas and the wastewater to simulate the waterline, another region that is generally highly corroded. Every seven days, the sewage was drained, and freshly collected wastewater was refilled and poured over the concrete exposed surface of the concrete, as shown in Figure 3-8.

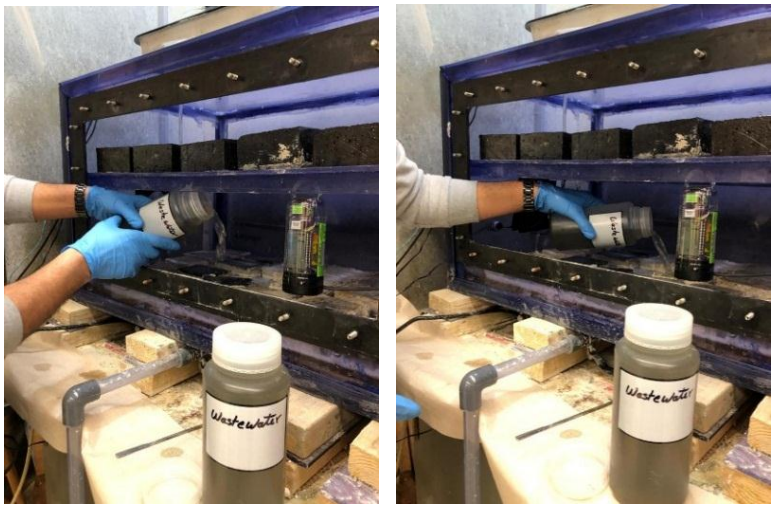

Figure 3-8, Domestic sewage addition (pictures by Mostafa Nasr)

3.1.4. Chamber Housing and Safety Guidance

Occupational Safety and Health Administration (OSHA) identified H_2S as a colorless, flammable, and extremely hazardous gas with a rotten egg smell. Hence, after passing the gas leak test, the chamber was transferred to the Environmental Science Lab (ESL) to be continually operated under a running fume hood. The fume hood was also tested to ensure proper ventilation of any accidental gas leaks and to alleviate the smell. Two portable H_2S gas detectors (BWC2-H714 by Honeywell) were also fixed on the fume hood's door and at the lab entrance as emergency warning alarms. In addition, a digital video camera, mounted on a tripod stand was fixed and connected to a remotely accessible laptop to allow live, remote monitoring. Proper personal protective equipment (PPE), including gloves, masks, splash shields, and coveralls, were also utilized while working in the lab. Figure 3-9 shows the safety measures and equipment used in the laboratory experiment.

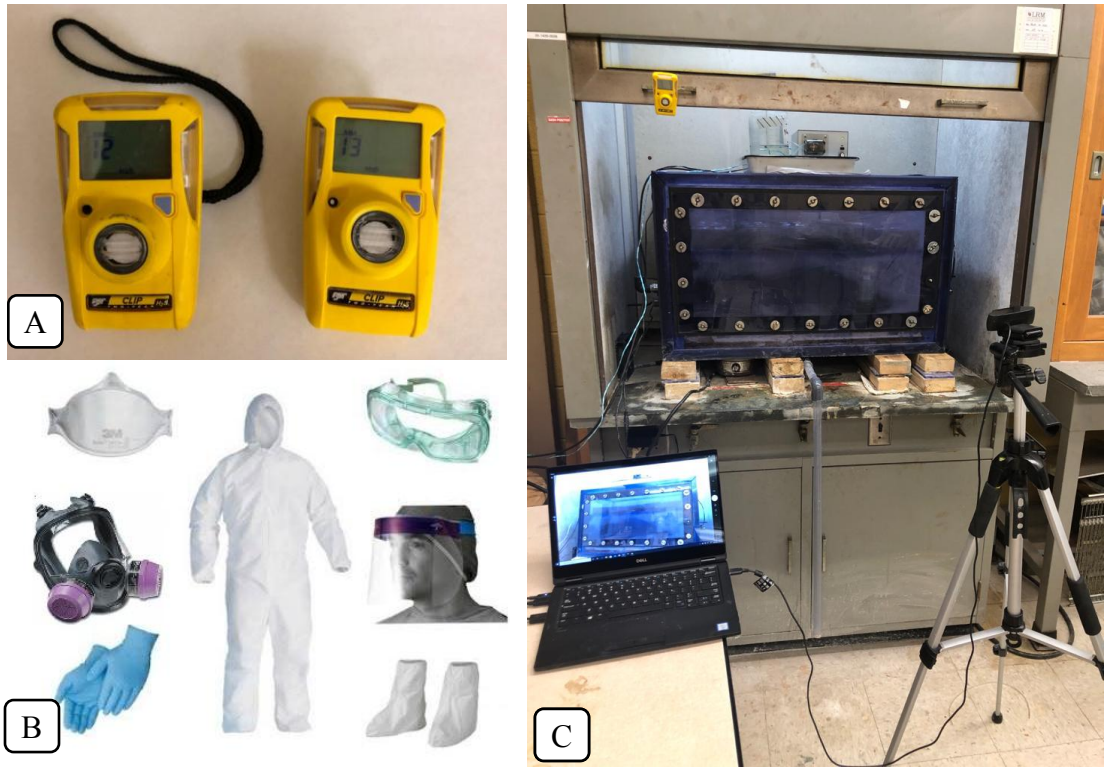

Figure 3-9, Safety measures and equipment, (A)H_2S gas detectors, (B)personal protective equipment (PPE), (C)digital monitoring camera for remote live monitoring.

3.1.5. H_2S Generation and Exposure

Once safety guidance and measures were established, gaseous H_2S was generated in the chamber using Equation 3-1. Generation of the H_2S gas was achieved by dosing a 0.5 M sodium sulfide (Na_2S) stock solution into a container with 8 M sulfuric acid (H_2SO_4). The Na_2S solution was pumped at a regulated rate through a silicon tube using a peristaltic pump (Figure 3-10, A) into the H_2SO_4 beaker to maintain the desired H_2S concentration in the chamber. Both the Na_2S and H_2SO_4 stock solutions were periodically refilled and replaced as needed.

$$H_2SO_4\ (aq) + Na_2S\ (aq) \rightarrow H_2S\ (g) + Na_2SO_4\ (aq) \qquad \textbf{Equation 3-1}$$

As the H_2S gas is heavier than air with a relative density of 1.19, a waterproof axial fan (Figure 3-10, B) was mounted right above the H_2SO_4 beaker to disperse the H_2S throughout the chamber. Additionally, initial trials without stirring the H_2SO_4 solution proved impossible to maintain adequate generation of H_2S gas at a stable concentration. Therefore, the H_2SO_4 beaker was placed on a magnetic stir plate (VWR® Low Profile Magnetic Stirrer) placed under the incubation chamber, as shown in Figure 3-10 (C), as it was not H_2S resistant.

The H_2S gas concentration was measured in real-time using a portable data-logger (AcruLog™ H_2S Gas Monitor) with a detection range of 0-1000 PPM (Figure 3-10, D) intended to survive in the harsh environments typically found within the wastewater industry. According to the manufacturer's guidance, the data-logger is designed to be exposed to up to 1000 ppm H_2S for 30 days (at a time) and then requires ten days of fresh air. Therefore, two loggers were acquired so that one can be in use while the other rests in fresh air. These loggers have an RS485 output that can be connected to a serial data input

(National Instruments) and data acquisition system. As will be discussed in Section 3.1.6, this system was later programmed to adjust the pump flow rate in real-time and maintain a stable atmosphere of 50-150 ppm H_2S gas as needed.

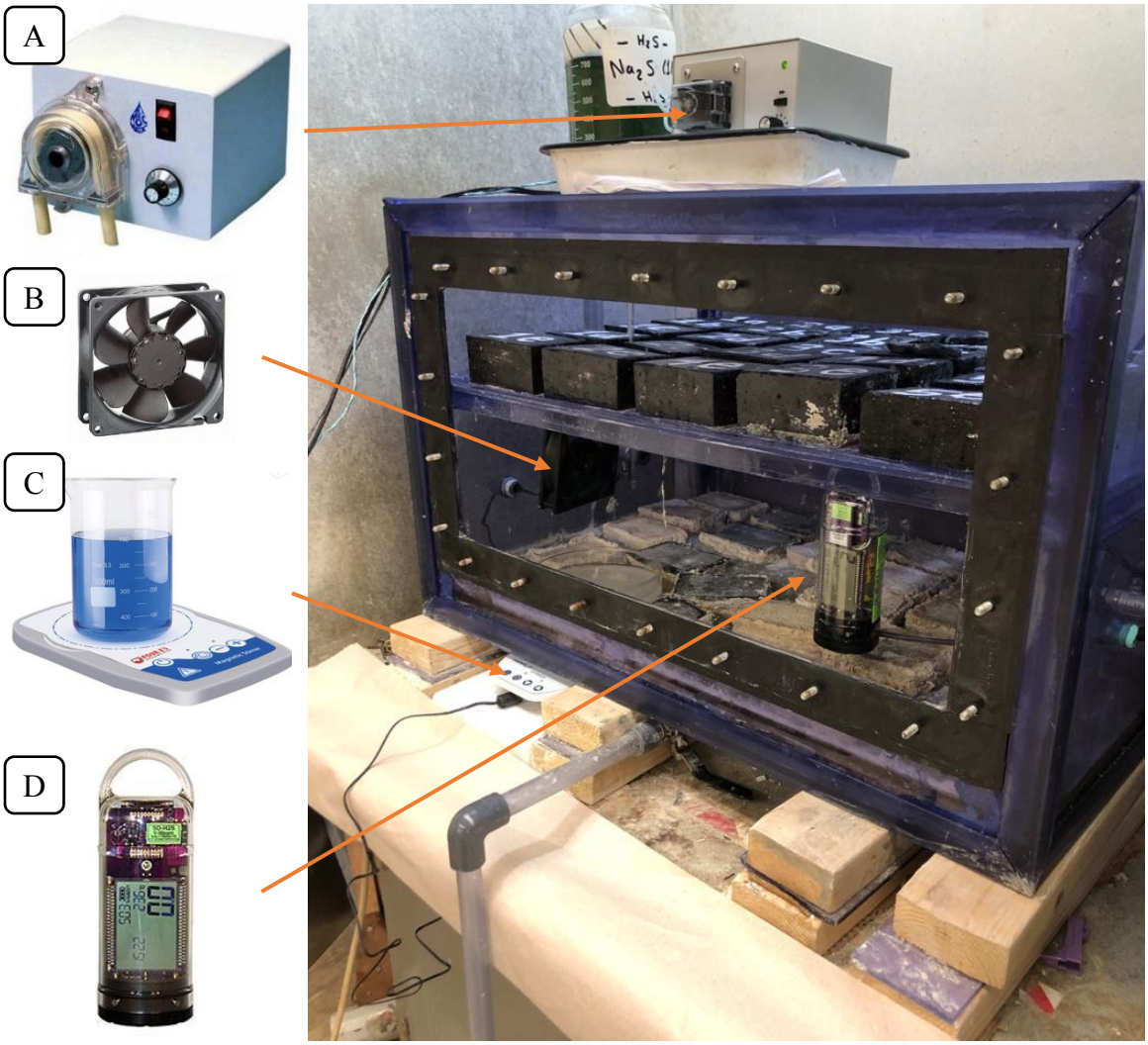

Figure 3-10, H_2S gas generation process and tools, (A)peristaltic pump, (B)waterproof axial fan, (C)magnetic stir plate, (D) AcruLog™ H_2S gas data-logger.

3.1.6. Data-Logging System and H_2S gas Concentration

To maintain the desired, stable H_2S concentration, a data-logging system was designed and programmed using LabVIEW controls software. An electronically controlled peristaltic pump was connected to a computer by way of a relay. The system was

configured to read the H_2S concentration from a self-contained AcruLog LL1000 Sensor and DAQ, with an RS485 interface. The system was connected to the computer through an RS485 input, which was then read into LabVIEW using the RS485 Modbus Protocol. The AcruLog LL1000 sensor outputs H_2S concentration (PPM), temperature (°C), and humidity (%) data in real time as shown in Figure 3-11. The data was read into LabVIEW, and then LabVIEW was programmed to actuate the relay and start/stop the pump as needed following the process diagram in Figure 3-12. The system was programmed to read and update at either 15, 30, or 60 second intervals, depending on the user's needs. The H_2S concentration (PPM), temperature (°C), and humidity (%) data, and time were also logged into a database. As an added safety feature, the system was programmed with a safety shutoff if the H_2S concentration exceeded a safe upper or lower limit. This feature was deemed necessary, as electrical failure of the fan or magnetic stirrer used in the MICC experimental chamber would result in the pump remaining in the on position, with a delay in H_2S generation, followed by a spike in the H_2S concentration. The system was configured and tested, and any desired H_2S concentration between 50 and 350 ppm (or higher if necessary) could be generated long-term with fluctuations on the order of ±5 percent, which was deemed acceptable for the experiment.

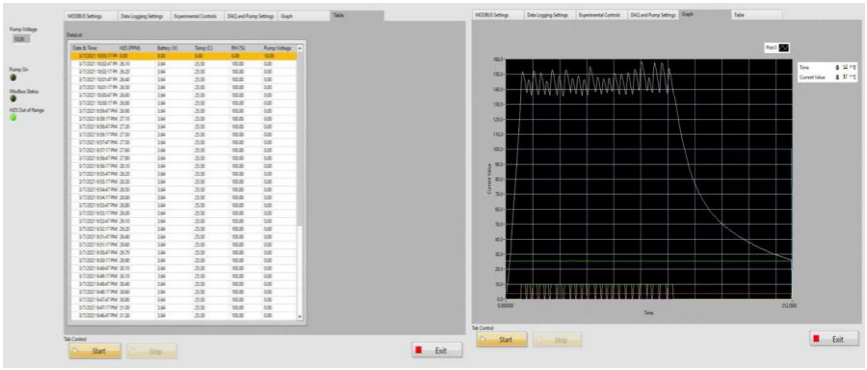

Figure 3-11, LabVIEW controls software (Designed and programmed by Richard Deschenes)

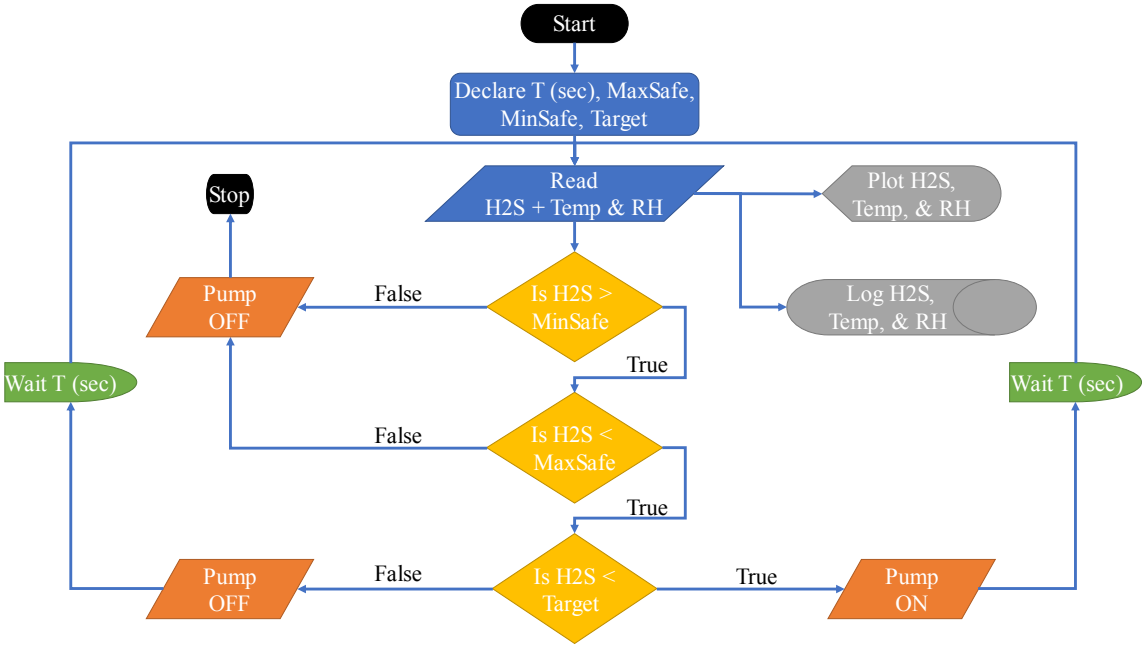

Figure 3-12, Process diagram of LabVIEW controls software (Designed and programmed by Richard Deschenes)

3.1.7. Gas-Phase Temperature and Relative Humidity

The temperature and relative humidity inside the chamber were recorded in real-time and plotted using the data logger and the LabVIEW application. Influenced by the controlled room temperature, the chamber's gas-phase temperature was maintained at 23-26 ˚C, as shown in Section 7.2- Appendix B, Table A1. Likewise, the gas phase relative humidity inside the chamber was maintained at 95-100%. Under any circumstances, the chamber's periodic opening for maintenance or replacing the H_2SO_4 solution had to be quick and short. Otherwise, the relative humidity will drop down, and the concrete surface will dry up, which consequently inhibits the anaerobic SOB growth rates.

3.1.8. Disposal of Wastewater and Toxic Chemicals

An essential consideration of this research was the generation and disposal of wastewater and toxic chemicals. Safe disposal of chemical and biological waste was a

significant logistical portion of the ongoing research and required established safety protocols to ensure no H_2S gas was released into the lab. Mixing sodium sulfide (Na_2S) and sulfuric acid (H_2SO_4) generates H_2S gas and a mixture of sodium sulfate, sulfuric acid, and sodium hydroxide. This waste mixture solution is characterized by a low pH of around 1 and can keep generating H_2S gas when agitated. For safe disposal, the waste material was doused with an excess of sodium hydroxide (NaOH) until the pH was greater than 11. At this point, all remaining H_2S goes into the solution and remains stable so long as pH is maintained above 10. The waste material was then collected and sent for disposal at an approved lab. On the other hand, the wastewater, periodically drained out of the incubation chamber, was stored in a labeled, sealed container and returned to the wet well location during the next site visit.

3.2. Field Investigation

The second aspect of the experimental investigation is the field investigation of surface treatments. Working with the Mahoning County Sanitary Engineers Office (MCSE), wet well locations in the Mahoning County-Ohio were selected for rehabilitation and treatment. The first site visit took place at a severely corroded wet well at Meadowood Cir, Youngstown, OH. Surface pH and core samples were collected at this location. However, as previously shown in Figure 3-4, the deterioration was severe, and it was deemed impossible to apply surface treatments. Since pressure washing and shotcrete were out of the scope of this research program, a new location was selected for surface treatment. The new wet well location, in Ellsworth-Ohio, has been recently rehabilitated by pressure washing and shotcrete application. The Meadowood Circle wet well (first location) will be considered as a possible location for future rehabilitation and validation of the best performing treatment method.

The under-investigation wet well, located at 11025 W. Akron-Canfield Road in Ellsworth- Ohio, was in a severe corrosion condition and was rehabilitated in 2015. The rehabilitation process involved pressure washing to remove loose, corroded concrete. The surface was then refinished by applying shotcrete, which was then troweled to provide a smooth, brushed surface finish. This location was selected for treatment investigation as the concrete surface did not require further rehabilitation before surface treatments were applied.

The H_2S concentration and gas-phase temperature inside the wet well were continuously measured using two OdaLog Longlife H_2S loggers (Figure 3-13, A). The OdaLog loggers are like those used in the laboratory experiment; these data-loggers are also designed to be exposed to up to 1000 ppm H_2S for 30 days (at a time) and then require ten days of fresh air. Therefore, one logger was left suspended from a rope while the wet well access door remained closed, as shown in Figure 3-13 (B). Every 21 days, the logger was replaced with the other one and then the data was retrieved and plotted on the cumulative monitoring graph. After few weeks of monitoring, the selected treatments were applied, as described in Section 3.3. Subsequent site visits have been to the wet well to replace loggers, collect concrete cores, and collect wastewater samples. Immediately after each visit, the collected concrete cores undergo the same measurement methods, as discussed in Section 3.4, to evaluate the efficacy of each treatment.

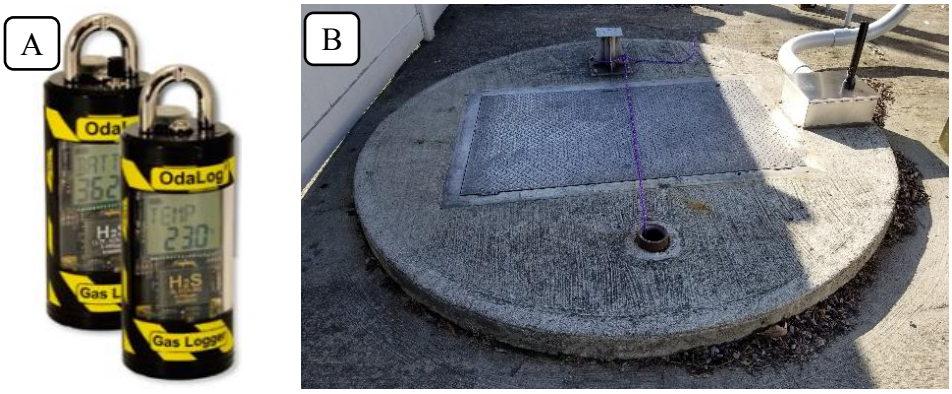

Figure 3-13, Wet well location in Ellsworth- Ohio, (A) H2S data-logger, (B)Monitoring H_2S gas concentration inside the wet well (picture by Dr. Richard Deschenes)

3.2.1. Concrete Cores and Wastewater Sample collection

Periodically (approximately every 45 days), a site visit was scheduled with MCSE to collect concrete cores, replace loggers and collect domestic wastewater samples required for the laboratory investigation. Upon arrival, the wet well access door was opened for aeration and a blower pump was lowered for extra ventilation. Before working inside the well, the H_2S gas logger was lowered to measure H_2S gas concentration and ensure the H_2S level is low enough for safe entry (< 10 PPM per OSHA Guidelines). For additional health safety, personal protective equipment (PPE), including a protective face mask, safety goggles, waterproof gloves, and liquid-repellent coveralls, were utilized while handling the sewage. A safety harness suspended from a truck-mounted hoist was used to lower the technician into the well as shown in Figure 3-14 (A). Concrete cores were cut using a hammer drill with an attached core bit of 2 inches internal diameter (Figure 3-14, B). Each visit, two concrete cores from each treatment plus the control (10 cores total) were cut from the well wall for further laboratory investigation (Figure 3-14, C). Also, eight litters of domestic sewage were collected to be used in the incubation chamber (Figure 3-14, D).

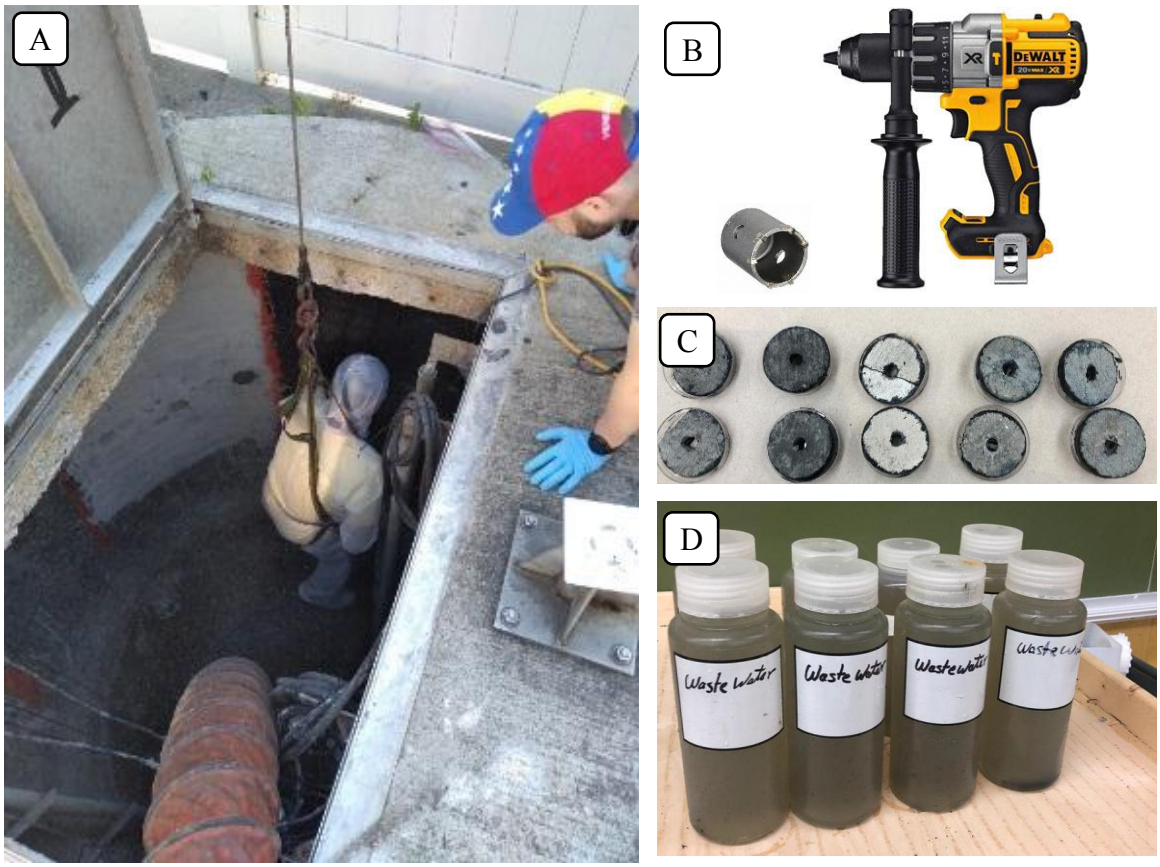

Figure 3-14, Sample collection from the Ellsworth wet well, (A) Author wearing PPE and harness while collecting core samples. (B) Hammer drill used for cutting cores, (C) Core samples, (D) WW samples (pictures by M. Nasr & Asad Khan).

3.3. Treatments

Based on treatment methods identified in the literature review, four surface treatments were selected and applied to eight subsets of the incubated concrete coupons. Simultaneously, the same treatments were applied to the internal perimeter wall of the Ellsworth wet well location. The applied surface treatments included: (i) epoxy mastic, (ii) free nitric acid (HNO_3)—via sodium nitrite ($NaNO_2$) plus hydrogen peroxide (H_2O_2), (iii) chemical biocide (mixed with mortar), and (iv) ARC sealant—surface applied permeability reducing treatment. The first two treatments were selected based on the literature review (Section 2.4), while the second two were recommended by several manufacturers of

concrete admixture and surface treatment. The commercial names of these products have been withheld at the request of the manufacturer.

The four treatments could also be categorized into two different types of treatments. Both the epoxy mastic and the ARC sealant are considered corrosion-resistant surface coatings. These coatings are used to reduce the concretes surface permeability and inhibit the biofilm adhesion, composition, diffusion, and development, as mentioned in Section 2.4.3. While on the other hand, sodium nitrite and the biocide with mortar belong to the biocidal inhibitor treatment category mentioned in Section 2.4.2. These biocide treatments are applied to the concrete surface to increase the surface pH and deactivate the SOB activities.

3.3.1. Treatments Application in the Lab

For approximately four months, concrete coupons were exposed to an atmosphere of 50 ppm H_2S gas and periodically exposed to wastewater to simulate and accelerate MICC deterioration. Once the second corrosion stage started and surface pH declined below 9, the coupons were removed from the incubation chamber, rinsed with water, and then sprayed with hydrogen peroxide 60 gm/L (1.76 M [6%]), as shown in Figure 3-15 (A). After that, coupons were left to dry at room temperature for 24 hours, and then the four treatments were applied to the exposed surface of the coupons. Subset of five coupons from the upper set and five coupons from the lower set (10 coupons for each treatment) were simultaneously coated with each treatment, as shown in Figure 3-15 (B). Details on the different treatment methods are provided in Sections 3.3.1.1-3.3.1.4, including concentrations, application rates, and application methods. After treatment, coupons were left to dry for another 24 hours and then returned into the chamber. After drying, the second

stage of the MICC corrosion process was expedited by exposing the coupons to a higher H_2S gas concentration of 165 ppm on average.

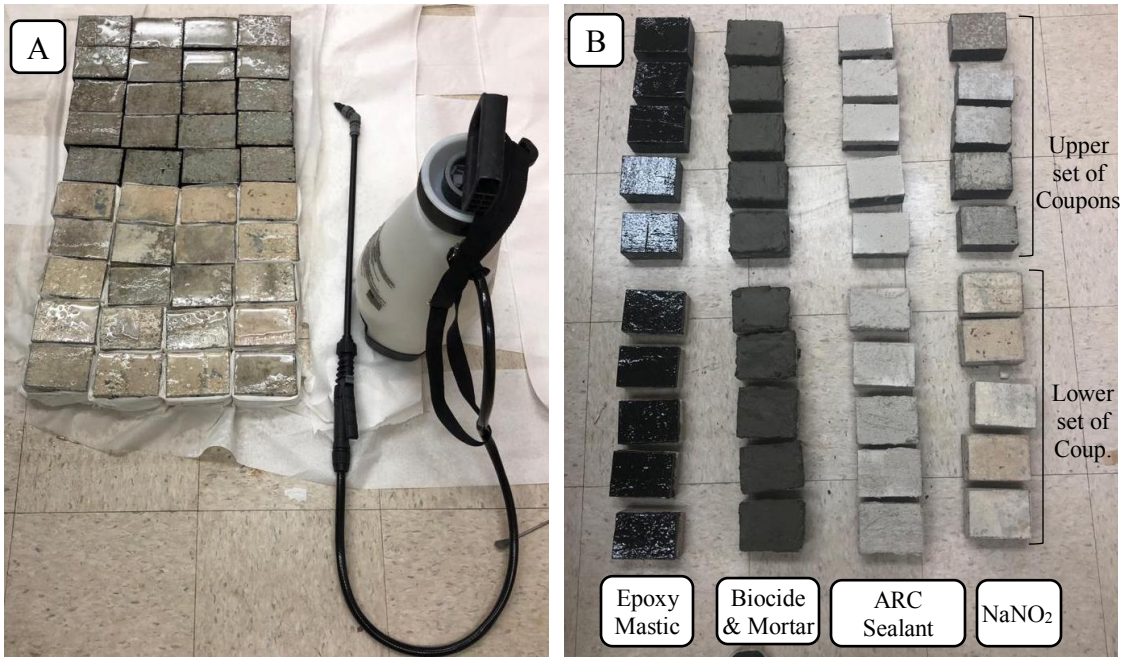

Figure 3-15, Treatments application on concrete coupons, (A)Spraying all coupons with H_2O_2, (B) Air drying of coupons after treatment application (pictures by Mostafa Nasr)

3.3.1.1. Epoxy

The epoxy mastic surface treatment was used to prevent MICC by reducing the concrete permeability, which impedes the biofilm progression and penetration efficacy, as discussed in Section 2.4.3. High-performance epoxy mastic is designed for long-term use in moderate to severe corrosion environments, and it can be sprayed, brushed, or rolled on the concrete surface. Black semi-gloss 9100 DTM Epoxy Mastic by Rust-Oleum. (Mfr. Model # 9179402) was mixed, 1:1 by volume, with Fast Cure Activator (Mfr. Model # 9104402) following the manufacturer's instructions. The two-component product was then applied to the surface with a paintbrush to obtain a 1-2 mm coat thickness. After 2 hours, a second coat was applied. This product is advertised as being durable in severe, wet H_2S environments for prolonged periods (Rust-Oleum Corporation; 2001). The material should

be essentially inert on exposure to wet, H_2S environments; however, the Long-term exposure to acids may cause some discoloration.

3.3.1.2. ARC Sealant (C-S-H forming) Compound

Comparable to the epoxy, the ARC Sealant is a surface-applied permeability reducing treatment. ARC Sealant is a slag and crystalline silica (quartz) based hydrating mixture (two-part) that is applied to the concrete surface by spraying or brushing. This product is advertised to form C-S-H and other hydration products within the concrete pore structure, thereby reducing the permeability of the concrete surface as discussed in Section 2.4.3. Moreover, ARC sealant is a mineral coating that is applied to the concrete surfaces to protect against strong acids and hydrogen sulfide gas. The acids, such as sulfuric acid, will chemically react with the sealant to form an acid resistant shell that protects the concrete substrate. The mixture was prepared following the manufacturer's instructions and then applied to the surface with a paint roller. Two applications were applied, 30 minutes apart. The commercial name of this product has been withheld at the request of the manufacturer.

3.3.1.3. Biocide with Mortar

The biocide admixture is a 3-(Trimethoxysilyl) propyldimethyloctadecyl ammonium chloride-based admixture that is added to concrete mortar to inhibit the growth of fungal and biological films on the concrete surface and within the pore structure as discussed in Section 2.4.2. A mortar mixture was designed with a standard mixture ratio of 1:1.5:0.4 (Portland cement: sand: water, by weight). The biocide admixture was added to the concrete mixing water in accordance with the manufacturer's recommended dosage. The mortar was then applied to the surface of the coupon with an average thickness of 0.25 inches. The commercial name of this product has been withheld at the request of the manufacturer.

3.3.1.4. Free Nitric acid- via $NaNO_2$ plus H_2O_2 biocide

Comparable to the biocide with mortar, free nitric acid is used to reduce the biological sulfide oxidizing activity rate through SOB disruption, as discussed in Section 2.4.2. Free nitric acid was applied via sodium nitrite at a concentration of 40.9 gm of $NaNO_2$/liter (0.714 liter/m²). The sodium nitrite ($NaNO_2$) was applied at a controlled rate using the sprayer shown in Figure 3-15 (A). The surface was pretreated with hydrogen peroxide (0.6%) to boost the efficacy of the sodium nitrite.

3.3.2. Treatments Application on-site

Periodic site visits to the Ellsworth wet well location were required to evaluate the progression of the corrosion condition. Like the lab coupons, after the surface pH dropped below 9 and the second stage of corrosion started, the treatments were applied. The surface treatments required ambient air and concrete temperature above 4.4 °C (40 °F). Therefore, the treatments were applied in late March 2020, when the weather was favorable. The same four surface treatments used in the experimental investigation were applied to the wet well walls, at the same application rate and using the same application method.

Wearing all required PPE and suspended from a truck mounted hoist and harness, the technician was lowered with the application equipment into the wet well (Figure 3-16, A). The well's perimeter was first divided into five sections for the four treatments and control (Figure 3-16, B). The surface was pretreated with hydrogen peroxide (0.6%) to boost the efficacy of all treatments. The four treatments were successively applied using the same mixing ratios and application procedures followed in the lab (Figure 3-16, C). The epoxy and the ARC sealant were applied in two layers as recommended by the manufacturer. The sodium nitrite was applied at a controlled rate using a sprayer and at a concentration of 40.9 gm of $NaNO_2$/liter (0.714 liter/m²) as recommended by Sun et al. (2015) and Jiang et

al. (2013). The biocide was mixed with mortar and then troweled to the surface with an average thickness of ~0.25 inches.

Figure 3-16, Treatments application at Ellsworth-Ohio wet well location (pictures by Dr. Richard Deschenes).

3.4. Measurements

Following an inclusive review of several measures employed to monitor and analyze corrosion rates in wastewater infrastructure, four measuring methods were selected to determine the effectiveness of applied treatments. These approaches included the periodic measuring of surface pH, Sulfide Uptake Rate (SUR), live/dead staining, and visual inspection of both the concrete coupons and site cores. These methods are considered accurate, rapid, inexpensive, and non-destructive. The outcomes of these testing methodologies were gathered to evaluate the applicability, practicality, cost-effectiveness, and service life of different treatments.

3.4.1. Surface pH

As mentioned in Section 2.5.1, the first key indicator of any successful mitigation of MICC is the surface pH which should remain high in healthy concrete. Accordingly, a

periodic surface pH measurement procedure was performed monthly to evaluate the resistance to acidic attacks and surface pH reduction of each of the treatment methods. The surface pH of concrete coupons and cores was measured directly using an Extech surface pH meter (PH100). The surface was pre-cleaned with deionized water to remove any existing dirt, concrete sealers, or adhesive residues. Afterward, 2 ml of ultrapure water, pH ~ 7.00 ± 0.2, were dripped with a pipet on the concrete surface and allowed to equilibrate for 30 seconds. The flat surface pH electrode was then placed on the concrete surface and allowed to obtain a steady reading. The average surface pH was calculated from 3 different measurements performed at random locations on the surface of each coupon and core. The results were plotted on two separate graphs, one for the experimental coupons and the other for collected concrete cores. These graphs were then used to analyze and compare different treatment mitigation efficacy.

Figure 3-17, Surface pH measurement (pictures by Mostafa Nasr)

3.4.2. Sulfide Uptake Rate (SUR)

The chemical and biological sulfide oxidation to sulfuric acid (H_2SO_4) leads to the dissolution of the cementitious matrix, neo-formation of sulfate salts, and consequent mass loss of concrete (Grengg et al., 2018, Islander et al., 1991). Therefore, effective diminishing of the sulfide uptake rate (SUR) is essential for any successful MICC mitigation treatment.

Monitoring the H_2S uptake rates for both the concrete coupons and site cores was conducted through the SUR test documented by Sun et al., 2014. The method involved exposing concrete specimens to a specific volume of H_2S gas and then monitoring the rate at which the gas was taken up over time.

The apparatus involved a gas-tight PVC chamber used to hold a concrete coupon, H_2S data logger (AcruLog^{TM}), fan, and enough sulfuric acid to generate the desired volume of H_2S gas. The testing chamber was designed as two separate parts, a base and a cover, made of clear PVC with internal dimensions of 17.25 in. (length) X 9.85 in. (width) X 13 in (height). The data logger was used to measure and record the H_2S gas concentration (PPM), RH (%), and temperature (°C) values at 30-second intervals. The fan was controlled by a voltage regulator to maintain a constant mixing action within the chamber. Continuous agitation of the sulfuric acid was attained by running a magnetic stirrer beneath the base.

The first step of the procedure is to place the concrete specimen on the base of the chamber. The entire chamber is elevated to leave space underneath for the magnetic stirrer (Figure 3-18, A). The coupon is temporarily covered with a small PVC box suspended from the chamber ceiling. The box is placed over the specimen to prevent any exposure to the H_2S gas during the progressive gas generation. The larger PVC enclosure is placed over the base and fixed by weights to prevent any leakage (Figure 3-18, B). A small glass tube through the top is used to pipet a known volume of sodium sulfide solution into the beaker of sulfuric acid to initiate the H_2S gas generation in the chamber. Once the targeted gaseous H_2S concentration (~75 ppm) is reached, the specimen enclosure is pulled up, exposing the coupon surface to the H_2S gas environment (Figure 3-18, C). The H_2S concentration

gradually decreases over a one-hour testing period. The recorded data is later retrieved and plotted to determine the rate of change.

In each experimental, to determine the net SUR of the coupon alone, the background H_2S uptake rate (adsorbed by moist air and/or the reactor materials) was initially measured for the empty chamber and subtracted from the measured slope. After each test, the exposed surface area is measured, and the surface specific H_2S uptake rate calculated using Equation 2-2. The entire experiment is conducted under a fume hood for safety, as shown in Figure 3-18 (D).

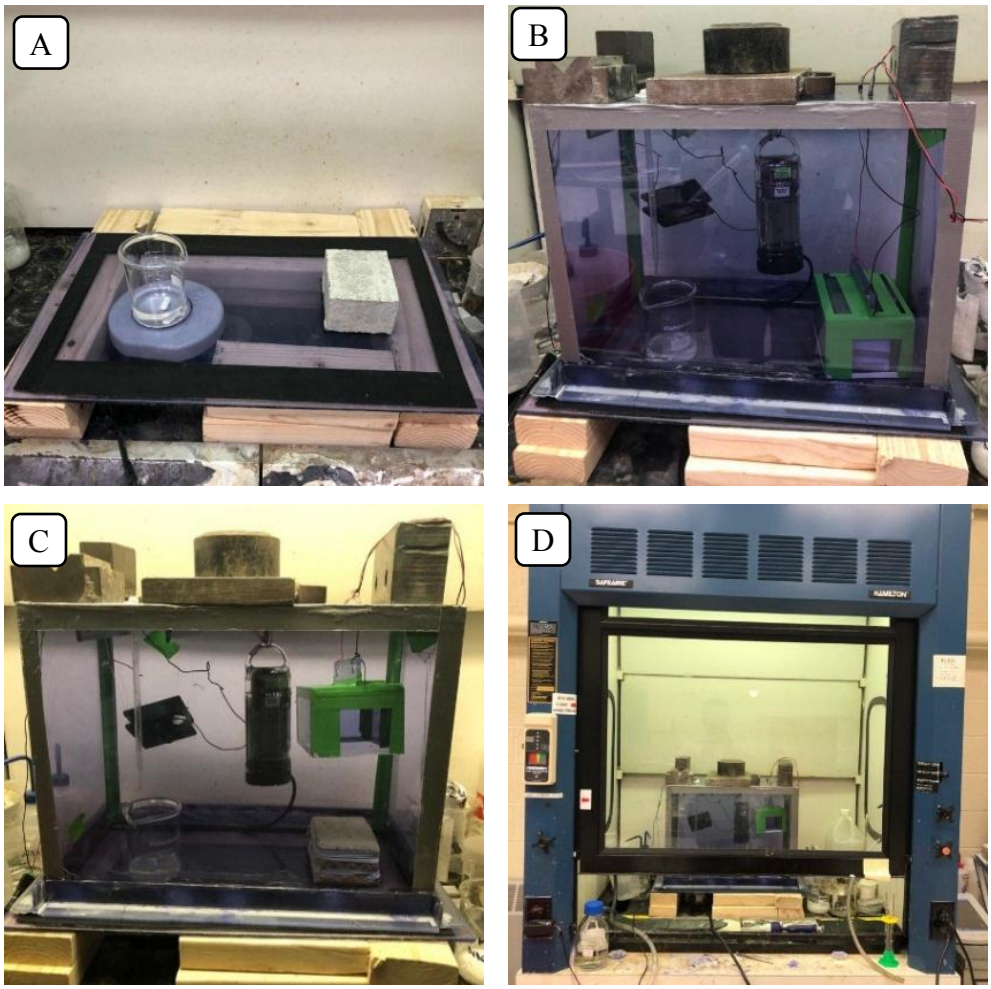

Figure 3-18, SUR test set up showing (A) PVC base with a stirrer, a beaker of H_2SO_4 acid, and coupon, (B) sealed chamber during H_2S generation with the data logger, covered specimen and fan, (C), sealed chamber during exposure of the specimen to the H_2S environment, (D) entire experiment is shown in a fume hood as required for safety (pictures by Mostafa Nasr)

The chamber was tested several times while empty to determine and minimize the average background uptake rate that occurs during chemical adsorption and oxidation of H_2S by the confined air and/or the apparatus (e.g., fan, sensor, and PVC). After several trials, the background uptake rate was successfully minimized, as discussed in Section 4.1.3. Periodic SUR tests were carried out monthly to monitor the change in H_2S uptake rates at different corrosion stages. During testing, each specimen was moved into the SUR test chamber immediately after being withdrawn from the incubation chamber to maintain the existing SOB population on the surface. For consistency between various tests, the temperature was controlled at 25 ± 1.5 ˚C, and the relative humidity was controlled at 75 ± 10 %.

3.4.3. Live/ Dead Staining

Several Live/Dead (L/D) staining trials were done to determine the viability of bacterial cells in the corrosion layers scraped from the concrete coupon surface. The process largely followed that of Sun et al. (2015), mentioned in section 2.5.3, except for the florescent microscope as a confocal laser scanning microscope was not available. Therefore, a Zeiss Axio Observer A1 inverted fluorescence microscope with a N-Achroplan 20× objective lens and Axiocam 503 CCD camera was used. The live and dead cells are imaged using FITC (Excitation/Emission: 503/530 nm) and TRITC (Excitation/Emission: 530/620 nm) filter set. After imaging, the live/dead cell counts were determined by image analysis software. The captured images were processed by quantitative image analysis to count the abundance of live or dead cells, which appear in the image as green or red pixels, respectively.

At this time, the corrosion process is moving from stage 1 to stage 2, and as such microbial growth on the surface of the concrete has not reached the levels where L/D

straining will show sufficient resolution for analysis. During the rest of stage 2 and stage 3 of corrosion, which will occur as part of the next phase of the project, L/D staining will be utilized to further understand the efficacy of the various treatment methods.

4. Chapter 4 Results and Discussion

This chapter presents a detailed and comprehensive discussion of the experimental results of all tests performed herein to evaluate the MICC mitigation measures both on-site and via experimental simulation at the lab. This research program involved continuous monitoring of MICC, treatments application, periodic testing, and data analysis for lab coupons and site cores monitored over approximately one year. During this period, coupons were exposed to an aggressive environment to simulate accelerated MICC. In the sewer wet well of Ellsworth-Ohio, MICC also advanced but at a much slower rate. Initial evaluations of the applied treatments were obtained. However, further investigations are still ongoing to cover the 3rd stage of corrosion and obtain more inclusive results. This complementary work will be done and included in a future aspect of this research program.

4.1. Lab Experiment

The progress of laboratory simulated MICC and the efficacy of treatments were periodically monitored, analyzed, and recorded, as summarized in the following section. Over a one year period, the surface pH of the upper coupons declined from an average of 10.5 down to an average of 6.5, indicating that the 2nd stage of corrosion is in progress. The surface pH of lower control coupons decreased faster and is nearing 4, indicating that stage 3 of Islander's three-step corrosion model (see Section 2.2) is initiating. Sulfide uptake rate (SUR) test results for concrete coupons are also included herein. Live/Dead staining tests will be included in future research, as the microbial growth on the surface of the concrete has not reached the levels where L/D straining will show sufficient resolution for analysis.

4.1.1. Average H_2S Gas Concentration in the Incubation Chamber

After constructing and testing the MICC incubation chamber (see Section 3.1.1), concrete coupons were placed into the chamber, and 4.0 liters of fresh wastewater added.

In February 2020, H_2S gas generation began. The gas concentration was controlled by the data-logging system (detailed in Section 3.1.6) and was also recorded every 5 minutes and logged onboard the AcruLog™ logger. Periodically, the logger was removed from the chamber and the data offloaded to a computer. The average weekly H_2S gas concentration and temperature are summarized in Figure 4-1 (data is provided in Section 7.2, Table A1).

Over the first few weeks, the H_2S concentration was low and unstable as the sodium sulfide solution flow rate and concentration were adjusted and optimized to establish a stable gas concentration. During this time, it was also discovered that the stirring of sulfuric acid was required to generate a stable gas concentration. These parameters were adjusted and refined, and then a stable concentration of H_2S was safely achieved.

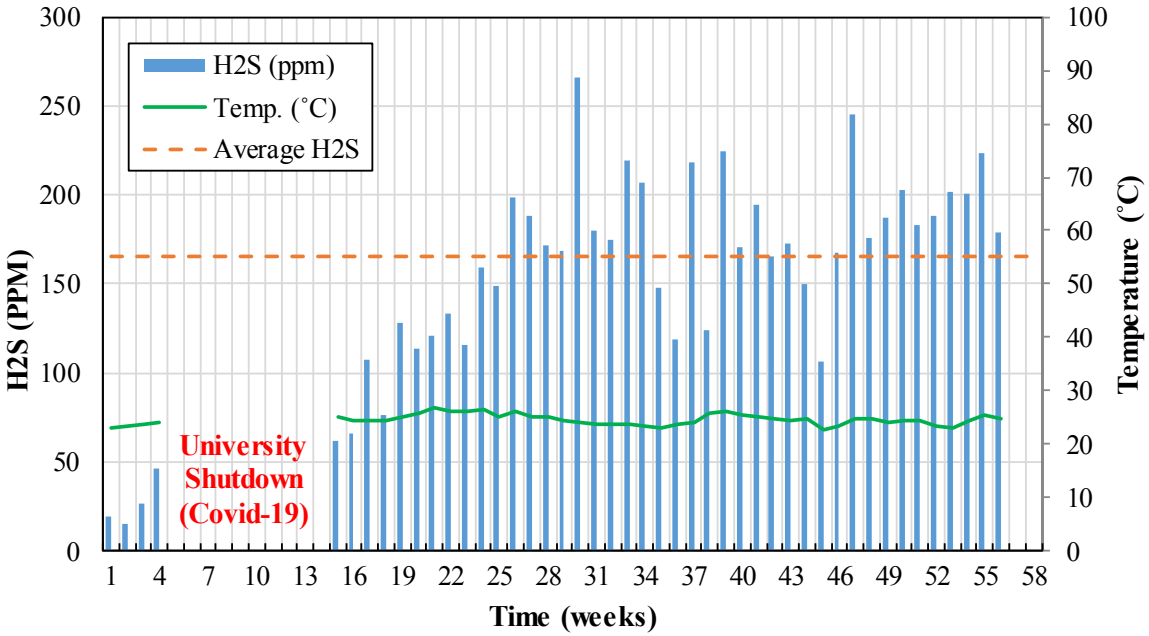

Figure 4-1, Average H_2S exposure concentration (ppm) for laboratory trials, measured using AcruLog™ H_2S gas data-logger.

In March 2020, YSU was locked down in response to the state of emergency. As access to lab facilities was prevented, the experiment was safely shut down for two months.

During this period, no H_2S generation or data collection was conducted. As the concrete coupons were not exposed to H_2S during the shutdown, the SRB and SOB species present on the concrete became dormant or died. As a result, a conditioning period was required to reestablish healthy bacteria in the concrete corrosion zone.

The experiment resumed in May 2020, and since then a stable H_2S environment has been maintained. The H_2S concentration was increased from the initially proposed concentration of ~50 PPM to accelerate the passivation of the concrete and the development of SOB biofilm. The concrete was exposed to H_2S gas concentration varying between 150 and 250 PPM throughout the following duration of the experiment. The average weekly H_2S gas concentration (the horizontal dash line in Figure 4-1) was later calculated as 165.6 PPM, which was sufficient to accelerate MICC in the chamber. Likewise, the temperature and relative humidity in the chamber were maintained at 24±1 ˚C and 95-100%, respectively, to expedite the corrosion process.

4.1.2. Surface pH for Lab Coupons

The surface pH was periodically measured for the concrete coupons following the method described in Section 3.4.1 and then tabulated as shown in Section 7.3-Appendix C, Table A3-Table A10. The initial average surface pH of the coupons was between 10.32 and 10.68, which is in line with the research published by Joseph et al. 2010. The coupons were then placed into the incubation chamber, and the MICC simulation process started. Throughout the experiment duration, surface pH was periodically measured for both the upper and lower sets of coupons. At the time of this writing, the obtained results indicate that surface pH is declining faster in the lower coupons exposed directly to wastewater than upper coupons exposed to only H_2S gas (and periodically to wastewater). Also, the surface

pH of lower coupons is nearing 4, indicating that the 3rd stage of the MICC is starting, a level where microbes will begin to thrive and MICC will accelerate.

4.1.2.1. Surface pH for Upper Coupons (exposed to humid, H_2S only)

The surface pH of the upper set of coupons, suspended on the shelf, was measured monthly and tabulated in Table 4-1. Three months after exposure, the surface pH decreased from ~10.36 to ~8.48, indicating that the second corrosion stage has started. After surface treatments were applied to the coupons, the average surface pH increased to 9.46 and 9.11 for the biocide with mortar and sodium nitrite ($NaNO_2$) treatments, respectively. The surface pH of ARC sealant also increased slightly to 8.74. However, surface pH of the epoxy treated coupons stabilized near 7.49, as the epoxy is inert in the presence of humid, H_2S gas and has an expected surface pH of ~7 (when tested using ultrapure water). On the other hand, the surface pH of the control samples continued to decrease towards 7, as no treatment was applied.

Table 4-1, Average surface pH for upper concrete coupons exposed to H_2S gas only.

Date	Month	Treatments				
		Control	Epoxy	ARC Sealant	Biocide	NaNO2
02/19/2020	0	10.33±0.06	10.44±0.16	10.34±0.17	10.36±0.11	10.32±0.17
02/19/2020	0	**H_2S gas generation started**				
07/28/2020	5	8.23±0.13	8.62±0.22	8.33±0.15	8.31±0.22	8.93±0.19
08/06/2020	5	**Treatments were applied**				
08/13/2020	6	7.27±0.10	7.49±0.08	8.74±0.25	9.46±0.13	9.11±0.10
09/10/2020	7	7.16±0.10	7.32±0.31	7.92±0.10	8.74±0.18	8.90±0.07
11/12/2020	9	6.95±0.14	6.93±0.13	7.64±0.09	8.61±0.27	9.12±0.24
12/22/2020	10	6.62±0.20	6.92±0.22	7.51±0.24	8.95±0.16	9.15±0.19
01/27/2021	11	6.41±0.29	6.87±0.27	7.40±0.27	8.64±0.25	8.85±0.18
03/15/2021	13	6.26±0.11	6.84±0.07	6.84±0.13	8.47±0.25	9.00±0.13

* ± values indicate the 95% CI of the mean (n=6).

Over the following seven months, surface pH of the control specimens continued to trend downward from 7.27 to 6.26 with a rate of -0.14 per month. Simultaneously, the surface pH of epoxy-treated specimens also trended downward but with a 36 percent slower

monthly rate of 0.09/month to reach pH 6.69 by the end of the same period. Likewise, the coupons treated with ARC sealant declined over time but with a faster rate of 0.27/ month. In the case of biocide treatment, the increase in surface pH, caused by applying the biocide through a fresh layer of mortar (pH ~10), trended down with the same rate of -0.14/month as that of the control coupons. However, the surface pH of the sodium nitrite ($NaNO_2$) treated samples has remained almost constant at ~9 with nearly zero rate of decrease throughout the same time period.

Observing the surface pH results summarized in Figure 4-2, the biocidal treatments, including the biocide in mortar and sodium nitrite ($NaNO_2$), indicated marked improvement after treatment with the pH jumping back up. However, the surface pH started for samples treated with biocide in mortar declined at the same rate as the untreated control while $NaNO_2$ remained constant. The increase in surface pH for these biocidal treatments is likely caused by killing the SOB species living on the surface of the concrete. This hypothesis will be tested through Live/Dead staining of the concrete surface, which will occur in the next part of this research program. Epoxy also performed better than the control with a 36 percent slower decline in surface pH. However, the ARC sealant was less effective and the surface pH declined faster than control. Overall, the sodium nitrite ($NaNO_2$) performed the best (89 percent slower rate of decrease in surface pH relative to the control) while ARC sealant performed worst with an 88 percent faster rate of decrease in surface pH than that of the control coupons.

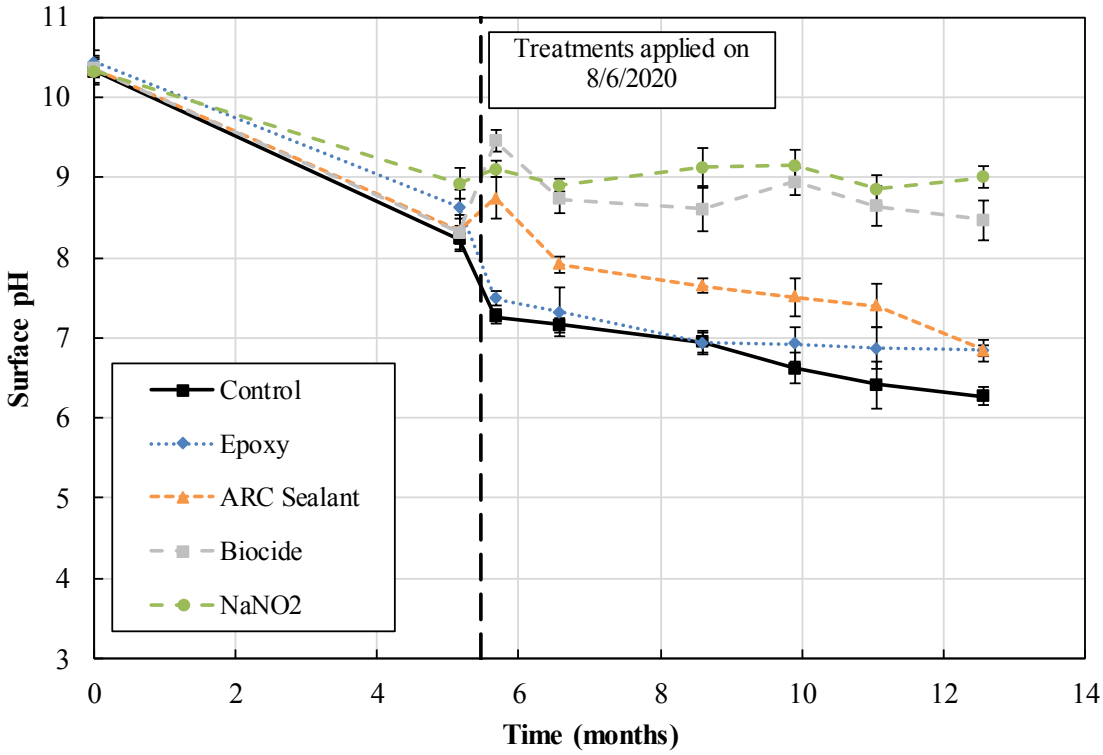

Figure 4-2, Surface pH measurements over time for laboratory upper coupons exposed to humid, H_2S gas only. Error bars indicate the 95% CI of the mean for n=6.

4.1.2.2. Surface pH for Lower Coupons (exposed to humid, H_2S gas and WW) For the lower samples (exposed to wastewater and humid H_2S gas), the surface pH trends were similar to the upper set of coupons, as shown in Table 4-2 and Figure 4-4. However, the surface pH was observed to decrease faster than in the upper coupons. This observation indicates that direct exposure to wastewater and H_2S gas together may exacerbate deterioration compared to exposure to H_2S gas, with limited exposure to wastewater. This is perhaps due to the primarily biogenic corrosion in the lower coupons as compared to primarily chemical corrosion in the upper coupons. After three months of H_2S gas exposure and frequent wastewater replenishment, the surface pH of the

specimens decreased from ~10.54 to ~7.43. This pH drop indicated the concrete surface had been neutralized by exposure to H_2S, and a biofilm of SOB has begun to grow, leading to accelerated passivation and an increasing corrosion rate.

Table 4-2, Average surface pH for lower conc. coupons exposed to H_2S gas and WW.

Date	Month	Treatments				
		Control	Epoxy	ARC Sealant	Biocide	NaNO2
02/19/2020	0	10.37±0.11	10.63±0.15	10.68±0.14	10.43±0.15	10.59±0.09
02/19/2020	0	**H_2S gas generation started**				
07/28/2020	5	7.56±0.25	7.28±0.44	7.43±0.25	7.60±0.31	7.26±0.37
08/06/2020	5	**Treatments were applied**				
08/13/2020	6	7.10±0.25	7.51±0.21	8.52±0.18	9.10±0.22	8.36±0.49
09/10/2020	7	6.81±0.23	6.97±0.60	7.69±0.28	8.88±0.20	7.47±0.51
11/12/2020	9	4.69±0.15	6.31±0.13	4.84±0.19	7.84±0.15	4.64±0.13
12/31/2020	10	4.46±0.13	5.84±0.11	4.36±0.27	7.24±0.14	4.16±0.26
01/27/2021	11	4.20±0.25	4.74±0.15	3.97±0.32	6.82±0.25	4.50±0.19
03/15/2021	13	4.05±0.16	4.69±0.29	4.25±0.16	5.92±0.13	4.48±0.17

* ± values indicate the 95% CI of the mean (n=6).

After surface treatments were applied to the coupons, the average surface pH rose to 8.52, 9.10, and 8.36 for the coupons treated with ARC sealant, biocide, and sodium nitrite ($NaNO_2$), respectively. This temporary increase in pH is due to the chemical composition of the treatments. The surface pH for coupons treated with epoxy also slightly increased to stabilize near 7.51, supporting the notion that epoxy has an expected surface pH of ~7 (when tested using ultrapure water). Control coupons, on the contrary, were the only set that sustained a lower surface pH, which decreased towards 7. An interesting observation regarding the epoxy treatment was found when testing the surface pH without first washing the exposed surface. It appears a biofilm will form on the surface of the epoxy with a low pH (< 3). However, this biofilm can be washed off by rinsing with tap water for 15 seconds, leaving the surface pH near 7. This result indicates the epoxy may prove a viable treatment option as the biofilm on the surface provides a means of stripping H_2S from the air without

harming the concrete. The biofilm contains SOB that converts H_2S into H_2SO_4, which is then converted to insoluble sulfur species. This process may provide a means of removing some of the excess H_2S from the wet well environment rather than trapping the gas in an inert system. More testing is required to determine the longevity of the epoxy when exposed to a humid, H_2S rich environment.

Over the seven months since treatments were applied, the surface pH for the control specimens continued to decline from 7.10 to 4.05. This rate of decrease in surface pH was 0.44/month in the lower control coupons, which is 3.14 times faster than that in the upper control specimens (0.14/month). This observation indicates the corrosion rate at the waterline of sewer structures, represented by lower coupons, is much higher than that occurring at the upper portion of the structure, like those observed in the crown of sewer pipes. The surface pH of epoxy-treated coupons also trended downward with a 24 percent slower rate (relative to the control) of 0.33/month to reach a pH 5.84 after five months. However, a sudden drop in the surface pH was recorded in the 6^{th} month. This decrease was accompanied by a change in color of the epoxy surface from shiny-glossy to matte texture, as shown in Figure 4-3. The change in the epoxy color might indicate that the epoxy compound has started to break down. However, the epoxy is still performing well in SUR testing, as shown in Section 4.2.3. Also, when scraping the epoxy from the surface and measuring the surface pH underneath the epoxy coating, the concrete was found to maintain a surface pH greater than 7. This indicates that epoxy is still functioning, protecting the concrete surface from acidic attacks even after losing the neutralized surface compound. Further investigation on the epoxy application method and the number and thickness of coats are highly recommended for future investigation.

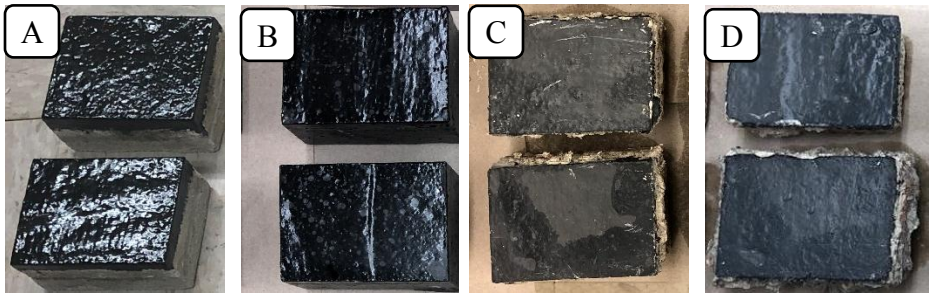

Figure 4-3, Change in surface texture color of Epoxy treatment over time (A)Freshly applied Glossy black Epoxy, (B) After 1 months of H_2S exposure, (C) After 4 months of H_2S exposure, (D) After 7 months of H_2S exposure.

The surface pH of the ARC sealant declined over time, at a faster rate of 0.61/ month, to a final surface pH of 4.25 by the end of the 7th month. Again, the biocide with mortar treatment revealed a similar rate of decrease (0.45/month) to that of the untreated control coupons (0.44/month). This similar trend could be interpreted by the assumption that the biocide has no or limited effect on the chemical oxidation, which is the primary factor leading MICC throughout the current 1st and 2nd stages. However, given that the biocide is mixed inside the applied mortar, the treatment might decrease the further invasion of SOB species into the concrete, which will hinder the biological oxidation occurring through the 3rd stage of corrosion. Similarly, sodium nitrite ($NaNO_2$) did not indicate improvement when compared to the control. For the specimens treated with sodium nitrite, the temporary increase in surface pH that was observed after treatment diminished rapidly in the first two months, and then stabilized around a pH of ~4.5. One explanation for the poor performance, could be that frequent contact with wastewater might have inactivated the sodium nitrite ($NaNO_2$) from the surface. During the second year of the experiment, different application rates and frequencies of application for the $NaNO_2$ are recommended to be evaluated to determine the most effective treatment method.

Observing the surface pH results summarized in Figure 4-4, the decrease in surface pH of the lower coupons is more severe than that recorded in the upper set of coupons. The two biocidal treatments, biocide with mortar and $NaNO_2$, again indicated a marked improvement by increasing the pH, albeit temporarily. Over time, the surface pH of the biocide treatment declined at a similar rate parallel to control, while the $NaNO_2$ declined faster. However, it is expected that the $NaNO_2$ treatment will require repeated applications to kill SOB on the surface and inhibit MICC during the upcoming third stage of corrosion. The permeability reducers, ARC sealant and epoxy, also showed a similar decreasing trend. However, epoxy performed the best, slowing the change in surface pH over time, while ARC sealant performed worse with a faster rate of decrease in the surface pH than the untreated control.

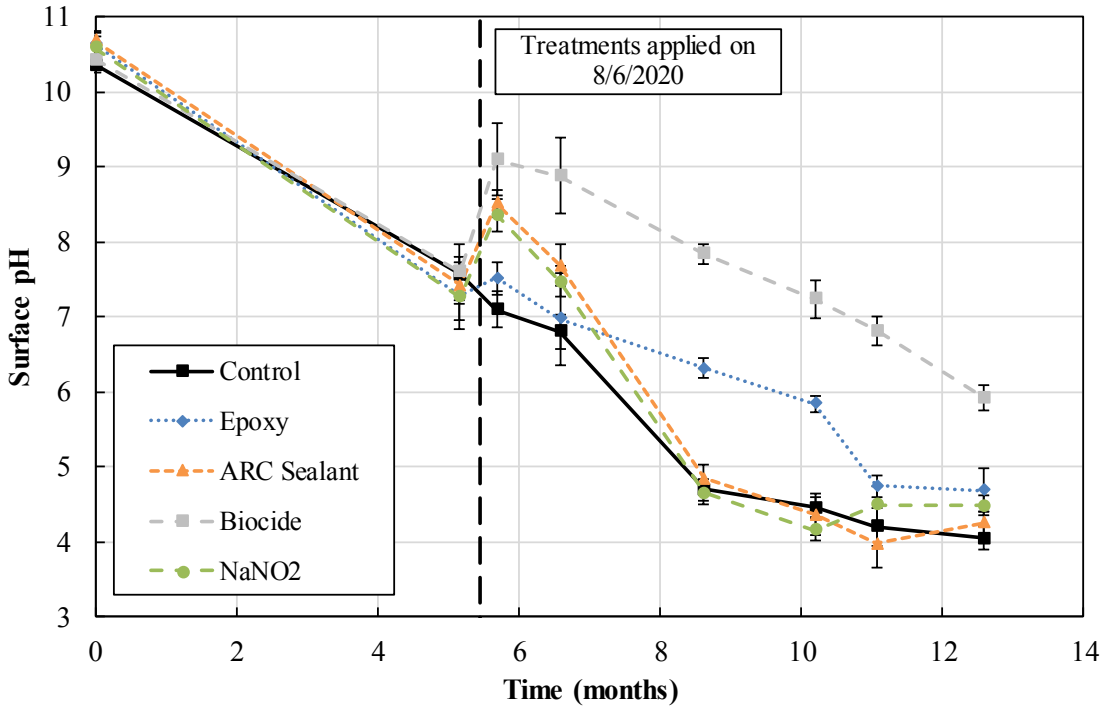

Figure 4-4, Surface pH measurements over time for laboratory lower coupons exposed to humid, H_2S gas and wastewater. Error bars indicate the 95% CI of the mean for n=6.

4.1.3. Sulfide Uptake Rate (SUR) for Lab Coupons

Sulfide uptake rates (SUR) have been periodically measured for the concrete coupons from the laboratory experiment and then tabulated and plotted as shown in Section 7.4-Appendix D, Table A11-Table A23. As discussed in Sections 2.5.2 and 3.4.2, SUR is calculated from the mass of sulfur consumed onto the exposed surface of a concrete coupon over a fixed period, using Equation 2-2. The sulfur consumed is determined from the change in H_2S concentration d[H_2S] in (PPM) after deducting the background uptake over a fixed observation period. The change in H_2S concentration was calculated as the difference between the highest initial H_2S concentration (~75 PPM) and the final concentration after a one-hour test period. In this case, the time change (dt) is 1 hour, the total gas volume in the Reactor ($V_{reactor}$) was calculated as 0.035 m^3, and the surface area of concrete is equal to the exposed surface of the concrete coupon in square meters (m^2). During the test, the temperature was maintained at 25±1˚C, and the relative humidity was also at 75±10%. Measuring the SUR for each sample required approximately 2 hours for generating the initial gas concentration, exposing the sample, and preparing the apparatus. Therefore, measuring the SUR for 5 lower coupons, 5 upper coupons, and 5 core samples required approximately 30 hours, not including the time required to collect the core samples from the wet well. Therefore, it was infeasible to conduct duplicate SUR measurements due to time and resource limitations. The SUR results presented herein do not include error bars, since duplicate measurements were not collected.

High SUR indicates a higher consumption (biological or chemical) of H_2S, which is assumed to be converted to sulfuric acid either biologically (via SOB) or chemically (interaction with surface water). Therefore, SUR is an indirect measure of the biological activity on the exposed concrete surface (so long as chemical uptake is controlled and

measured). The experimental chamber, discussed in Section 3.4.2, was designed to prevent any H_2S gas leakage and to minimize chemical uptake by the chamber materials. The chamber was tested several times without any concrete samples to determine and minimize the average background uptake rate that occurs during chemical adsorption or oxidation of H_2S into water in the confined atmosphere or the apparatus. After several trials, the background uptake rate was successfully minimized from ~9 PPM/hour to only ~4 PPM/hour (23.33 mg-S m^{-2} h^{-1}). Before each set of tests, the background UR was first measured and then subtracted from the H_2S concentration change to determine the net SUR for the specimen alone. Moreover, all sides of the lower coupons except the upper exposed surface were tightly covered with Teflon tape during testing to limit the SUR to the upper exposed surface only.

The initial SUR of the concrete coupons was measured before H_2S or wastewater exposure, and the results are summarized in Figure 4-5. The specimens C#1 and C#2 were uncoated, while specimens C#3 and C#4 were coated on all but one face with epoxy mastic. The coated specimens had a much slower SUR, as the H_2S gas had only reacted with the fresh concrete on the single exposed face. After deducting the background UR and normalizing both measurements by the exposed surface area, the average initial SUR was evaluated as 52.39 mg-S m^{-2} h^{-1} for fresh concrete. This measurement is in line with the research results published by Sun et al. 2014, as the SUR for fresh coupons was recorded as 57±4 mg-S m^{-2} h^{-1} under the same testing conditions (75ppm, 75% RH, and 25˚C). Over time, as MICC progresses on the concrete surface, an increase in the SUR was observed and recorded, as shown in the following sections. All sulfide uptake rate (SUR)

measurements presented herein are in units of mg-S m^{-2} h^{-1} (milligram of sulfur per square meter per hour)

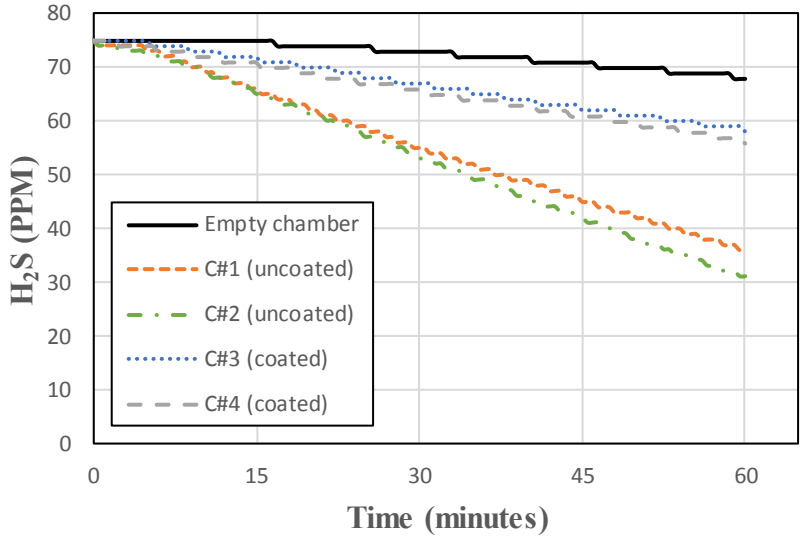

Figure 4-5, Initial sulfide uptake rate (SUR) of coupons before exposure or treatment.

4.1.3.1. SUR for Upper Coupons (exposed to humid, H_2S only)

The sulfide uptake rate (SUR) of the upper concrete coupons exposed to H_2S gas (but not directly to wastewater) was periodically measured throughout the duration of the experiment. The SUR results are summarized in Table 4-3 and Figure 4-6. Three months after exposure, the SUR of the control increased from ~52 to ~82, indicating that MICC is progressing and the 2nd stage of corrosion had started. Once surface treatments were applied to the coupons, SUR measurement for all treated specimens dropped. The epoxy treated coupons showed a significant decrease in SUR to 35.04, which is 57% lower than the control (81.77) and 33% lower than the initial SUR of fresh concrete (52.39). Similarly, the SUR of ARC sealant dropped to 58.41, while the SUR of the biocide with mortar and sodium nitrite ($NaNO_2$) decreased slightly to 70.09. The control was the only one that maintained a higher SUR of 81.77 as no treatment was applied.

Table 4-3, SUR for upper concrete coupons exposed to H_2S gas.

Date	Month	SUR (mg-S m^{-2} hr^{-1})				
		Control	Epoxy	ARC Sealant	Biocide	NaNo2
03/17/2020	0	52.39	-	-	-	-
08/06/2020	5	Treatments were applied				
08/27/2020	5	81.77	35.04	58.41	70.09	70.09
09/29/2020	7	52.88	23.50	23.50	47.00	35.25
11/16/2020	8	52.23	0.00	11.61	17.41	5.80
12/28/2020	10	81.89	35.10	46.80	52.64	58.49
01/25/2021	11	58.40	0.00	23.36	17.52	11.68
03/09/2021	12	81.65	23.33	64.15	34.99	29.16

During the seven months following treatment application, SUR measurements for all upper coupons varied over time. Consistent differences in SUR values are apparent, as shown in Figure 4-6. SUR measurements of the control specimens varied between ~52 and ~83, which were the highest recorded values among all tests. The epoxy treated coupons performed best overall with the lowest uptake rate of zero in some tests, while the highest was 35.10 in only one test, which was still 60 percent lower than that of the control at the same trial. ARC Sealant also indicated a lower uptake rate of 11.61 and 23.36 in some tests. However, a single higher measurement of 64.15 was recorded at the last test. Although the SUR reading was 22 percent lower than that of the control on the same test day, it made a significant change in the SUR trendline of the ARC sealant. In the case of the biocide in mortar, the variation in SUR measurements was between 17.52 (66 percent lower than control) and 70.09 (15 percent lower than control). Sodium nitrite ($NaNO_2$) treatment had a similar trend. The lowest SUR measurement for $NaNO_2$ was 5.8 (89 percent lower than control) while the highest was 70.09 (15 percent lower than control). It is apparent that the later SUR measurements for both biocidal treatments were lower than those recorded right after the treatment application, indicating that both treatments maintained efficacy over time.

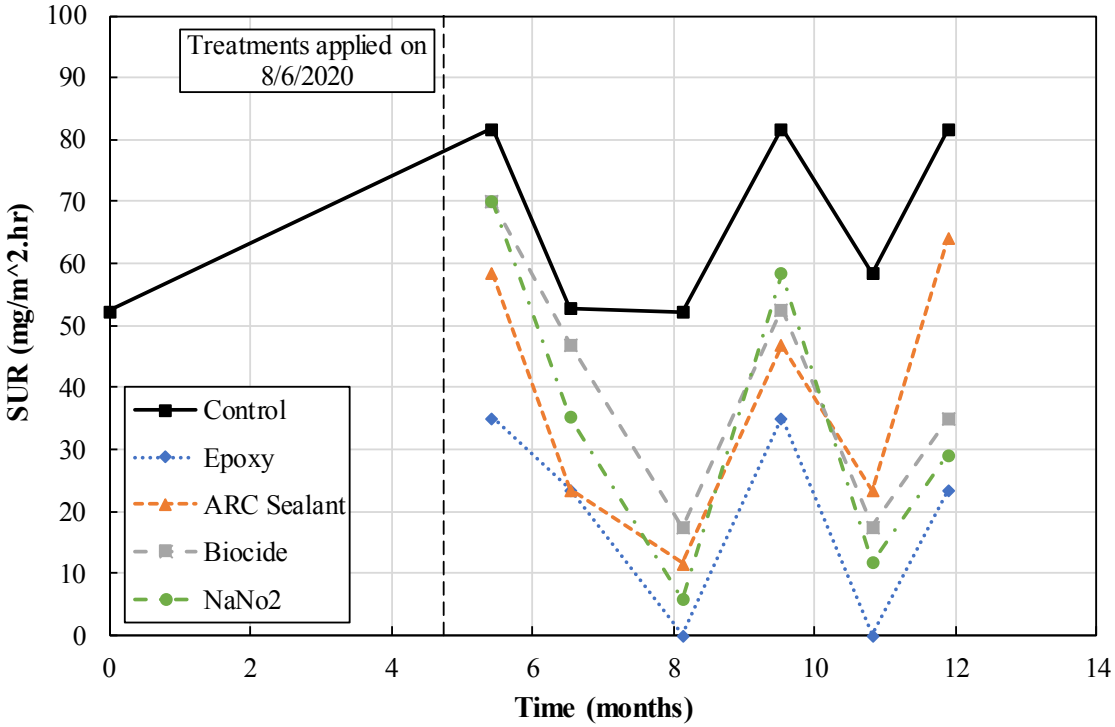

Figure 4-6, Sulfide uptake rate (SUR) over time for laboratory upper coupons exposed to humid, H_2S gas only. Error bars not included because duplicate measurements were not performed due to time and resource constraints.

Overall, all treatment options resulted in improvement when compared with the control coupons. The highest SUR was measured for the control samples, while the samples treated with epoxy indicated the most significant improvement. Epoxy treatment performed better than the fresh, never exposed concrete. During all measurement trials, the SUR of epoxy was 56-100% less than the untreated control coupons. ARC sealant also managed to reduce SUR. However, its mitigation performance appears to be decreasing over time. Likewise, biocidal treatments showed improvements as compared to the control, with the efficacy appearing to be more stable over time.

4.1.3.2. SUR for Lower Coupons (exposed to humid, H_2S gas and WW)

Sulfide uptake rates (SUR) of the lower coupons exhibited similar trends to those observed in the upper set of coupons. However, higher uptake rates and larger differences

between treatments are apparent, as shown in Table 4-4 and Figure 4-7. After four months of H_2S gas exposure and periodic replenishment of wastewater, the SUR of the control increased from ~52 to ~100, which is 47 percent higher than that of the upper coupons (52.88) after the same exposure time. The higher SUR with the lower surface pH confirms that exposure to both wastewater and H_2S gas together expedites the deterioration compared to exposure only to H_2S gas. Parallel to the results for the upper coupons, the SUR measurement for all treatments decreased immediately after treatment. The epoxy treated coupons dropped to 47.03, which is 53% lower than the control on the same test (99.94) and 10% lower than the initial SUR of fresh concrete (52.39). The ARC sealant did not show a significant enhancement, as the SUR dropped slightly by 6 percent to 94.06. SUR of the biocide with mortar and sodium nitrite ($NaNO_2$) also decreased to 76.42 and 70.54, respectively. The control was the only sample that maintained a higher SUR of 99.94 as no treatment was applied.

Table 4-4, SUR for lower concrete coupons exposed to H_2S gas and wastewater.

Date	Month	SUR (mg-S m^{-2} hr^{-1})				
		Control	Epoxy	ARC Sealant	Biocide	NaNo2
03/17/2020	0	52.39	-	-	-	-
08/06/2020	5	**Treatments were applied**				
10/15/2020	7	99.94	47.03	94.06	76.42	70.54
11/19/2020	8	201.47	15.11	65.48	191.40	156.14
12/31/2020	10	75.97	11.69	23.37	58.44	29.22
01/26/2021	11	93.37	40.85	81.70	64.19	58.36
03/10/2021	12	93.40	40.86	70.05	64.21	58.37

Throughout the months following treatment application, SUR measurements for all treatments and the control coupons varied over time, as shown in Figure 4-7. SUR measurements of the control varied between ~76 and ~201, which was the highest recorded values among all SUR tests. Once more, the epoxy treated coupons exhibited a stable decrease in SUR with lower measurements than the fresh never-exposed concrete (52.39)

in all test trials. The SUR of epoxy varied between 11.69 and 40.86, which were 85 percent and 56 percent lower than the control, respectively, as measured on the same day. SUR of ARC sealant also trended down to 65.48 and 23.37. However, the SUR measurements returned to 81.70 and 70.05 at the last two measurements. Future SUR testing will reveal if this rising trend continues.

The biocidal treatments and control samples indicated a sharp increase in SUR (November 2020 readings—8 months) that were not observed in the other two treatments. The reason for these spikes is unknown but could be explained by one of two assumptions. First, the increase might have occurred due to an error in the test measurement procedure so long as these sharp increases did not repeat in other SUR tests. Second, the results might be valid measurements that indicate the biocide and $NaNO_2$ treatments are ineffective in mitigating biofilm growth on the surface of the concrete, resulting in a healthy biofilm with greater SOB activity. The SOB activity of the biofilm is expected to fluctuate over time due to changes in temperature, average H_2S concentration, humidity, changes in wastewater characteristics, and other controlling factors. Therefore, the SUR might have increased in the control, biocide with mortar, and $NaNO_2$ specimens due to an unmeasured change in one of these factors that returned to normal levels in subsequent measurements. The most likely factor subject to changes is the wastewater characteristics as the remaining factors were controlled and measured.

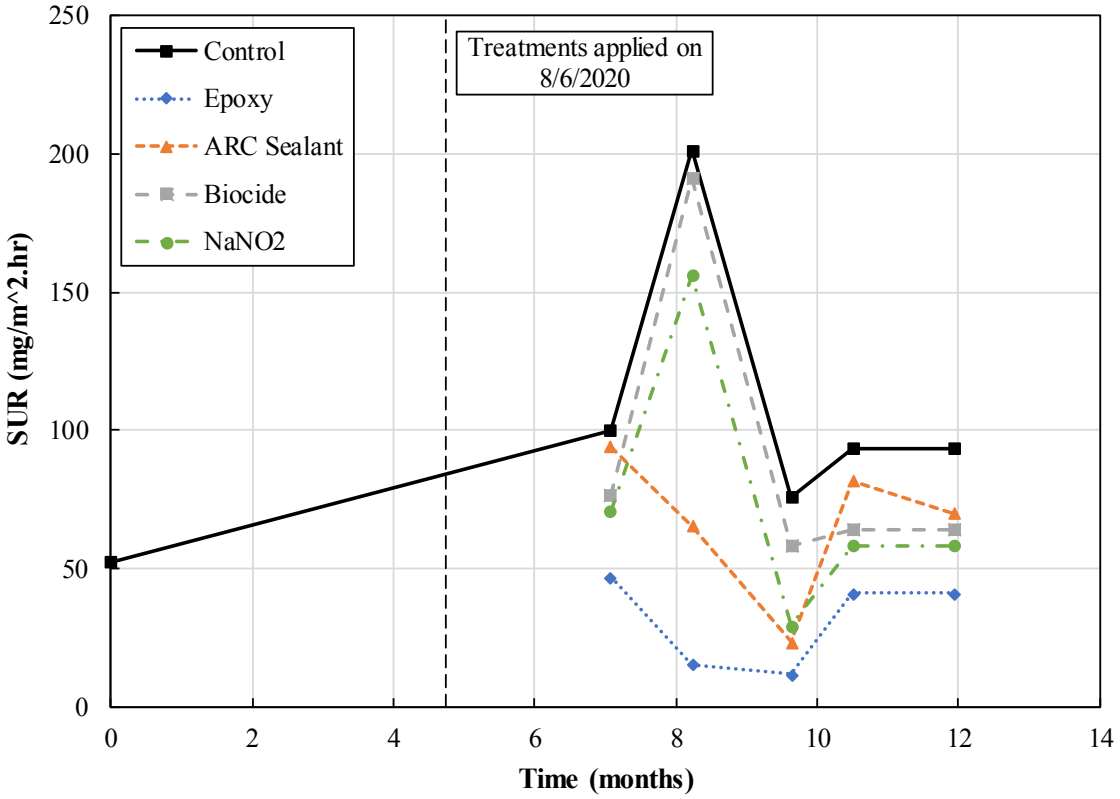

Figure 4-7, Sulfide uptake rate (SUR) over time for laboratory lower coupons exposed to humid, H_2S gas and wastewater. Error bars not included because duplicate measurements were not performed due to time and resource constraints.

A change in wastewater characteristics may affect the specimens differently as both epoxy and ARC sealant modify the surface characteristics of the concrete, thereby inhibiting bacteria ingress. At this stage, the available information is not sufficient to favor either of the two hypotheses. However, future investigation will reveal more information and confirm or disprove these hypotheses. Nevertheless, in all subsequent trials, both biocide and $NaNO_2$ performed better than the control. The SUR measurements for the biocide with mortar varied between 58.44, and 64.21, which were 23 percent, and 31 percent better than the control at the same trials, respectively. Sodium nitrite ($NaNO_2$) also performed better than the control by 62 percent and 38 percent as measured on the same date (12/31/20).

Overall, all treatment options resulted in improvement when compared with the control coupons. ARC sealant managed to control the SUR, while the samples treated with epoxy showed the most significant improvement. Once again, epoxy treatment performed better than the fresh never-exposed concrete. During all trials, the SUR of epoxy was 53-93 percent less than the control, indicating epoxy could be the best treatment option to be applied at the waterline of sewer structures found in manholes and wet wells. Likewise, biocidal treatments showed efficient improvements compared to the control. However, further investigation is required to better understand the ambiguous increase and decrease measured at 8 months.

4.2. Field Investigation Results

The same four treatments were evaluated in the field through periodic sample collection, testing, and monitoring. The test data was recorded and analyzed for the wet well location at Ellsworth-Ohio, as summarized in the following sections. The surface pH of site cores declined from ~7.8 to ~ 7.3 over 11 months, indicating that the 2nd stage of MICC is in progress. The slower on-site progress of MICC compared to the lab confirms that the laboratory simulation process expedited MICC as planned. Sulfide uptake rate (SUR) test results for site cores are also included herein. However, Live/Dead staining tests will be included in the second year of the research program, as the microbial growth on the surface of the concrete has not reached the levels where L/D straining will show sufficient resolution for analysis.

4.2.1. Average H_2S Gas Concentration at Ellsworth-OH Wet Well

After several site visits to severely corroded wet well locations, the sewer wet well in Ellsworth-Ohio was chosen for MICC monitoring and further investigation, as discussed in Section 3.2. In March 2020, the MICC site monitoring process started. The H_2S

concentration and gas-phase temperature inside the wet well were continuously measured and recorded every 5 minutes using one of the two available H_2S loggers. Every three weeks, the logger was removed from the wet well, and the data offloaded to a computer. The average weekly H_2S gas concentration and temperature for the wet well location are summarized in Figure 4-8 (raw data is provided in Section 7.2-Appendix B, Table A2).

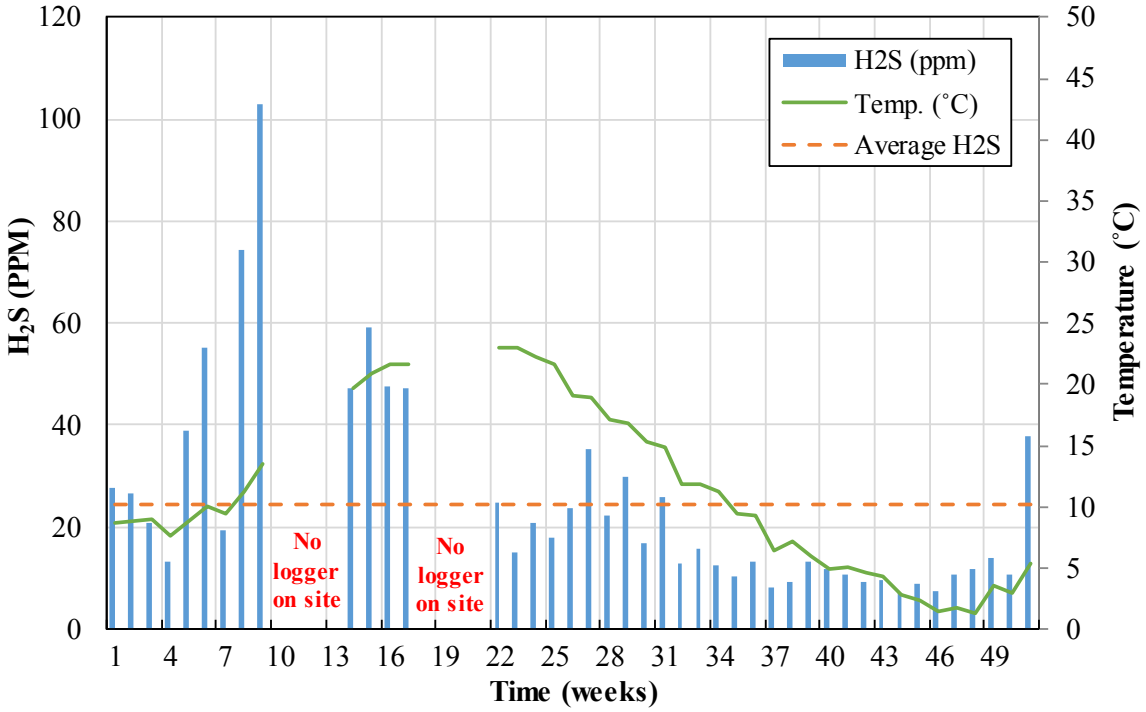

Figure 4-8, Average H_2S exposure (ppm) for the Ellsworth, Ohio wet well measured using an OdaLog LL1000, suspended at 10 feet below the wet well surface.

As previously mentioned, the OdaLog H_2S gas logger can only be exposed to an H_2S environment for 30 days at a time and then requires 10 days of fresh air. However, a long delay in delivering the replacement H_2S gas logger happened due to the Covid-19 pandemic. Therefore, there are some gaps in the record when the logger was removed from the wet well, and no replacement one was available (marked as "No logger on site").

Between March 2020 and March 2021, the H_2S gas concentration varied over time due in part to the ambient temperature and humidity conditions and changes in the wastewater characteristics. As expected, the average H_2S concentration increased in the summer months and then dropped as the weather cooled. It is also expected this trend will repeat over the next year of the program. The annual average H_2S gas concentration (represented by the horizontal dash line in Figure 4-8) was calculated as 24.6 PPM for the available data, excluding the 8 weeks gap periods. However, another calculation was done to estimate the maximum annual average of H_2S gas concentration without these data gaps. The average H_2S gas concentration of the two-month gap periods is assumed to be as high as 100 PPM; therefore, the maximum average annual could be estimated as 36.42 PPM. This overestimation is used to compare and link the MICC investigation results from the wet well to the lab simulation results.

The average H_2S gas concentration, temperature, and relative humidity in the lab chamber were maintained at ~166 PPM, 23-25˚C, and 100%, respectively. However, the estimated maximum average H_2S gas concentration, temperature, and relative humidity at the wet well were calculated and recorded as ~36 PPM, 2-23˚C, and 90-100%, respectively, during winter-summer times. The difference in these controlling factors between the lab and the site exposure conditions supports the assumption that the MICC simulation process in the lab is accelerated relative to the wet well.

4.2.2. Surface pH for Site Cores

Using the same methodology as the lab coupons, the surface pH was periodically measured for the concrete cores from the Ellsworth-OH wet well location following the method described in Section 3.4.1 and then tabulated as summarized in Section 7.5-Appendix E, Table A24-Table A29. The average surface pH of the concrete prior to

treatment was 7.79, indicating the 2nd stage of MICC is progressing in the concrete, and passivation of the concrete has occurred. Fresh concrete should have a surface pH between 12 and 13. However, exposure to H_2S has decreased the pH towards 7.79 over the past five years since the wet well concrete surface was rehabilitated with a fresh coating of mortar (0.25 – 0.4 inches thickness). Throughout the 11-month monitoring duration, the surface pH of all treatments and the control was periodically measured and tabulated, as summarized in Table 4-5 and Figure 4-9.

Table 4-5, Average surface pH for concrete cores from Ellsworth, Ohio wet well location

Date	Month	Treatments				
		Control	Epoxy	ARC Sealant	Biocide	NaNO2
02/21/2020	0	7.79±0.02	-	-	-	-
03/25/2020	1	**Treatments were applied**				
06/25/2020	4	7.68±0.08	7.62±0.25	8.06±0.26	7.92±0.22	7.65±0.22
08/20/2020	6	7.54±0.37	7.67±0.10	7.48±0.29	7.77±0.25	6.85±0.20
10/13/2020	8	7.44±0.17	7.56±0.10	6.61±0.12	7.83±0.10	6.73±0.16
12/09/2020	9	7.34±0.18	7.55±0.20	6.67±0.08	7.82±0.12	7.46±0.42
01/21/2021	11	7.33±0.15	7.54±0.19	6.63±0.11	7.66±0.17	7.46±0.22

* ± values indicate the 95% CI of the mean (n=4).

The pH measurements for the site cores were not tested during the 3 consecutive months after treatment due to the previously mentioned Covid-19 pandemic shutdown, which prevented access to lab facilities. Three months after treatment, the surface pH had increased from 7.79 to 8.06 and 7.92 for the ARC sealant and biocide with mortar, respectively. The ARC sealant appears to have an average initial surface pH of ~8.5, as it was measured in all 3 cases of the laboratory upper and lower coupons and the site cores. The increase in surface pH for the biocide with mortar treatments is likely due to the application of fresh mortar and the ability of the biocide in killing the SOB species living on the surface of concrete. The surface pH of the epoxy treated concrete cores stabilized again near 7.62, as the epoxy is inert in the presence of humid, H_2S gas and has an expected

surface pH of ~7 (when tested using ultrapure water). Sodium nitrite ($NaNO_2$), on the other hand, exhibited a comparable decreasing trend to 7.65 to that of the control, indicating that $NaNO_2$ had no immediate mitigation effect on the surface pH.

Over the following seven months, the surface pH of the control continued to trend downward from 7.68 to 7.33 with a decreasing rate of 0.05/ month. Concurrently, the surface pH of epoxy treated cores also trended downward but with an 80 percent slower rate of 0.01/month to reach pH 7.54 by the end of the same period. Again, the cores treated with ARC sealant declined over time with the fastest rate of 0.2/month. The temporary increase in surface pH of biocidal treatments, which had occurred after treatment application, reversed and trended back down at a relatively slower rate than the control. Surface pH of the biocide with mortar declined at a rate of ~0.04/month (26 percent slower than control), while $NaNO_2$ declined at a rate of 0.03/ month (46 percent slower pH rate than the control).

Overall, by observing the surface pH results summarized in Figure 4-9, the ARC sealant and biocide with mortar indicated a slight improvement after treatment with the pH jumping back up. However, the surface pH of the ARC treatment declined faster than the untreated control. Biocidal treatments and epoxy revealed a slower change in surface pH, with the epoxy performing best (80 percent slower rate of decrease in surface pH as compared to the control). The ARC sealant performed worse, with a rate of decrease in pH 309 percent faster pH than the control.

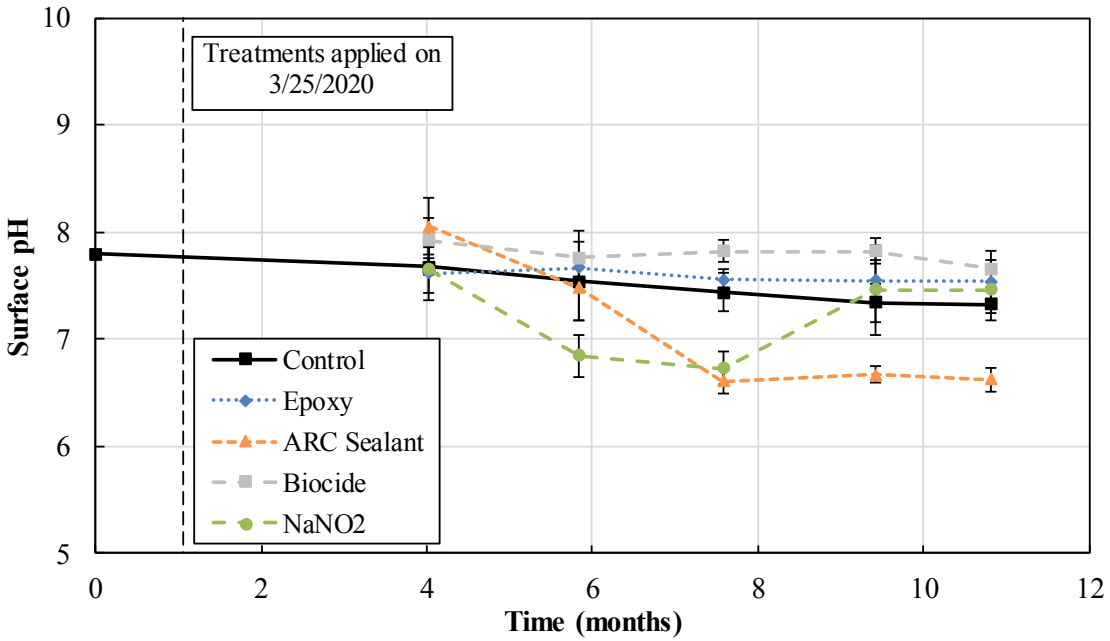

Figure 4-9, Surface pH measurements over time for concrete cores from Ellsworth, Ohio wet well location, Error bars indicate the 95% CI of the mean for n=4.

4.2.3. Sulfide Uptake Rate (SUR) for site cores

Following the same procedure used for the lab coupons, sulfide uptake rates (SUR) have been periodically measured for concrete cores collected from the Ellsworth, Ohio wet well location following the method described in Sections 2.5.2 and 3.4.2. The SUR results were then tabulated and plotted as shown in Section 7.6, Table A30-Table A33. SUR was also calculated using Equation 2-2. All the variables, including $d[H_2S]$, dt, $V_{reactor}$, etc., were evaluated in the same manner mentioned in Section 4.1.3. However, due to the smaller surface area for the core samples, as compared to the concrete coupons, two core samples (per treatment) are tested in the SUR reaction chamber at the same time. Therefore, the surface area of the specimen (S_{area}) is equal to the total exposed surface area of two concrete cores placed together into the testing chamber.

During all SUR tests, the temperature was again controlled at 25±1˚C, and the relative humidity was maintained at 75±10%. The background uptake rate was also minimized from ~9 PPM/hour to only ~4 PPM/hour (23.33 mg-S m^{-2} h^{-1}). In each set of tests, the background uptake rate was also measured and then subtracted from the H_2S concentration change to determine the net SUR for the specimen alone. Furthermore, all sides but the upper exposed surface of the cores were painted with epoxy to limit SUR measurement to the upper exposed surfaces only. Although core samples were collected on February 21, 2020, the SUR was not measured immediately after sample collection due to complications arising during COVID-19. As such, the initial SUR of the untreated concrete was assumed to be approximately 58 mg-S m^{-2} h^{-1} based on the average SUR from samples measured after the laboratory reopened. This approximate value falls in line with SUR values from core samples collected on April 22, 2020. All upcoming sulfide uptake rate (SUR) results presented herein are in units of mg-S m^{-2} h^{-1} (milligrams of sulfur per meter squared per hour).

Sulfide Uptake Rates (SUR) of the concrete cores from the wet well indicated comparable trends to the lab coupons. However, the SUR trends were more uniform, and fewer disparities are apparent, as shown in Table 4-6 and Figure 4-10. After two months of monitoring, the SUR of the control increased from ~58 to ~81, indicating that MICC is progressing as expected. However, after treatment, the SUR regressed to an increasing trend for all four treatments. The epoxy dropped after treatment to 40.38, which is 50 percent lower than the control and 31 percent lower than the initial SUR (58). Comparable to the results for the lower coupons evaluated in the laboratory, ARC sealant did not show a significant enhancement after treatment. The SUR measurement for ARC sealant dropped

slightly to 64.61, which is only 20 percent lower than the SUR of control on the same test run (80.76). However, the SUR of biocide with mortar performed better and declined to 48.45 (40 percent better than control). In the case of sodium nitrite ($NaNO_2$), a moderate drop occurred, as the SUR decreased to 56.53 (30 percent better than control on the same test run).

Table 4-6, SUR for concrete cores from Ellsworth, Ohio wet well location

Date	Month	SUR (mg-S m^{-2} hr^{-1})				
		Control	Epoxy	ARC Sealant	Biocide	NaNO2
02/21/2020	0	58.15	-	-	-	-
03/25/2020	1	**Treatments were applied**				
04/22/2020	2	80.76	40.38	64.61	48.45	56.53
10/20/2020	8	95.67	20.09	95.67	76.53	95.67
12/17/2020	10	163.20	0.00	113.80	79.22	123.07
01/27/2021	11	191.12	59.56	121.55	84.19	97.32

During the 10 months following treatment, SUR measurements for site cores also fluctuated over time. However, an overall increasing trend was apparent for the control samples and all treated samples, except for the epoxy. The SUR of the control cores increased consistently from ~81 to ~191, which were the highest values in all tests. Once again, the epoxy performed the best, with the lowest uptake rate of zero in some tests, while the highest (59.56) was nearly equal to the initially recorded SUR measurement at the beginning of monitoring (58.15) and 69 percent better than control on the same test run. This performance indicates that the epoxy has a significant capability to mitigate or even stop the severe effects of MICC on concrete in real world situations. ARC Sealant, on the contrary, was less effective with an increasing trendline and SUR measurements varying between ~96 and ~122 (0-36 percent lower SUR than control). SUR of the biocide with mortar also increased over time but slower compared to the control. The SUR measurements varied between 76.53 (20 percent lower than control) and 84.19 (66 percent

lower than control). Sodium nitrite ($NaNO_2$) treatment also indicated similar variation in the trend. The SUR measurement for $NaNO_2$ varied between 95.67 and 97.32, which were 0- 49 percent lower than control on the same trials. Some variations in SUR are expected due to changes in temperature, humidity, wastewater constituents, and other unmeasured variables. Therefore, a smooth trend is not expected.

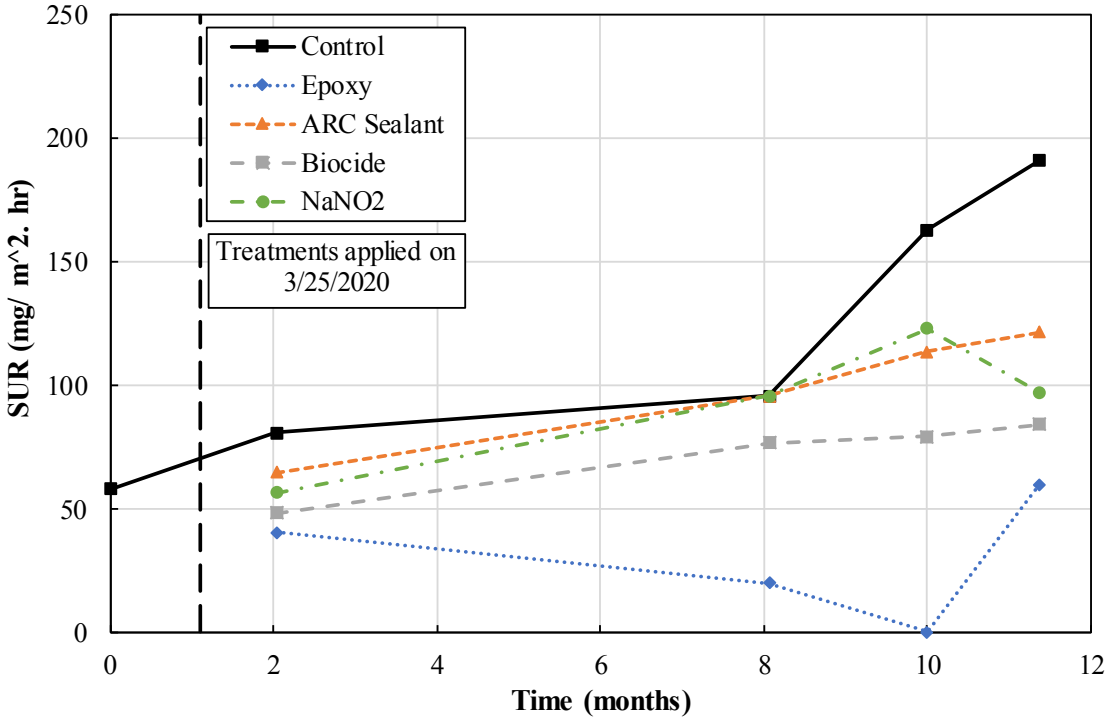

Figure 4-10, Sulfide Uptake Rate (SUR) over time for field concrete cores from Ellsworth, Ohio wet well location. Error bars not included because duplicate measurements were not performed due to time and resource constraints.

Overall, all treatment options resulted in improvement when compared with the control. The results from the wet well indicate higher overall SURs for all treatments and the control, as compared to the epoxy treatment, which showed an improvement. ARC sealant revealed a marginal improvement relative to the control. During all trials, the SUR of epoxy was equal or less than the initial SUR at the beginning of monitoring and 69-100 percent

less than the control, indicating epoxy has a magnificent capacity to mitigate or even stop MICC. The biocide with mortar treatment also revealed a marked improvement compared to the control, while $NaNO_2$ showed a moderate improvement. Again, the SUR will have to be measured periodically to assess changes over a longer period before any final conclusions are made on the better performing treatment.

4.3. Synthesis

Throughout the experiment, concrete coupons were exposed to a severely corrosive MICC environment than that in the wet well at Ellsworth, Ohio. The average H_2S gas concentration, temperature, and relative humidity in the simulation chamber were maintained at ~166 PPM, 23-25˚C, and 100%, respectively. However, the maximum average H_2S gas concentration, temperature, and relative humidity at the wet well were calculated and recorded as ~36 PPM, 2-23˚C, and 90-100%, respectively. The higher exposure conditions in the lab accelerated the passivation of the concrete and the development of SOB biofilm in the chamber, which was sufficient to accelerate MICC compared to that occurring in the sewer wet well. Accordingly, the surface pH diminishing rate of upper control coupons (0.14/month) was three times faster than that in wet well (0.04/month).

Periodic measurements also revealed the surface pH decreases faster in the lower control coupons than in the upper control coupons. This observation indicates exposure to wastewater and H_2S gas together exacerbate deterioration compared to exposure only to H_2S gas. The rate of decrease in surface pH in the lower coupons (0.44/month) was faster than that in the upper control (0.14/month), denoting the corrosion rate at the waterline of sewer structures may also be up to ~3 times higher than that occurring at the upper portion of the structure, like the crown of sewer pipes. Figure 4-11 illustrates the MICC progress

on the laboratory coupons after 1, 4, and 7 months from the treatment application. Periodic visual inspection indicates the concrete deterioration on the surface of lower coupons is faster than that on the surface of lower coupons.

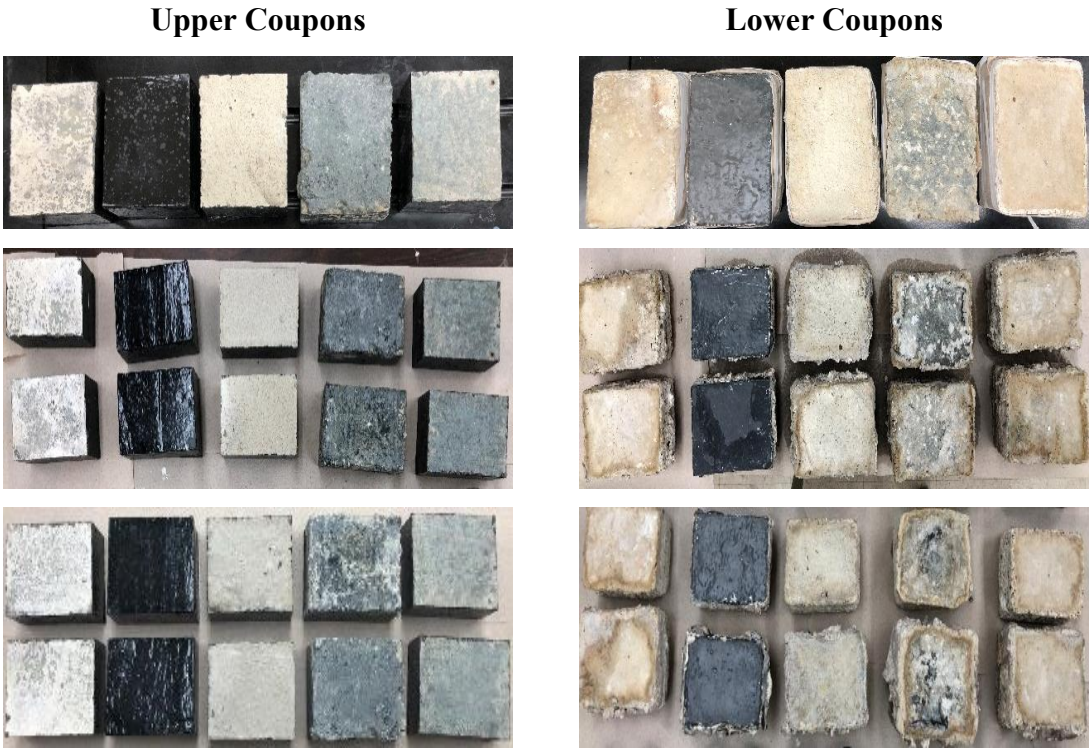

Figure 4-11, MICC progress after 1, 4 and 7 months from treatment application on upper coupons exposed to H_2S gas only (left side) and lower coupons exposed to H_2S gas and WW (right side) (pictures by Mostafa Nasr).

As previously mentioned, maintaining a high surface pH is a fundamental indicator for any successful MICC mitigation treatment. Also, effective control or decrease of the sulfide uptake rate (SUR) is essential for effective MICC mitigation. Therefore, periodic testing for the surface pH and SUR was conducted to monitor the performance of each treatment in mitigating MICC. A quantitative mitigation performance matrix was utilized to evaluate the overall performance of each treatment compared to the control, which is summarized in Table 4-7. However, it is unclear how surface pH should be weighted as

compared to SUR. Therefore, the ranking should serve only as a numerical comparison and not a final ranking of overall performance.

Table 4-7, Quantitative mitigation performance matrix of results.

Treatment	Surface pH declining rate (%)				SUR (%)				Overall (%)	Rank
	Upper coupons	Lower coupons	Site cores	**pH rank**	Upper coupons	Lower coupons	Site cores	**SUR Rank**		
Control	0	0	0	#	0	0	0	#	**0**	#
Epoxy mastic	+36	+8	+77	**1**	+71	+72	+77	**1**	**+57**	**1**
ARC sealant	-88	-40	-308	**4**	+44	+41	+25	**3**	**-54**	**4**
Biocide w/ mortar	-2	-4	+26	**3**	+41	+19	+46	**4**	**+21**	**3**
$NaNO_2$	+89	-27	+46	**2**	+49	+34	+30	**2**	**+37**	**2**

The rate of decline in surface pH of each treatment was calculated by normalizing the difference between the first and last pH reading, taken after treatment application, by the difference between the first and last reading of the control over the same period. SUR percent performance of each treatment was also calculated by normalizing the sum of SUR measurements taken after treatment application by the sum of all SUR measurements of the control over the same period. Therefore, the control performance was given the value zero as the reference line, while treatments are either +ve % or -ve %, depending on their performance rate vs. control. Accordingly, +ve % of surface pH change rate indicates slower declining pH rate than control (better performance). Similarly, +ve % of SUR indicates a lower uptake rate than control (better performance). Finally, the surface pH and SUR performance for upper, lower, and site samples were combined to evaluate the overall qualitative performance of each treatment against the control.

Overall, all surface treatments performed better than control in the SUR test. All surface treatments also performed better than control in surface pH, except for ARC sealant which indicated a faster decrease in surface pH than control. Epoxy mastic performed the best, with a significant overall mitigation performance of +57 percent. However, this performance evaluation could be increased, considering the actual surface pH of the concrete covered underneath the epoxy coat is much higher than that measured on top of the epoxy. The sodium nitrite ($NaNO_2$) and biocide with mortar ranked 2nd and 3rd performers, respectively, with overall mitigation performances of +37 percent and +21 percent. ARC sealant was the worst performer treatment with an overall performance of -54 percent. However, this performance could also increase if the concrete underneath maintains a high surface pH, which will be verified in the second year of the research program.

5. Chapter 5 Conclusions and Recommendations

5.1. Synopsis

The aim of this study was to extend the service life of wastewater infrastructures by investigating a series of mitigation strategies to control MICC in concrete sewers. The scope of the study consisted of evaluating the efficacy of mitigation measures to slow or inhibit MICC by controlling sulfide oxidation rates and concrete permeability using surface treatments. Permeability reducing surface treatments (epoxy mastic and ARC sealant) and surface applied biocidal treatments (biocide with mortar and sodium nitrite $NaNO_2$) were evaluated in a controlled laboratory experiment, where MICC conditions were simulated. The results obtained from the laboratory investigation were validated in a concrete wet well. Finally, the mitigation efficacy of the applied treatment was evaluated using periodic measurements of surface pH and SUR, while the Live/ Dead staining test will be utilized at the latter stages of corrosion during the second year of the research program.

5.2. Conclusions

Validation of the data included herein will require an additional year or more years of investigation. However, based on the first year of monitoring and data collection, some preliminary conclusions are provided:

1. The more aggressive environmental conditions in the lab accelerated the passivation of the concrete surface and the development of SOB biofilm in the chamber, which was sufficient to accelerate MICC compared to that occurring in the sewer wet well. The rate at which surface pH diminished for the upper control coupons (0.14/month), which was three times faster than that in wet well (0.04/month). In other words, one year of MICC laboratory simulation is considered equivalent to approximately 3 years in Ellsworth, Ohio wet well location.

2. Exposure to wastewater and H_2S gas together exacerbate deterioration compared to exposure to H_2S without direct exposure to wastewater. The rate at which surface pH diminished in the lower coupons (0.44/month) was approximately three times faster than that in the upper control (0.14/month). As a result, the corrosion rate at the waterline of sewer structures may be up to 3 times higher than that occurring at the upper portion of the structure, like the crown of sewer pipes.
3. The epoxy may prove a viable treatment option as the biofilm on the surface provides a means of stripping H_2S from the air without harming the concrete. The biofilm contains SOB that convert H_2S into H_2SO_4, which is then converted to insoluble sulfur species. This process may provide a means of removing some of the excess H_2S from the wet well environment rather than trapping the gas in an inert system.
4. All surface treatments performed better than the control in the SUR test. The SUR measurements for all treatments decreased immediately after treatment. Moreover, through the following months of the treatment application, the lab coupons and site cores of all treatments maintained a lower SUR measurement over time than the untreated control.
5. All surface treatments performed better than control in the surface pH test, except for ARC sealant which indicated a faster decrease in surface pH than control. Given that the ARC sealant can be used in conjunction with the biocide, it may prove more effective when a fresh coat of mortar. The mortar should be applied to the concrete with biocide included, followed by surface treatment with the ARC sealant. Together these treatments will inhibit growth of the biofilm and inhibit bacteria transport into the concrete.

6. Epoxy mastic performed the best, with a significant overall mitigation performance of +57 percent compared to the untreated control. Moreover, this performance evaluation could be increased, considering the actual surface pH of the concrete covered underneath the epoxy coat is much higher than that measured on top of the epoxy.
7. Sodium nitrite ($NaNO_2$) performed the second, with an overall mitigation performance of +37 percent compared to the untreated control.
8. The biocide with mortar performed the third, with an overall mitigation performance of +21% compared to the untreated control.
9. ARC sealant was the worst performer treatment with an overall performance of -54 percent. However, this performance could also increase if the concrete underneath maintains a high surface pH, which should be verified in the second year of the research program.

5.3. Recommendations for Future Work

Through the first year of experimental observations, results validation, and preliminary conclusions, the following recommendations are provided for future investigation.

1. Periodic Live/Dead staining tests should be performed once Stage-3 deterioration initiate in the concrete. The L/D staining is a crucial indicator to evaluate the efficacy of treatments in slowing or inhibiting microbial growth on the biofilm. Live/Dead staining is used, especially in later corrosion stages, to quantify the amount of living and dead bacteria present in the biofilm after treatment application.
2. Further investigation on the practical application method of epoxy and the number and thickness of coats requires further investigation. The difficulty of preparing the concrete surface for epoxy coating due to the damped condition of deteriorated concrete is the main constraint. Coatings may not bond to the existing concrete

structure unless the corroded concrete is entirely removed by pressure washing, which increases the overall mitigation cost. Moreover, more testing is required to determine the longevity of the epoxy when exposed to humid, aggressive H_2S environments.

3. The duration between application and frequencies of application of the free nitric acid treatment via sodium nitrite ($NaNO_2$) and hydrogen peroxide (H_2O_2) requires further investigation to confirm the short and long-term effects on controlling SOB species on the surface of the concrete. Sodium nitrite ($NaNO_2$) is considered a feasible, cost-effective treatment option: however, the longevity and durability of each application trial needs more investigation.
4. Future investigations should include multiple wet wells for better validation of the results. The Meadowood Circle, Ohio wet well location could be considered a possible location for future rehabilitation and validation of the best performing treatment method.

6. References

Alexander, M., Bertron, A., De Belie, N. (2013). Performance of Cement-based Materials in Aggressive Aqueous Environments, first ed. Springer, Ghent.

Alexander, M., Goyns, A., Fourie, C., 2008. Experiences with a full-scale experimental sewer made with CAC and other cementitious binders in Virginia, South Africa. *Proceedings of the Centenary Conference on Calcium Aluminate Cements*. IHS, Avignon, pp. 279-292.

Berger, C., Falk, C., Hetzel, F., Pinnekamp, J., Roder, S., Ruppelt, J. (2016). State of the Sewer System in Germany : Results of the DWA survey 2015. KA - Korrespondenz Abwasser. Abfall 1, 26-41.

Berndit, M.L. (2011). Evaluation of coatings, mortars and mix design for protection of concrete against sulphur oxidising bacteria. *Construction and Building Materials*, 25(10), 3893-3902.

Cayford, B.I., Dennis, P.G., Keller, J., Tyson, G.W., Bond, P.L. (2012). High-throughput amplicon sequencing reveals distinct communities within a corroding concrete sewer system. *Applied Environmental Microbiology* 78 (19), 7160-7162.

Chen, K.Y., and Morris, J.C. (1972). Kinetics of oxidation of aqueous sulfide by oxygen. *Environmental Sciences & Technol*ogy, 6 (6), 529-537.

De Belie, N., Monteny, J., Beeldens, A., Vincke, E., Van Gemert, D., Verstraete, W. (2004). Experimental research and prediction of the effect of chemical and biogenic sulfuric acid on different types of commercially produced concrete sewer pipes. *Cement and Concrete Research*, 34, 2223-2236.

De Muynck, W., De Belie, N., Verstraete, W. (2009). Effectiveness of admixtures, surface treatments and antimicrobial compounds against biogenic sulfuric acid corrosion of concrete. *Cement and Concrete Composites*, 31(3), 163-170.

Firer, D., Friedler, E., Lahav, O. (2008). Control of sulfide in sewer systems by dosage of iron salts: comparison between theoretical and experimental results, and practical implications. *Science of the Total Environment* 392 (1), 145-156.

Ganigue, R., Gutierrez, O., Rootsey, R., Yuan, Z. (2011). Chemical dosing for sulfide control in Australia: an industry survey. *Water Research*, 45 (19), 6564-6574.

Gomez-Alvarez, V., Revetta, R.P., Domingo, J.W. (2012). Metagenome analyses of corroded concrete wastewater pipe biofilms reveal a complex microbial system. *BMC Microbiology*, 12, 122.

Grengg, C., Mittermayr, F., Baldermann, A., Böttcher, M.E., Leis, A., Koraimann, G., Grunert, P., Dietzel, M. (2015). Microbiologically induced concrete corrosion: a case study from a combined sewer network. *Cement and Concrete Research*, 77, 16-25.

Grengg, C., Mittermayr, F., Koraimann, G., Konrad, F., Szab_o, M., Demeny, A., Dietzel, M. (2017). The decisive role of acidophilic bacteria in concrete sewer networks: a new model for fast progressing microbial concrete corrosion, *Cement and Concrete Research*, 101, 93-101.

Grengg, C., Mittermayr, F., Ukrainczyk N., Koraimann, G., Sabine Kienesberger, S., Dietzel, M. (2018). Advances in concrete materials for sewer systems affected by microbial induced concrete corrosion. A review. *Water Research*, 134, 341-352.

Grengg, C., Müller, B., Staudinger, C., Mittermayr, F., Breininger, J., Ungerböck, B., Borisov, S.M., Mayr, T. and Dietzel, M. (2019). High-resolution optical pH imaging of concrete exposed to chemically corrosive environments. *Cement and Concrete Research*, 116, pp.231-237.

Gutierrez, O., Mohanakrishnan, J., Sharma, K.R., Meyer, R.L., Keller, J., Yuan, Z. (2008). Evaluation of oxygen injection as a means of controlling sulfide production in a sewer system. *Water Research*, 42, 4549-4561.

Gutierrez, O., Park, D., Sharma, K.R., Yuan, Z. (2009). Effects of long-term pH elevation on the sulfate-reducing and methanogenic activities of anaerobic sewer biofilms. *Water Research*, 43 (9), 2549-2557.

Gutierrez, O., Sudarjanto, G., Ren, G., Ganigue, R., Jiang, G., Yuan, Z. (2014). Assessment of pH shock as a method for controlling sulfide and methane formation in pressure main sewer systems. *Water Research*, 48, 569-578.

Gutiérrez-Padilla, M.G.D., Bielefeldt, A., Ovtchinnikov, S., Hernandez, M., Silverstein, J. (2010). Biogenic sulfuric acid attack on different types of commercially produced concrete sewer pipes. *Cement and Concrete Research* , 40, 293-301.

Haile, T., and Nakhla, G. (2010). The inhibitory effect of antimicrobial zeolite on the biofilm of acidithiobacillus thiooxidans. *Biodegradation,* 21 (1), 123-134.

Herisson, J., van Hullebusch, E.D., Moletta-Denat, M., Taquet, P., Chaussadent, T. (2013). Toward an accelerated biodeterioration test to understand the behavior of Portland and calcium aluminate cementitious materials in sewer networks. *International Biodeterioration and Biodegradation,* 84, 236-243.

Islander, B.R.L., Devinny, J.S., Member, A., Mansfeld, F., Postyn, A., Shih, H. (1991). Microbial ecology of crown corrosion in sewers. *Journal of Environmental Engineering*, 117, 1991, 751-770.

Jensen, H.S., Lens, P.N.L., Nielsen, J.L., Bester, K., Nielsen, A.H., Hvitved-Jacobsen, T., Vollertsen, J. (2011). Growth kinetics of hydrogen sulfide oxidizing bacteria in corroded concrete from sewers. *Journal of Hazardous Materials*, 189 (3), 685-691.

Jiang, G., Gutierrez, O., Sharma, K.R., Keller, J., Yuan, Z. (2011a). Optimization of intermittent, simultaneous dosage of nitrite and hydrochloric acid to control sulfide and methane production in sewers. *Water Research,* 45 (18), 6163-6172.

Jiang, G., Gutierrez, O., Yuan, Z. (2011b). The strong biocidal effect of free nitrous acid on anaerobic sewer biofilms. *Water Research*, 45 (12), 3735-3743.

Jiang, G., Keating, A., Corrie, S., O'halloran, K., Nguyen, L., Yuan, Z. (2013). Dosing free nitrous acid for sulfide control in sewers: results of field trials in Australia. *Water Research*, 47(13), pp.4331-4339.

Jiang, G., Sun, X., Keller, J., Bond, P.L. (2015). Identification of controlling factors for the initiation of corrosion of fresh concrete sewers. *Water Research*, 80, 30-40.

Jiang, G., and Yuan, Z. (2013). Synergistic inactivation of anaerobic wastewater biofilm by free nitrous acid and hydrogen peroxide. *Journal of Hazardous Materials, 250*, 91-98.

Jiang, G., Zhou, M., Chiu, T.H., Sun, X., Keller, J., Bond, P.L. (2016). Wastewater-enhanced microbial corrosion of concrete sewers. *Environmental Science and Technology,* 50, 8084-8092

Joseph, A.P., Keller, J., Bond, P.L. (2010). Examination of concrete corrosion using a laboratory experimental set up simulating sewer conditions. In: *6th International Conference on Sewer Processes and Networks*. Surfers Paradise, Gold Coast, Australia.

Joseph, A.P., Keller, J., Bustamante, H., Bond, P.L. (2012). Surface neutralization and H2S oxidation at early stages of sewer corrosion: influence of temperature, relative humidity and H2S concentration. *Water Research*, 46, 4235-4245.

Kakade, A.M. (2014). Measuring concrete surface pH-A proposed test method. *Concrete Repair Bulleting,* pp.16-20.

Li, X., Jiang, G., Kappler, U., Bond, P. (2017). The ecology of acidophilic microorganisms in the corroding concrete sewer environment. *Frontiers in Microbiology,* 8, 683

Matthews, J.C., Selvakumar, A., Sterling, R.L., Condit, W. (2014). Innovative rehabilitation technology demonstration and evaluation program. *Tunnelling and Underground Space Technology,* 39, 73-81.

Millero, F.J., Hubinger, S., Fernandez, M., Garnett, S. (1987). Oxidation of H2S in seawater as a function of temperature, pH, and ionic strength. *Environmental Science and Technology,* 21 (5), 439-443.

Mohanakrishnan, J., Gutierrez, O., Meyer, R.L., Yuan, Z. (2008). Nitrite effectively inhibits sulfide and methane production in a laboratory scale sewer reactor. *Water Research*, 42 (14), 3961-3971.

Mohanakrishnan, J., Gutierrez, O., Sharma, K.R., Guisasola, A., Werner, U., Meyer, R.L., Keller, J., Yuan, Z. (2009). Impact of nitrate addition on biofilm properties and activities in rising main sewers. *Water Research*, 43 (17), 4225-4237.

Mori, T., Nonaka, T., Tazaki, K., Koga, M., Hikosaka, Y., Noda, S. (1992). Interactions of nutrients, moisture and pH on microbial corrosion of concrete sewer pipes. *Water Research*, 26, 29-37.

Negishi, A., Muraoka, T., Maeda, T., Takeuchi, F., Kanao, T., Kamimura, K., Sugio, T. (2005). Growth inhibition by tungsten in the sulfur-oxidizing bacterium acidithiobacillus thiooxidans. *Bioscience, biotechnology, and biochemistry*, 69 (11), 2073-2080.

Nielsen, A.H., Vollertsen, J., Jensen, H.S., Wium-Andersen, T., Hvitved-Jacobsen, T. (2008). Influence of pipe material and surfaces on sulfide related odor and corrosion in sewers. *Water Research*, 42 (15), 4206-4214.

Okabe, S., Odagiri, M., Ito, T., Satoh, H. (2007). Succession of sulfur-oxidizing bacteria in the microbial community on corroding concrete in sewer systems. *Applied and Environmental Microbiology,* 73, 971-980.

Parker C. D. and Prisk J. (1953). The oxidation of inorganic compounds of sulfur by various sulfur bacteria. *Journal of general microbiology,* 8(3), 344-364.

Peyre Lavigne, M., Lors, C., Valix, M., Herrison, J., Paul, E., Bertron, A. (2016). Microbial induced concrete deterioration in sewers environment: mechanisms and microbial populations. In: *Microorganisms-cementitious Materials Interactions,* pp. 1-17.

Predicala, B., Nemati, M., Stade, S., Lague, C. (2008). Control of H2S emission from swine manure using Na-nitrite and Namolybdate. *Journal of Hazardous Materials,* 154 (1-3), 300-309.

Rees, M.J., Sickerdick, L.M., van Merkestein, R., Dowd, A. (2003). An evaluation of liquid magnesium hydroxide for the control of hydrogen sulfide gas odour. In: *Proceedings of OzWater 2003. In: AWA 20th Convention*, Perth, Western Australia.

Roberts, D.J., Nica, D., Zuo, G., Davis, J.L. (2002). Quantifying microbially induced deterioration of concrete: initial studies. *International Journal of Biodeterioration and Biodegradation,* 49 (4), 227-234.

Rust-Oleum Corporation (2001). Chemical Resistance Guide - Form No. 9575990. Rust-Oleum Corporation, Rev. 07/2001. 2 pg

Satoh, H., Odagiri, M., Ito, T., Okabe, S. (2007). Succession of sulfuroxidizing bacteria in the microbial community on corroding concrete in sewer systems. *Applied Environmental Microbiol*ogy, 73 (3), 971-980.

Satoh, H., Odagiri, M., Ito, T., Okabe, S. (2009). Microbial community structures and insitu sulfate-reducing and sulfur-oxidizing activities in biofilms developed on mortar specimens in a corroded sewer system. *Water Research*, 43, 4729-4739.

Sun, X., Jiang, G., Bond, P.L., Keller, J., Yuan, Z. (2015). A novel and simple treatment for control of sulfide induced sewer concrete corrosion using free nitrous acid. *Water Research*, 70, pp.279-287.

Sun, X., Jiang, G., Bond, P.L., Wells, T., Keller, J. (2014). A rapid, nondestructive methodology to monitor activity of sulfideinduced corrosion of concrete based on H2S uptake rate. *Water Research,* 59, 229-238.

US Environmental Protection Agency, July (2010). State of Technology for Rehabilitation of Wastewater Collection Systems. US Environmental Protection Agency, Office

of Research and Development. EPA/600/R-10/078, *Environmental Protection Agency.*

US EPA. (1985). Designmanual, odour and corrosion control in sanitary sewerage systems and treatment. plants EPA/625/1-85/018*, Environmental Protection Agency.*

Vincke, E., Verstichel, S., Monteny, J., Verstraete,W. (2000). A New Test Procedure for Biogenic Sulfuric Acid Corrosion of Concrete. *Biodegradation,* pp. 421-428.

Vollertsen, J., Nielsen, A.H., Jensen, H.S., Wium-Andersen, T., Hvitved-Jacobsen, T. (2008). Corrosion of concrete sewers - the kinetics of hydrogen sulfide oxidation. *Science of the total environment,* 394 (1), 162-170.

Wiener, M.S., Salas, B.V., Quintero-Nu´ n˜ ez, M., Zlatev, R. (2006). Effect of H2S on corrosion in polluted waters: a review. *Corrosion engineering, science and technology*, 41(3), 221-227.

World Health Organization (2000). Hydrogen sulfide. In: *Air Quality Guidelines for Europe*. Copenhagen, p. 7.

Yamanaka, T., Aso, I., Togashi, S., Tanigawa, M., Shoji, K., Watanabe, T., Watanabe, N., Maki, K., Suzuki, H. (2002). Corrosion by bacteria of concrete in sewerage systems and inhibitory effects of formates on their growth. *Water Research*, 36 (10), 2636-2642.

Yongsiri, C., Vollertsen, J., Hvitved-Jacobsen, T. (2004a). Effect of temperature on airewater transfer of hydrogen sulfide. *Journal of Environmental Engineering,* 130 (1), 104-109.

Yongsiri, C., Vollertsen, J., Hvitved-Jacobsen, T. (2005). Influence of wastewater constituents on hydrogen sulfide emission in sewer networks. *Journal of Environmental Engineering,* 131 (12), 1676-1683.

Yongsiri, C., Vollertsen, J., Rasmussen, M., Hvitved-Jacobsen, T. (2004b). Air-water transfer of hydrogen sulfide: an approach for application in sewer networks. *Water Environment Research*, 76 (1), 81-88.

Yuan, H., Dangla, P., Chatellier, P., Chaussadent, T. (2015). Degradation modeling of concrete submitted to biogenic acid attack. *Cement and Concrete Research*, 70, 29-38.

Zhang, L., Keller, J., Yuan, Z. (2009a). Inhibition of sulfate-reducing and methanogenic activities of anaerobic sewer biofilms by ferric iron dosing. *Water Research,* 43 (17), 4123-4132.

Zhang, L., Mendoza, L., Marzorati, M., Verstraete, W. (2009b). Decreasing sulfide generation in sewage by dosing formaldehyde and its derivatives under anaerobic conditions. *Water Science and Technology*, 59 (6), 1248-1254.

Zivica, V. and Bajza, A. (2001). Acidic Attack of Cement-Based Materials—A Review. Part 1. Principle of Acidic Attack. *Construction and Building Materials*, 15, 331-340.

7. Appendix

7.1. Appendix A, Drawing Details of MICC Incubation Chamber

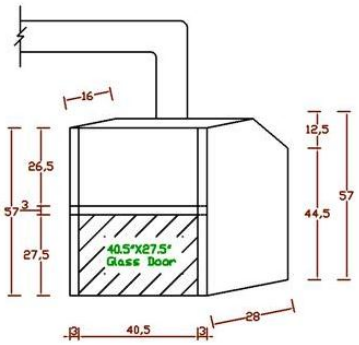

Fume Hood

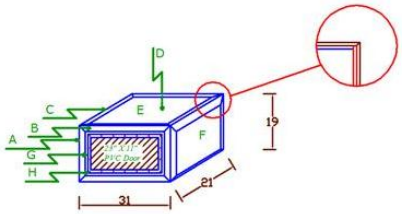

Chamber

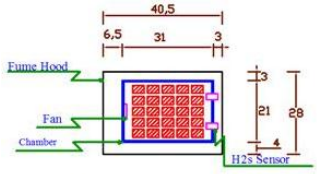

Plane View

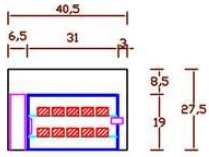

Elevation View

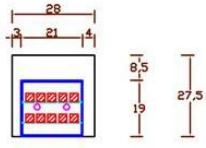

Side View

Element	Qty.	Section	Elevation	3D View	Location
A	4		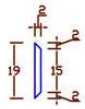	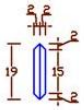	Vertical exterior edges
B	4	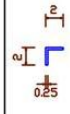	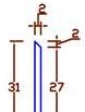	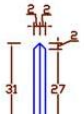	Horizontal exterior edges
C	4	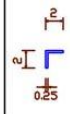	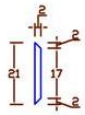	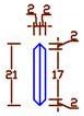	Horizontal exterior side edges
D	1	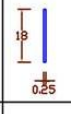			Vertical back side
E	2	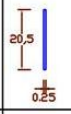		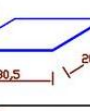	Horizontal Upper & Lower sides
F	2	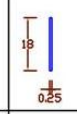	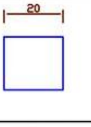	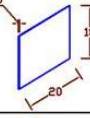	Vertical Right & Left sides
G	1	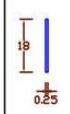	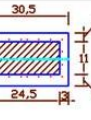	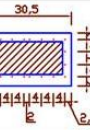	Vertical Front side
H	1	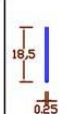			Access PVC door
I	1	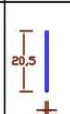	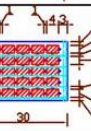	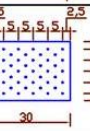	interior shelf
J	4	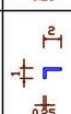	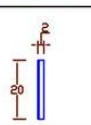	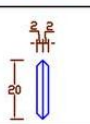	interior shelf side supports
K	2	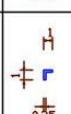	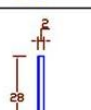	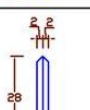	interior shelf back support

7.2. Appendix B, Average H_2S Gas Concentration and Temperature

Table A1, Average H_2S gas concentration and temperature in the incubation chamber.

Week #	From	To	H_2S (PPM)	Temperature (˚C)
1	2/19/2020	2/25/2020	18.9	23.2
2	2/26/2020	3/3/2020	15.0	23.4
3	3/4/2020	3/10/2020	26.4	23.8
4	3/11/2020	3/18/2020	46.56	24.20
5	3/18/2020	3/24/2020	**University Shutdown "COVID 19"**	
6	3/25/2020	3/31/2020		
7	4/1/2020	4/7/2020		
8	4/8/2020	4/14/2020		
9	4/15/2020	4/21/2020		
10	4/22/2020	4/28/2020		
11	4/29/2020	5/5/2020		
12	5/6/2020	5/12/2020		
13	5/13/2020	5/19/2020		
14	5/20/2020	5/26/2020		
15	5/26/2020	6/1/2020	61.72	25.08
16	6/2/2020	6/8/2020	66.25	24.34
17	6/9/2020	6/15/2020	107.07	24.41
18	6/16/2020	6/22/2020	76.12	24.38
19	6/23/2020	6/29/2020	128.39	24.98
20	6/30/2020	7/6/2020	114.01	25.95
21	7/7/2020	7/13/2020	120.55	26.96
22	7/14/2020	7/20/2020	133.66	25.98
23	7/21/2020	7/27/2020	115.52	26.11
24	7/28/2020	8/3/2020	159.16	26.39
25	8/4/2020	8/10/2020	148.69	25.21
26	8/11/2020	8/17/2020	198.28	26.29
27	8/18/2020	8/24/2020	188.56	24.99
28	8/25/2020	8/31/2020	171.36	25.09
29	9/1/2020	9/7/2020	169.06	24.48
30	9/8/2020	9/14/2020	266.39	24.22
31	9/15/2020	9/21/2020	179.97	23.58
32	9/22/2020	9/28/2020	174.55	23.85
33	9/29/2020	10/5/2020	218.88	23.66
34	10/6/2020	10/12/2020	207.20	23.32
35	10/13/2020	10/19/2020	147.59	23.19
36	10/20/2020	10/26/2020	119.18	23.78
37	10/27/2020	11/2/2020	218.61	24.10
38	11/3/2020	11/9/2020	124.45	25.62
39	11/10/2020	11/16/2020	224.76	26.11
40	11/17/2020	11/23/2020	170.89	25.47
41	11/24/2020	11/30/2020	194.48	25.24
42	12/1/2020	12/7/2020	165.07	24.71
43	12/8/2020	12/14/2020	173.16	24.31
44	12/15/2020	12/21/2020	150.39	24.72

Week #	From	To	H_2S (PPM)	Temperature (˚C)
45	12/22/2020	12/28/2020	106.48	22.77
46	12/29/2020	1/4/2021	167.09	23.50
47	1/5/2021	1/11/2021	245.48	24.84
48	1/12/2021	1/18/2021	176.15	24.70
49	1/19/2021	1/25/2021	187.71	24.14
50	1/26/2021	2/1/2021	203.28	24.30
51	2/2/2021	2/8/2021	182.73	24.31
52	2/9/2021	2/15/2021	188.40	23.44
53	2/16/2021	2/22/2021	201.60	23.11
54	2/23/2021	3/1/2021	200.86	24.26
55	3/2/2021	3/8/2021	223.67	25.48
56	3/9/2021	3/15/2021	179.30	24.58
	Average		**165.6**	**24.6**

Table A2, Average H_2S gas concentration and temperature in Ellsworth-OH wet well.

Week #	From	To	H_2S (PPM)	Temperature (˚C)
1	3/25/2020	3/31/2020	27.54	8.74
2	4/1/2020	4/7/2020	26.47	8.82
3	4/8/2020	4/14/2020	20.66	8.98
4	4/15/2020	4/21/2020	13.35	7.61
5	4/22/2020	4/28/2020	38.74	8.85
6	4/29/2020	5/5/2020	55.14	10.08
7	5/6/2020	5/12/2020	19.29	9.37
8	5/13/2020	5/19/2020	74.49	11.27
9	5/20/2020	5/26/2020	102.94	13.55
10	5/26/2020	6/1/2020	**No logger on site "COVID 19"**	
11	6/2/2020	6/8/2020		
12	6/9/2020	6/15/2020		
13	6/16/2020	6/22/2020		
14	6/23/2020	6/29/2020	47.18	19.69
15	6/30/2020	7/6/2020	59.14	20.91
16	7/7/2020	7/13/2020	47.43	21.69
17	7/14/2020	7/20/2020	47.26	21.66
18	7/21/2020	7/27/2020	**No logger on site "COVID 19"**	
19	7/28/2020	8/3/2020		
20	8/4/2020	8/10/2020		
21	8/11/2020	8/17/2020		
22	8/18/2020	8/24/2020	24.85	23.01
23	8/25/2020	8/31/2020	15.16	22.99
24	9/1/2020	9/7/2020	20.83	22.21
25	9/8/2020	9/14/2020	17.81	21.63

Week #	From	To	H_2S (PPM)	Temperature (˚C)
26	9/15/2020	9/21/2020	23.72	19.10
27	9/22/2020	9/28/2020	35.12	18.95
28	9/29/2020	10/5/2020	22.22	17.12
29	10/6/2020	10/12/2020	29.98	16.80
30	10/13/2020	10/19/2020	16.95	15.31
31	10/20/2020	10/26/2020	25.74	14.92
32	10/27/2020	11/2/2020	13.02	11.81
33	11/3/2020	11/9/2020	15.62	11.89
34	11/10/2020	11/16/2020	12.60	11.23
35	11/17/2020	11/23/2020	10.51	9.48
36	11/24/2020	11/30/2020	13.32	9.34
37	12/1/2020	12/7/2020	8.29	6.43
38	12/8/2020	12/14/2020	9.25	7.10
39	12/15/2020	12/21/2020	13.33	5.96
40	12/22/2020	12/28/2020	11.66	4.95
41	12/29/2020	1/4/2021	10.65	5.07
42	1/5/2021	1/11/2021	9.29	4.61
43	1/12/2021	1/18/2021	9.56	4.33
44	1/19/2021	1/25/2021	7.23	2.83
45	1/26/2021	2/1/2021	8.72	2.40
46	2/2/2021	2/8/2021	7.33	1.44
47	2/9/2021	2/15/2021	10.79	1.73
48	2/16/2021	2/22/2021	11.88	1.36
49	2/23/2021	3/1/2021	13.84	3.48
50	3/2/2021	3/8/2021	10.59	3.02
51	3/9/2021	3/15/2021	37.80	5.30
Average			**24.59**	**11.09**

7.3. Appendix C, Surface pH for Laboratory Concrete Coupons

Table A3, Initial concrete coupons surface pH readings as of February 2020.

	Control		Epoxy mastic		ARC Sealant		Biocide (mixed with mortar)		Sodium Nitrite and Hydrogen Peroxide	
	Coup#	pH	Coup#	pH	Coup#	pH	Coup#	pH	Coup#	pH
Upper Coupons (H_2S gas only)	**1a**	10.22 10.36	**2a**	10.67 10.43	**3a**	10.36 10.66	**4a**	10.49 10.65	**5a**	10.34 10.34
	1b	10.29 10.20	**2b**	10.72 10.22	**3b**	10.36 10.25	**4b**	10.24 10.33	**5a**	10.01 10.33
	1c	10.36 10.47	**2c**	10.08 10.10	**3c**	10.12 10.33	**4c**	10.48 10.20	**5a**	10.00 10.26
	1d	10.38 10.43	**2d**	10.61 10.76	**3d**	10.02 9.97	**4d**	10.43 10.43	**5a**	10.32 10.73
	1e	10.19 10.35	**2e**	10.51 10.29	**3e**	10.81 10.53	**4e**	10.06 10.27	**5a**	10.83 10.08
Avg.		**10.33**		**10.44**		**10.34**		**10.36**		**10.32**
STDEV		**0.10**		**0.25**		**0.27**		**0.17**		**0.28**
Lower Coupons (H_2S gas & wastewater)	**1f**	10.54 10.50	**2f**	11.13 10.25	**3f**	10.55 10.71	**4f**	10.32 10.38	**5a**	10.53 10.60
	1g	10.29 10.15	**2g**	10.55 10.65	**3g**	10.66 10.42	**4g**	10.17 10.02	**5a**	10.52 10.39
	1h	10.50 10.41	**2h**	10.51 10.87	**3h**	10.78 11.20	**4h**	10.30 10.50	**5a**	10.78 10.83
	1i	10.53 10.46	**2i**	10.35 10.67	**3i**	10.53 10.85	**4i**	10.54 10.73	**5a**	10.48 10.66
	1j	10.15 10.12	**2j**	10.72 10.64	**3j**	10.59 10.54	**4j**	10.56 10.78	**5a**	10.44 10.66
Avg.		**10.37**		**10.63**		**10.68**		**10.43**		**10.59**
STDEV		**0.17**		**0.25**		**0.22**		**0.24**		**0.14**

Table A4, Concrete coupons surface pH readings as of July 2020

	Control		Epoxy mastic		ARC Sealant		Biocide (mixed with mortar)		Sodium Nitrite and Hydrogen Peroxide	
	Coup#	pH	Coup#	pH	Coup #	pH	Coup #	pH	Coup#	pH
Upper Coupons (H_2S gas only)	**1a**	8.29 8.09	**2a**	8.47 8.56	**3a**	8.24 8.21	**4a**	8.06 7.88	**5a**	8.95 8.64
	1b	7.94 8.21	**2b**	8.56 9.53	**3b**	8.21 7.83	**4b**	8.14 8.66	**5b**	9.22 8.94
	1c	8.14 8.53	**2c**	8.15 8.51	**3c**	8.38 8.42	**4c**	8.19 8.15	**5c**	9.38 8.78
	1d	8.16 8.00	**2d**	8.58 8.42	**3d**	8.34 8.34	**4d**	8.03 8.25	**5d**	8.56 9.38
	1e	8.55 8.42	**2e**	8.78 8.68	**3e**	8.74 8.58	**4e**	8.93 8.84	**5e**	8.59 8.81
Avg.		**8.23**		**8.62**		**8.33**		**8.31**		**8.93**
STDEV		**0.21**		**0.36**		**0.24**		**0.36**		**0.31**
Lower Coupons (H_2S gas & waste water)	**1f**	7.99 8.16	**2f**	7.96 7.43	**3f**	7.76 7.88	**4f**	7.98 8.11	**5f**	7.50 7.25
	1g	7.18 7.80	**2g**	6.45 6.79	**3g**	7.27 7.40	**4g**	7.71 7.49	**5g**	6.59 6.98
	1h	7.15 7.28	**2h**	6.46 6.42	**3h**	6.71 6.77	**4h**	6.88 6.67	**5h**	6.36 6.71
	1i	7.78 6.98	**2i**	7.99 8.30	**3i**	7.82 7.53	**4i**	8.12 7.84	**5i**	7.93 8.21
	1j	7.56 7.74	**2j**	7.76 7.23	**3j**	7.55 7.56	**4j**	7.39 7.78	**5j**	7.33 7.71
Avg.		**7.56**		**7.28**		**7.43**		**7.60**		**7.26**
STDEV		**0.40**		**0.72**		**0.41**		**0.50**		**0.60**

Table A5, Concrete coupons surface pH readings as of August 2020

	Control		Epoxy mastic		ARC Sealant		Biocide w/ mortar		$NaNO_2 + H_2O_2$	
	Coup#	PH	Coup#	PH	Coup #	PH	Coup #	PH	Coup#	PH
Upper Coupons	**1a**	7.22	**2a**	7.40	**3a**	8.51	**4a**	9.51	**5a**	9.23
		7.24		7.59		8.53		9.28		9.00
	1b	7.19	**2b**	7.53	**3b**	8.94	**4b**	9.43	**5b**	9.05
		7.41		7.45		8.99		9.60		9.14
Avg.		**7.27**		**7.49**		**8.74**		**9.46**		**9.11**
STDEV		**0.10**		**0.08**		**0.26**		**0.14**		**0.10**
Lower Coupons	**1f**	7.28	**2f**	7.75	**3f**	8.64	**4f**	8.88	**5f**	8.25
		7.36		7.60		8.69		8.97		7.70
	1g	6.87	**2g**	7.26	**3g**	8.44	**4g**	9.39	**5g**	8.81
		6.89		7.43		8.29		9.16		8.68
Avg.		**7.10**		**7.51**		**8.52**		**9.10**		**8.36**
STDEV		**0.26**		**0.21**		**0.18**		**0.23**		**0.50**

Table A6, Concrete coupon surface pH readings as of September 2020

	Control		Epoxy mastic		ARC Sealant		Biocide w/ mortar		$NaNO_2 + H_2O_2$	
	Coup#	PH	Coup#	PH	Coup #	PH	Coup #	PH	Coup#	PH
Upper Coupons	**1a**	7.28	**2a**	7.32	**3a**	7.85	**4a**	8.91	**5a**	8.82
		7.10		7.70		7.93		8.88		8.87
	1b	7.18	**2b**	7.33	**3b**	7.83	**4b**	8.54	**5b**	9.00
		7.06		6.93		8.05		8.61		8.91
Avg.		**7.16**		**7.32**		**7.92**		**8.74**		**8.90**
STDEV		**0.10**		**0.31**		**0.10**		**0.19**		**0.08**
Lower Coupons	**1f**	7.02	**2f**	6.55	**3f**	8.06	**4f**	8.68	**5f**	7.65
		6.48		6.65		7.61		8.79		6.70
	1g	6.87	**2g**	6.79	**3g**	7.69	**4g**	8.89	**5g**	7.84
		6.86		7.88		7.38		9.16		7.68
Avg.		**6.81**		**6.97**		**7.69**		**8.88**		**7.47**
STDEV		**0.23**		**0.62**		**0.28**		**0.21**		**0.52**

Table A7, Concrete coupon surface pH readings as of November 2020

	Control		Epoxy mastic		ARC Sealant		Biocide w/ mortar		$NaNO_2 + H_2O_2$	
	Coup#	PH	Coup#	PH	Coup #	PH	Coup #	PH	Coup#	PH
Upper Coupons		6.86		6.92		7.52		8.33		9.05
	1a	7.24	**2a**	6.85	**3a**	7.67	**4a**	8.93	**5a**	9.03
		6.95		7.02		7.60		9.12		8.61
		6.73		6.75		7.81		8.54		9.25
	1b	7.01	**2b**	7.21	**3b**	7.54	**4b**	8.44	**5b**	9.41
		6.88		6.85		7.72		8.28		9.38
Avg.		**6.95**		**6.93**		**7.64**		**8.61**		**9.12**
STDEV		**0.17**		**0.16**		**0.11**		**0.34**		**0.30**
Lower Coupons		4.48		6.15		4.93		7.68		4.76
	1f	4.76	**2f**	6.14	**3f**	4.61	**4f**	7.98	**5f**	4.82
		4.57		6.22		5.21		7.76		4.61
		4.95		6.44		4.57		8.15		4.43
	1g	4.82	**2g**	6.38	**3g**	4.92	**4g**	7.79	**5g**	4.48
		4.56		6.53		4.81		7.68		4.75
Avg.		**4.69**		**6.31**		**4.84**		**7.84**		**4.64**
STDEV		**0.18**		**0.16**		**0.24**		**0.19**		**0.16**

Table A8, Concrete coupons surface pH readings as of December 2020

	Control		Epoxy mastic		ARC Sealant		Biocide w/ mortar		$NaNO_2 + H_2O_2$	
	Coup#	PH	Coup#	PH	Coup #	PH	Coup #	PH	Coup#	PH
Upper Coupons		6.80		7.04		7.93		8.64		8.97
	1a	6.70	**2a**	7.23	**3a**	7.42	**4a**	8.97	**5a**	9.28
		6.53		6.83		7.79		8.89		9.34
		6.83		6.72		7.27		9.26		9.36
	1b	6.16	**2b**	7.17	**3b**	7.17	**4b**	9.03	**5b**	8.77
		6.70		6.53		7.46		8.88		9.16
Avg.		**6.62**		**6.92**		**7.51**		**8.95**		**9.15**
STDEV		**0.25**		**0.27**		**0.30**		**0.20**		**0.23**
Lower Coupons		4.25		6.01		3.93		7.18		4.40
	1f	4.48	**2f**	5.89	**3f**	4.62	**4f**	7.30	**5f**	3.90
		4.44		5.65		4.48		7.27		4.16
		4.58		5.74		3.99		6.96		3.88
	1g	4.69	**2g**	5.94	**3g**	4.77	**4g**	7.51	**5g**	4.67
		4.32		5.78		4.38		7.19		3.92
Avg.		**4.46**		**5.84**		**4.36**		**7.24**		**4.16**
STDEV		**0.16**		**0.13**		**0.34**		**0.18**		**0.32**

Table A9, Concrete coupons surface pH readings as of January 2021

	Control		Epoxy mastic		ARC Sealant		Biocide w/ mortar		$NaNO_2 + H_2O_2$	
	Coup#	PH	Coup#	PH	Coup #	PH	Coup #	PH	Coup#	PH
Upper Coupons		6.38		7.37		7.34		8.24		8.79
	1a	6.62	**2a**	6.88	**3a**	6.95	**4a**	9.08	**5a**	9.03
		6.08		6.57		7.58		8.73		9.22
		7.02		6.93		7.21		8.31		8.71
	1b	6.33	**2b**	6.43	**3b**	7.95	**4b**	8.67	**5b**	8.62
		6.05		7.05		7.37		8.82		8.73
Avg.		**6.41**		**6.87**		**7.40**		**8.64**		**8.85**
STDEV		**0.36**		**0.34**		**0.34**		**0.32**		**0.23**
Lower Coupons		4.27		4.50		4.77		6.52		4.59
	1f	3.58	**2f**	4.72	**3f**	3.85	**4f**	6.88	**5f**	4.28
		4.21		4.89		3.77		6.73		4.87
		4.31		4.93		3.88		6.63		4.29
	1g	4.42	**2g**	4.54	**3g**	3.76	**4g**	7.39	**5g**	4.63
		4.39		4.85		3.79		6.74		4.31
Avg.		**4.20**		**4.74**		**3.97**		**6.82**		**4.50**
STDEV		**0.31**		**0.18**		**0.39**		**0.31**		**0.24**

Table A10, Concrete coupons surface pH readings as of March 2021

	Control		Epoxy mastic		ARC Sealant		Biocide w/ mortar		$NaNO_2 + H_2O_2$	
	Coup#	PH	Coup#	PH	Coup #	PH	Coup #	PH	Coup#	PH
Upper Coupons		6.45		6.88		6.86		8.34		8.92
	1a	6.32	**2a**	6.82	**3a**	6.64	**4a**	8.08	**5a**	9.17
		6.39		6.83		6.88		8.71		9.15
		6.13		6.71		6.81		8.52		8.99
	1b	6.13	**2b**	6.97	**3b**	7.13	**4b**	8.24	**5b**	8.73
		6.16		6.85		6.73		8.92		9.04
Avg.		**6.26**		**6.84**		**6.84**		**8.47**		**9.00**
STDEV		**0.14**		**0.08**		**0.17**		**0.31**		**0.16**
Lower Coupons		4.12		4.16		4.52		6.12		4.80
	1f	3.89	**2f**	4.42	**3f**	4.23	**4f**	5.97	**5f**	4.56
		4.22		4.59		4.40		6.09		4.61
		3.95		4.96		4.20		5.86		4.22
	1g	3.81	**2g**	4.88	**3g**	3.93	**4g**	5.77	**5g**	4.31
		4.31		5.12		4.21		5.73		4.40
Avg.		**4.05**		**4.69**		**4.25**		**5.92**		**4.48**
STDEV		**0.20**		**0.36**		**0.20**		**0.16**		**0.21**

7.4. Appendix D, Sulfide Uptake Rate (SUR) for Laboratory Concrete Coupons

Table A11, Upper concrete coupons SUR readings as of March 2020

Samples: Upper Coupons **Test date** 3/17/2020

H_2S test start: 75 ppm
Avg temp. (˚C): 26.74
Background UR 7

	1 Side exposed			all Sides exposed		
	L (in)	W (in)	H (in)	L (in)	W (in)	H (in)
Coupon #1	4	3	2	4	3	2
Exposed Surface area	0.007742			0.033548		
Avg. Change in H_2S (PPM)	17			41.5		
SUR (mg-S m^{-2} hr^{-1})	**58.33**			**46.44**		
Avg. SUR (mg-S m^{-2} hr^{-1})	**52.39**					

Equation Variables

Gas Constant	R	8.3145	N-m/(mol-K)
Temperature	T	299.8927	K
Atmospheric Pressure	P	101.3250	kPa
Molecular Weight of Sulfer	M.W.-S	32.0650	g/mol
Exposed Surface area	Area	0.0010	m^2
Chamber Volume	$V_{reactor}$	0.0347	m^3

Volume calculation

	variables	inch	meter
Coupon	L	4	0.10160
	W	3	0.07620
	H	2	0.05080
	Volume	24	0.00039
logger	D	2.25	0.05715
	H	5.5	0.13970
	Volume	21.88	0.00036
Fan + other	Volume	48	0.00079
Test Chamber	L	17.25	0.43815
	W	9.85	0.25019
	H	13	0.33020
	Vol.	2208.86	0.03620
Net Volume	$V_{reactor}$	2114.99	0.03466

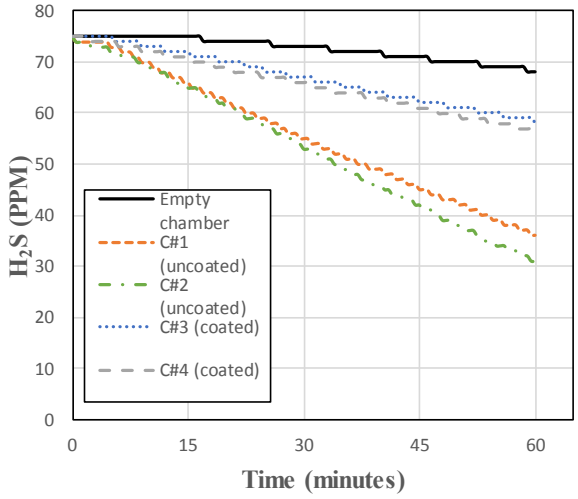

$$r_{H2S} := \frac{-\Delta H2S}{\Delta t} \cdot P_{atm} \cdot \frac{MW_{Sulfur}}{R \cdot T} \cdot \frac{V_{reactor}}{S_{area}} = 79.707 \ \frac{mg}{m^2 \cdot hr}$$

Table A12, Upper concrete coupons SUR readings as of August 2020

Samples: Upper Coupons **Test date** 8/27/2020 **H2S test start:** 70 ppm

Temperature (˚C): 26.35

Background UR 8

	Control	Epoxy	ARC Sealant	Biocide	NaNo2
Change in H_2S (PPM)	22	14	18	20	20
SUR (mg-S m^{-2} hr^{-1})	81.77	35.04	58.41	70.09	70.09

Equation Variables

Gas Constant	R	8.3145	N-m/(mol-K)
Temperature	T	299.50	K
Atmospheric Pressure	P	101.325	kPa
Molecular Weight of Sulfer	M.W.-S	32.065	g/mol
Exposed Surface area	Area	0.007742	m^2
Chamber Volume	Vreactor	0.035	m^3

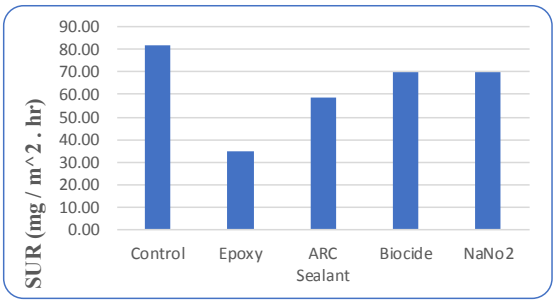

Volume calculation

	variables	inch	meter
Coupon	L	4	0.10160
	W	3	0.07620
	H	2	0.05080
	Volume	24	0.00039
logger	D	2.25	0.05715
	H	5.5	0.13970
	Volume	21.88	0.00036
Fan + other	Volume	48	0.00079
Test Chamber	L	17.25	0.43815
	W	9.85	0.25019
	H	13	0.33020
	Vol.	2208.86	0.03620
Net Volume	Vreactor	2114.99	0.03466

$$r_{H2S} := \frac{-\Delta H2S}{\Delta t} \cdot P_{atm} \cdot \frac{MW_{Sulfur}}{R \cdot T} \cdot \frac{V_{reactor}}{S_{area}} = 79.707 \ \frac{mg}{m^2 \cdot hr}$$

Table A13, Upper concrete coupons SUR readings as of September 2020

Samples: Upper Coupons **Test date** 9/29/2020 **H2S test start:** 70 ppm

Temperature (˚C): 24.58

Background UR 10

	Control	Epoxy	ARC Sealant	Biocide	NaNo2
Change in H2S (PPM)	19	14	14	18	16
SUR(mg-S m^{-2} h^{r-1})	52.88	23.50	23.50	47.00	35.25

Equation Variables

Gas Constant	R	8.3145	N-m/(mol-K)
Temperature	T	297.73	K
Atmospheric Pressure	P	101.325	kPa
Molecular Weight of Sulfer	M.W.-S	32.065	g/mol
Exposed Surface area	Area	0.007742	m^2
Chamber Volume	Vreactor	0.035	m^3

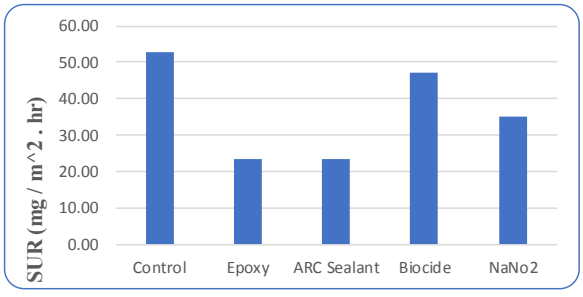

Volume calculation

	variables	inch	meter
Coupon	L	4	0.10160
	W	3	0.07620
	H	2	0.05080
	Volume	24	0.00039
logger	D	2.25	0.05715
	H	5.5	0.13970
	Volume	21.88	0.00036
Fan + other	Volume	48	0.00079
Test Chamber	L	17.25	0.43815
	W	9.85	0.25019
	H	13	0.33020
	Vol.	2208.86	0.03620
Net Volume	Vreactor	2114.99	0.03466

$$r_{H2S} := \frac{-\Delta H2S}{\Delta t} \cdot P_{atm} \cdot \frac{MW_{Sulfur}}{R \cdot T} \cdot \frac{V_{reactor}}{S_{area}} = 79.707 \ \frac{mg}{m^2 \cdot hr}$$

Table A14, Upper concrete coupons SUR readings as of November 2020

Samples: Upper Coupons **Test date** 11/16/2020 **H2S test start:** 75 ppm

Temperature (°C): 28.26

Background UR 10

	Control	Epoxy	ARC Sealant	Biocide	NaNo2
Change in H2S (PPM)	19	10	12	13	11
SUR(mg-S m^{-2} hr^{-1})	52.23	0.00	11.61	17.41	5.80

Equation Variables

Gas Constant	R	8.3145	N-m/(mol-K)
Temperature	T	301.41	K
Atmospheric Pressure	P	101.325	kPa
Molecular Weight of Sulfer	M.W.-S	32.065	g/mol
Exposed Surface area	Area	0.007742	m^2
Chamber Volume	Vreactor	0.035	m^3

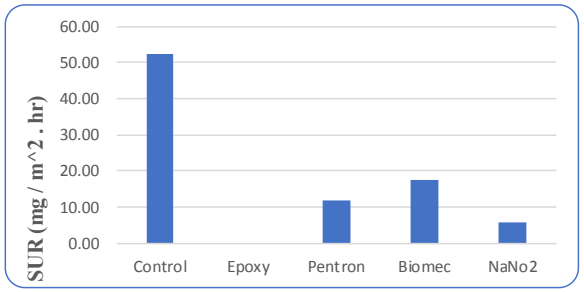

Volume calculation

	variables	inch	meter
Coupon	L	4	0.10160
	W	3	0.07620
	H	2	0.05080
	Volume	24	0.00039
logger	D	2.25	0.05715
	H	5.5	0.13970
	Volume	21.88	0.00036
Fan + other	Volume	48	0.00079
Test Chamber	L	17.25	0.43815
	W	9.85	0.25019
	H	13	0.33020
	Vol.	2208.86	0.03620
Net Volume	Vreactor	2114.99	0.03466

$$r_{H2S} := \frac{-\Delta H2S}{\Delta t} \cdot P_{atm} \cdot \frac{MW_{Sulfur}}{R \cdot T} \cdot \frac{V_{reactor}}{S_{area}} = 79.707 \ \frac{mg}{m^2 \cdot hr}$$

Table A15, Upper concrete coupons SUR readings as of December 2020

Samples: Upper Coupons **Test date** 12/28/2020 **H2S test start:** 75 ppm

Temperature (°C): 25.91

Background UR 12

	Control	Epoxy	ARC Sealant	Biocide	NaNo2
Change in H2S (PPM)	26	18	20	21	22
SUR (mg-S m^{-2} hr^{-1})	81.89	35.10	46.80	52.64	58.49

Equation Variables

Gas Constant	R	8.3145	N-m/(mol-K)
Temperature	T	299.06	K
Atmospheric Pressure	P	101.325	kPa
Molecular Weight of Sulfer	M.W.-S	32.065	g/mol
Exposed Surface area	Area	0.007742	m^2
Chamber Volume	Vreactor	0.035	m^3

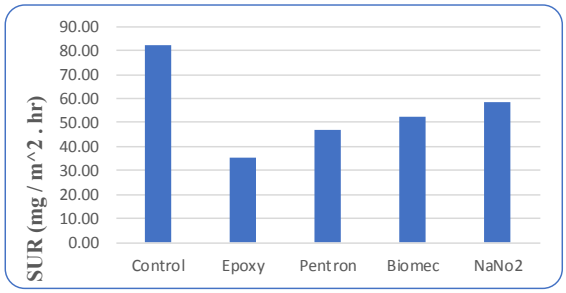

Volume calculation

	variables	inch	meter
Coupon	L	4	0.10160
	W	3	0.07620
	H	2	0.05080
	Volume	24	0.00039
logger	D	2.25	0.05715
	H	5.5	0.13970
	Volume	21.88	0.00036
Fan + other	Volume	48	0.00079
Test Chamber	L	17.25	0.43815
	W	9.85	0.25019
	H	13	0.33020
	Vol.	2208.86	0.03620
Net Volume	Vreactor	2114.99	0.03466

$$r_{H2S} := \frac{-\Delta H2S}{\Delta t} \cdot P_{atm} \cdot \frac{MW_{Sulfur}}{R \cdot T} \cdot \frac{V_{reactor}}{S_{area}} = 79.707 \ \frac{mg}{m^2 \cdot hr}$$

Table A16, Upper concrete coupons SUR readings as of January 2021

Samples: Upper Coupons **Test date** 1/25/2021

H2S test start: 75 ppm
Temperature (°C): 26.38
Background UR 4

	Control	Epoxy	ARC Sealant	Biocide	NaNo2
Change in H2S (PPM)	14	4	8	7	6
SUR (mg-S m^{-2} hr^{-1})	58.40	0.00	23.36	17.52	11.68

Equation Variables

Gas Constant	R	8.3145	N-m/(mol-K)
Temperature	T	299.53	K
Atmospheric Pressure	P	101.325	kPa
Molecular Weight of Sulfer	M.W.-S	32.065	g/mol
Exposed Surface area	Area	0.007742	m^2
Chamber Volume	Vreactor	0.035	m^3

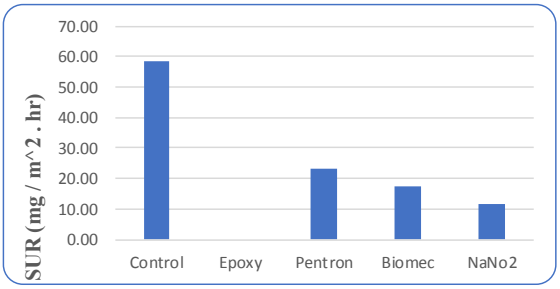

Volume calculation

	variables	inch	meter
Coupon	L	4	0.10160
	W	3	0.07620
	H	2	0.05080
	Volume	24	0.00039
logger	D	2.25	0.05715
	H	5.5	0.13970
	Volume	21.88	0.00036
Fan + other	Volume	48	0.00079
Test Chamber	L	17.25	0.43815
	W	9.85	0.25019
	H	13	0.33020
	Vol.	2208.86	0.03620
Net Volume	Vreactor	2114.99	0.03466

$$r_{H2S} := \frac{-\Delta H2S}{\Delta t} \cdot P_{atm} \cdot \frac{MW_{Sulfur}}{R \cdot T} \cdot \frac{V_{reactor}}{S_{area}} = 79.707 \ \frac{mg}{m^2 \cdot hr}$$

Table A17, Upper concrete coupons SUR readings as of March 2021

Samples: Upper Coupons **Test date** 3/9/2021

H2S test start: 75 ppm
Temperature (°C): 26.81
Background UR 4

	Control	Epoxy	ARC Sealant	Biocide	NaNo2
Change in H2S (PPM)	18	8	15	10	9
SUR (mg-S m^{-2} hr^{-1})	81.65	23.33	64.15	34.99	29.16

Equation Variables

Gas Constant	R	8.3145	N-m/(mol-K)
Temperature	T	299.96	K
Atmospheric Pressure	P	101.325	kPa
Molecular Weight of Sulfer	M.W.-S	32.065	g/mol
Exposed Surface area	Area	0.007742	m^2
Chamber Volume	Vreactor	0.035	m^3

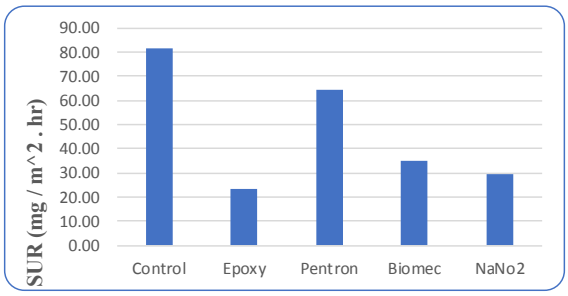

Volume calculation

	variables	inch	meter
Coupon	L	4	0.10160
	W	3	0.07620
	H	2	0.05080
	Volume	24	0.00039
logger	D	2.25	0.05715
	H	5.5	0.13970
	Volume	21.88	0.00036
Fan + other	Volume	48	0.00079
Test Chamber	L	17.25	0.43815
	W	9.85	0.25019
	H	13	0.33020
	Vol.	2208.86	0.03620
Net Volume	Vreactor	2114.99	0.03466

$$r_{H2S} := \frac{-\Delta H2S}{\Delta t} \cdot P_{atm} \cdot \frac{MW_{Sulfur}}{R \cdot T} \cdot \frac{V_{reactor}}{S_{area}} = 79.707 \ \frac{mg}{m^2 \cdot hr}$$

Table A18, Lower concrete coupons SUR readings as of March 2021

Samples: Upper Coupons **Test date** 3/17/2020

H_2S test start:	75 ppm
Avg temp. (˚C):	26.74
Background UR	7

	1 Side exposed			all Sides exposed		
	L (in)	W (in)	H (in)	L (in)	W (in)	H (in)
Coupon #1	4	3	2	4	3	2
Exposed Surface area	0.007742			0.033548		
Avg. Change in H_2S (PPM)	17			41.5		
SUR (mg-S m^{-2} hr^{-1})	**58.33**			**46.44**		
Avg. SUR (mg-S m^{-2} hr^{-1})	**52.39**					

Equation Variables

Gas Constant	R	8.3145	N-m/(mol-K)
Temperature	T	299.8927	K
Atmospheric Pressure	P	101.3250	kPa
Molecular Weight of Sulfer	M.W.-S	32.0650	g/mol
Exposed Surface area	Area	0.0010	m^2
Chamber Volume	$V_{reactor}$	0.0347	m^3

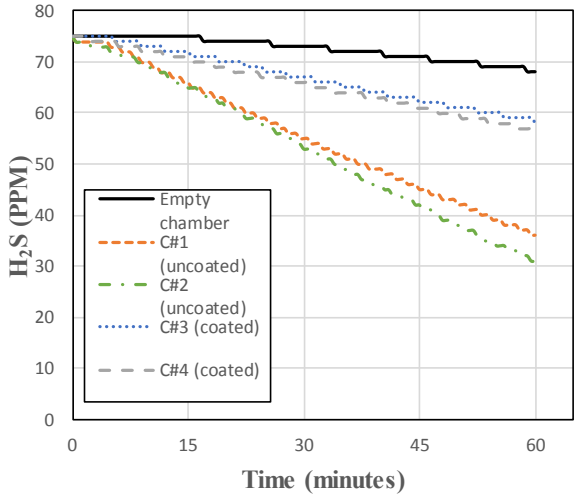

Volume calculation

	variables	inch	meter
Coupon	L	4	0.10160
	W	3	0.07620
	H	2	0.05080
	Volume	24	0.00039
logger	D	2.25	0.05715
	H	5.5	0.13970
	Volume	21.88	0.00036
Fan + other	Volume	48	0.00079
Test Chamber	L	17.25	0.43815
	W	9.85	0.25019
	H	13	0.33020
	Vol.	2208.86	0.03620
Net Volume	$V_{reactor}$	2114.99	0.03466

$$r_{H2S} := \frac{-\Delta H2S}{\Delta t} \cdot P_{atm} \cdot \frac{MW_{Sulfur}}{R \cdot T} \cdot \frac{V_{reactor}}{S_{area}} = 79.707 \ \frac{mg}{m^2 \cdot hr}$$

Table A19, Lower concrete coupons SUR readings as of October 2021

Samples: Lower Coupons **Test date** 10/15/2020 **H2S test start:** 70 ppm
Temperature (°C): 24.43
Background UR 4

	Control	Epoxy	ARC Sealant	Biocide	NaNo2
Change in H2S (PPM)	21	12	20	17	16
SUR (mg-S m^{-2} hr^{-1})	99.94	47.03	94.06	76.42	70.54

Equation Variables

Gas Constant	R	8.3145	N-m/(mol-K)
Temperature	T	297.58	K
Atmospheric Pressure	P	101.325	kPa
Molecular Weight of Sulfer	M.W.-S	32.065	g/mol
Exposed Surface area	Area	0.007742	m^2
Chamber Volume	Vreactor	0.035	m^3

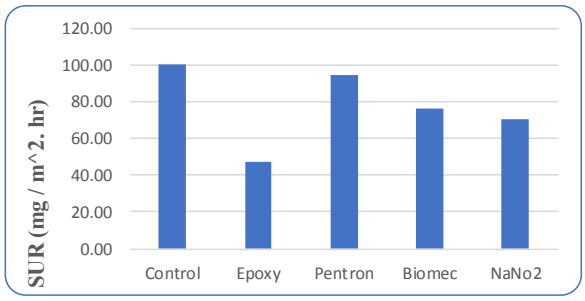

Volume calculation

	variables	inch	meter
Coupon	L	4	0.10160
	W	3	0.07620
	H	2	0.05080
	Volume	24	0.00039
logger	D	2.25	0.05715
	H	5.5	0.13970
	Volume	21.88	0.00036
Fan + other	Volume	48	0.00079
Test Chamber	L	17.25	0.43815
	W	9.85	0.25019
	H	13	0.33020
	Vol.	2208.86	0.03620
Net Volume	Vreactor	2114.99	0.03466

$$r_{H2S} := \frac{-\Delta H2S}{\Delta t} \cdot P_{atm} \cdot \frac{MW_{Sulfur}}{R \cdot T} \cdot \frac{V_{reactor}}{S_{area}} = 79.707 \ \frac{mg}{m^2 \cdot hr}$$

Table A20, Lower concrete coupons SUR readings as of November 2021

Samples: Lower Coupons **Test date** 11/19/2020 **H2S test start:** 75 ppm
Temperature (°C): 27.03
Background UR 12

	Control	Epoxy	ARC Sealant	Biocide	NaNo2
Change in H2S (PPM)	52	15	25	50	43
SUR (mg-S m^{-2} hr^{-1})	201.47	15.11	65.48	191.40	156.14

Equation Variables

Gas Constant	R	8.3145	N-m/(mol-K)
Temperature	T	300.18	K
Atmospheric Pressure	P	101.325	kPa
Molecular Weight of Sulfer	M.W.-S	32.065	g/mol
Exposed Surface area	Area	0.008911	m^2
Chamber Volume	Vreactor	0.034	m^3

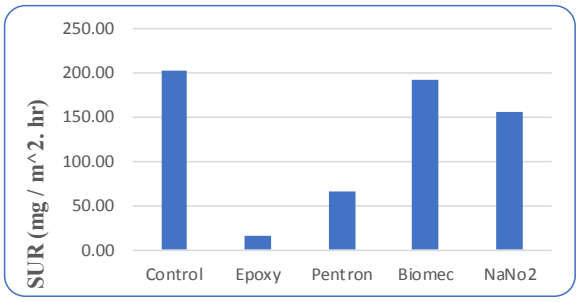

Volume calculation

	variables	inch	meter
Coupon	L	4.25	0.10795
	W	3.25	0.08255
	H	2	0.05080
	Volume	27.625	0.00045
logger	D	2.25	0.05715
	H	5.5	0.13970
	Volume	21.88	0.00036
Fan + other	Volume	55.25	0.00091
Test Chamber	L	17.25	0.43815
	W	9.85	0.25019
	H	13	0.33020
	Vol.	2208.86	0.03620
Net Volume	Vreactor	2104.11	0.03448

$$r_{H2S} := \frac{-\Delta H2S}{\Delta t} \cdot P_{atm} \cdot \frac{MW_{Sulfur}}{R \cdot T} \cdot \frac{V_{reactor}}{S_{area}} = 79.707 \ \frac{mg}{m^2 \cdot hr}$$

Table A21, Lower concrete coupons SUR readings as of December 2021

Samples: Lower Coupons **Test date** 12/31/2020 **H2S test start:** 75 ppm
Temperature (˚C): 26.20
Background UR 4

	Control	Epoxy	ARC Sealant	Biocide	NaNo2
Change in H2S (PPM)	17	6	8	14	9
SUR (mg-S m^{-2} hr^{-1})	75.97	11.69	23.37	58.44	29.22

Equation Variables

Gas Constant	R	8.3145	N-m/(mol-K)
Temperature	T	299.35	K
Atmospheric Pressure	P	101.325	kPa
Molecular Weight of Sulfer	M.W.-S	32.065	g/mol
Exposed Surface area	Area	0.007742	m^2
Chamber Volume	Vreactor	0.035	m^3

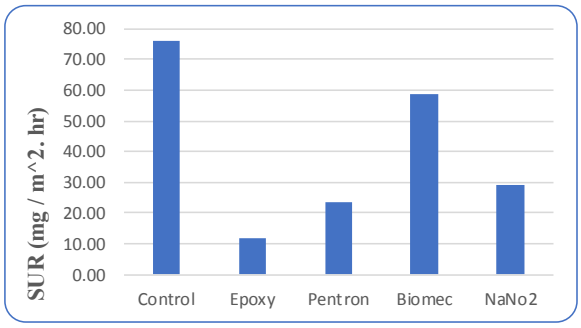

Volume calculation

	variables	inch	meter
Coupon	L	4	0.10160
	W	3	0.07620
	H	2	0.05080
	Volume	24	0.00039
logger	D	2.25	0.05715
	H	5.5	0.13970
	Volume	21.88	0.00036
Fan + other	Volume	48	0.00079
Test Chamber	L	17.25	0.43815
	W	9.85	0.25019
	H	13	0.33020
	Vol.	2208.86	0.03620
Net Volume	Vreactor	2114.99	0.03466

$$r_{H2S} := \frac{-\Delta H2S}{\Delta t} \cdot P_{atm} \cdot \frac{MW_{Sulfur}}{R \cdot T} \cdot \frac{V_{reactor}}{S_{area}} = 79.707 \ \frac{mg}{m^2 \cdot hr}$$

Table A22, Lower concrete coupons SUR readings as of January 2021

Samples: Lower Coupons **Test date** 1/26/2021 **H2S test start:** 75 ppm
Temperature (˚C): 26.62
Background UR 4

	Control	Epoxy	ARC Sealant	Biocide	NaNo2
Change in H2S (PPM)	20	11	18	15	14
SUR (mg-S m^{-2} hr^{-1})	93.37	40.85	81.70	64.19	58.36

Equation Variables

Gas Constant	R	8.3145	N-m/(mol-K)
Temperature	T	299.77	K
Atmospheric Pressure	P	101.325	kPa
Molecular Weight of Sulfer	M.W.-S	32.065	g/mol
Exposed Surface area	Area	0.007742	m^2
Chamber Volume	Vreactor	0.035	m^3

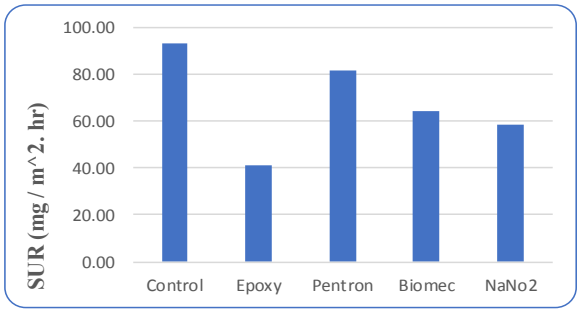

Volume calculation

	variables	inch	meter
Coupon	L	4	0.10160
	W	3	0.07620
	H	2	0.05080
	Volume	24	0.00039
logger	D	2.25	0.05715
	H	5.5	0.13970
	Volume	21.88	0.00036
Fan + other	Volume	48	0.00079
Test Chamber	L	17.25	0.43815
	W	9.85	0.25019
	H	13	0.33020
	Vol.	2208.86	0.03620
Net Volume	Vreactor	2114.99	0.03466

$$r_{H2S} := \frac{-\Delta H2S}{\Delta t} \cdot P_{atm} \cdot \frac{MW_{Sulfur}}{R \cdot T} \cdot \frac{V_{reactor}}{S_{area}} = 79.707 \ \frac{mg}{m^2 \cdot hr}$$

Table A23, Lower concrete coupons SUR readings as of March 2021

Samples: Lower Coupons **Test date** 3/10/2021 **H2S test start:** 75 ppm

Temperature (˚C): 26.53

Background UR 3

	Control	Epoxy	ARC Sealant	Biocide	NaNo2
Change in H2S (PPM)	19	10	15	14	13
SUR (mg-S m^{-2} hr^{-1})	93.40	40.86	70.05	64.21	58.37

Equation Variables

Gas Constant	R	8.3145	N-m/(mol-K)
Temperature	T	299.68	K
Atmospheric Pressure	P	101.325	kPa
Molecular Weight of Sulfer	M.W.-S	32.065	g/mol
Exposed Surface area	Area	0.007742	m^2
Chamber Volume	Vreactor	0.035	m^3

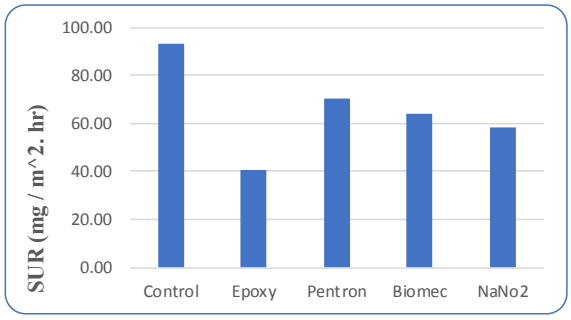

Volume calculation

	variables	inch	meter
Coupon	L	4	0.10160
	W	3	0.07620
	H	2	0.05080
	Volume	24	0.00039
logger	D	2.25	0.05715
	H	5.5	0.13970
	Volume	21.88	0.00036
Fan + other	Volume	48	0.00079
Test Chamber	L	17.25	0.43815
	W	9.85	0.25019
	H	13	0.33020
	Vol.	2208.86	0.03620
Net Volume	Vreactor	2114.99	0.03466

$$r_{H2S} := \frac{-\Delta H2S}{\Delta t} \cdot P_{atm} \cdot \frac{MW_{Sulfur}}{R \cdot T} \cdot \frac{V_{reactor}}{S_{area}} = 79.707 \ \frac{mg}{m^2 \cdot hr}$$

7.5. Appendix E, Surface pH for Concrete Cores from Ellsworth-OH Wet Well

Table A24, Initial concrete cores surface pH readings as of February 2020.

	Control		Epoxy mastic		ARC Sealant		Biocide w/ mortar		$NaNO_2 + H_2O_2$	
	Coup#	PH	Coup#	PH	Coup #	PH	Coup #	PH	Coup#	PH
Site cores	**1**	7.82 7.80	**1**	7.84 7.81	**1**	7.73 7.74	**1**	7.77 7.81	**1**	7.79 7.81
Avg.		**7.81**		**7.83**		**7.74**		**7.79**		**7.80**
STDEV		**0.01**		**0.02**		**0.01**		**0.03**		**0.01**

Table A25, Concrete cores surface pH readings as of June 2020

	Control		Epoxy mastic		ARC Sealant		Biocide w/ mortar		$NaNO_2 + H_2O_2$	
	Core#	PH	Core#	PH	Core#	PH	Core#	PH	Core#	PH
Site cores	**1**	7.72 7.64	**1**	7.75 7.49	**1**	8.19 7.92	**1**	7.81 8.03	**1**	7.54 7.76
Avg.		**7.68**		**7.62**		**8.06**		**7.92**		**7.65**
STDEV		**0.06**		**0.18**		**0.19**		**0.16**		**0.16**

Table A26, Concrete cores surface pH readings as of August 2020

	Control		Epoxy mastic		ARC Sealant		Biocide w/ mortar		$NaNO_2 + H_2O_2$	
	Core#	PH	Core#	PH	Core#	PH	Core#	PH	Core#	PH
Site cores	**1**	8.03 7.61	**1**	7.56 7.81	**1**	7.63 7.81	**1**	8.06 7.71	**1**	6.71 6.86
	2	7.14 7.39	**2**	7.63 7.66	**2**	7.14 7.33	**2**	7.44 7.85	**2**	7.13 6.69
Avg.		**7.54**		**7.67**		**7.48**		**7.77**		**6.85**
STDEV		**0.38**		**0.11**		**0.30**		**0.26**		**0.20**

Table A27, Concrete cores surface pH readings as of October 2020

	Control		Epoxy mastic		ARC Sealant		Biocide w/ mortar		$NaNO_2 + H_2O_2$	
	Core#	PH	Core#	PH	Core#	PH	Core#	PH	Core#	PH
Site cores	**1**	7.63 7.55	**1**	7.54 7.55	**1**	6.57 6.77	**1**	7.72 7.81	**1**	6.83 6.51
	2	7.31 7.27	**2**	7.69 7.45	**2**	6.59 6.49	**2**	7.81 7.96	**2**	6.87 6.72
Avg.		**7.44**		**7.56**		**6.61**		**7.83**		**6.73**
STDEV		**0.18**		**0.10**		**0.12**		**0.10**		**0.16**

Table A28, Concrete cores surface pH readings as of December 2020

	Control		Epoxy mastic		ARC Sealant		Biocide w/ mortar		$NaNO_2 + H_2O_2$	
	Core#	PH	Core#	PH	Core#	PH	Core#	PH	Core#	PH
Site cores	**1**	7.13	**1**	7.34	**1**	6.71	**1**	7.71	**1**	7.15
		7.29		7.41		6.75		7.99		7.03
	2	7.58	**2**	7.68	**2**	6.58	**2**	7.76	**2**	7.78
		7.36		7.76		6.63		7.83		7.88
Avg.		**7.34**		**7.55**		**6.67**		**7.82**		**7.46**
STDEV		**0.19**		**0.20**		**0.08**		**0.12**		**0.43**

Table A29, Concrete cores surface pH readings as of January 2020

	Control		Epoxy mastic		ARC Sealant		Biocide w/ mortar		$NaNO_2 + H_2O_2$	
	Core#	PH	Core#	PH	Core#	PH	Core#	PH	Core#	PH
Site cores	**1**	7.45	**1**	7.55	**1**	6.60	**1**	7.92	**1**	7.61
		7.47		7.82		6.79		7.61		7.69
	2	7.21	**2**	7.42	**2**	6.59	**2**	7.55	**2**	7.33
		7.18		7.38		6.52		7.57		7.21
Avg.		**7.33**		**7.54**		**6.63**		**7.66**		**7.46**
STDEV		**0.15**		**0.20**		**0.12**		**0.17**		**0.23**

7.6. Appendix F, Sulfide Uptake Rate (SUR) for Site Cores from Ellsworth-OH

Table A30, Concrete cores SUR readings as of April 2020

Samples: Wet Well Cores
Site visit 4/22/2020
H_2S test start: 50 ppm
Location: Ellsworth-OH wet well
Test date 5/28/2020
Temperature (˚C): 26.00
Background UR 6

	Control		Epoxy		ARC Sealant		Biocide W/ morter		NaNo2	
	D (in)	d (in)	D (in)	d (in)	D (in)	d (in)	D (in)	d (in)	D (in)	d (in)
Coupon #1	1.9	0.35	1.9	0.35	1.9	0.35	1.9	0.35	1.9	0.35
Coupon #2	1.9	0.35	1.9	0.35	1.9	0.35	1.9	0.35	1.9	0.35
Exposed Surface area	0.002436		0.002436		0.002436		0.002436		0.002436	
Change in H2S (PPM)	26		16		22		18		20	
SUR (mg/ m^2. hr)	**80.76**		**40.38**		**64.61**		**48.45**		**56.53**	

Equation Variables

Gas Constant	R	8.31	N-m/(mol-K)
Temperature	T	299.15	K
Atmospheric Pressure	P	101.33	kPa
Mol. Weight of Sulfer	M.W.-S	32.07	g/mol
Exposed Surface area	Area	0.00	m^2
Chamber Volume	$V_{reactor}$	0.01	m^3

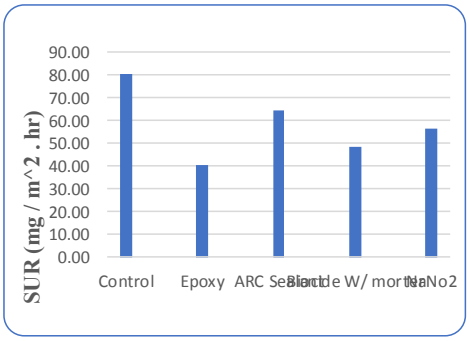

Volume calculation

	variables	inch	meter
Cores (2)	D	1.9	0.04826
	d	0.35	0.00889
	H	0.25	0.00635
	Volume	0.943839286	0.0000027
logger	D	2.25	0.05715
	H	5.5	0.13970
	Volume	21.88	0.00036
Fan + other	Volume	48.13580357	0.00014
T. Chamber	L	7	0.17780
	W	7	0.17780
	H	10	0.25400
	Vol.	490.00	0.00803
Net Vol.	$V_{reactor}$	419.04	0.00753

$$r_{H2S} := \frac{-\Delta H2S}{\Delta t} \cdot P_{atm} \cdot \frac{MW_{Sulfur}}{R \cdot T} \cdot \frac{V_{reactor}}{S_{area}} = 79.707 \frac{mg}{m^2 \cdot hr}$$

Table A31, Concrete cores SUR readings as of October 2020

Samples: Wet Well Cores **Site visit** 10/13/2020 **H_2S test start:** 70 ppm

Location: Ellsworth-OH wet well **Test date** 10/20/2020 **Temperature (˚C)** 26.16

Background UR 9

	Control		Epoxy		ARC Sealant		Biocide W/ morter		NaNo2	
	D (in)	d (in)	D (in)	d (in)	D (in)	d (in)	D (in)	d (in)	D (in)	d (in)
Coupon #1	1.9	0.35	1.9	0.35	1.9	0.35	1.9	0.35	1.9	0.35
Coupon #2	1.9	0.35	1.9	0.35	1.9	0.35	1.9	0.35	1.9	0.35
Exposed Surface area	0.002436		0.002436		0.002436		0.002436		0.002436	
Change in H2S (PPM)	14		10.05		14		13		14	
SUR (mg/ m^2. hr)	**95.67**		**20.09**		**95.67**		**76.53**		**95.67**	

Equation Variables

Gas Constant	R	8.31	N-m/(mol-K)
Temperature	T	299.31	K
Atmospheric Pressure	P	101.33	kPa
Mol. Weight of Sulfer	$M.W_S$	32.07	g/mol
Exposed Surface area	Area	0.00	m^2
Chamber Volume	$V_{reactor}$	0.04	m^3

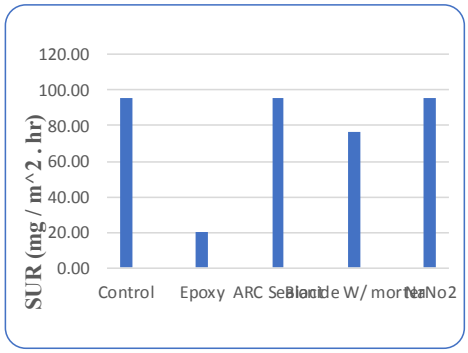

Volume calculation

	variables	inch	meter
Cores (2)	D	1.9	0.04826
	d	0.35	0.00889
	H	0.25	0.00635
	Volume	0.94384	0.0000027
logger	D	2.25	0.05715
	H	5.5	0.13970
	Volume	21.88	0.00036
Fan + other	Volume	48.1358	0.00014
T. Chamber	L	17.25	0.43815
	W	9.85	0.25019
	H	13	0.33020
	Vol.	2208.86	0.03620
Net Vol.	$V_{reactor}$	2137.91	0.03570

$$r_{H2S} := \frac{-\Delta H2S}{\Delta t} \cdot P_{atm} \cdot \frac{MW_{Sulfur}}{R \cdot T} \cdot \frac{V_{reactor}}{S_{area}} = 79.707 \ \frac{mg}{m^2 \cdot hr}$$

Table A32, Concrete cores SUR readings as of December 2020

Samples: Wet Well Cores **Site visit** 12/9/2020 **H_2S test start:** 75 ppm
Location: Ellsworth-OH wet well **Test date** 12/17/2020 **Temperature (˚C)** 26.70
Background UR 11

	Control		Epoxy		ARC Sealant		Biocide W/ morter		NaNo2	
	D (in)	d (in)	D (in)	d (in)	D (in)	d (in)	D (in)	d (in)	D (in)	d (in)
Coupon #1	1.83	0.52	2.09	0.3	2.02	0.35	1.84	0.4	2.04	0.42
Coupon #2	1.91	0.42	2.12	0.31	2.04	0.35	1.94	0.34	1.8	0.44
Exposed Surface area	0.001995		0.003285		0.002862		0.002349		0.002268	
Change in H2S (PPM)	18		11		18		15		17	
SUR (mg/ m^2. hr)	**163.20**		**0.00**		**113.80**		**79.22**		**123.07**	

Equation Variables

Gas Constant	R	8.31	N-m/(mol-K)
Temperature	T	299.85	K
Atmospheric Pressure	P	101.33	kPa
Mol. Weight of Sulfer	$M.W_S$	32.07	g/mol
Exposed Surface area	Area	0.00	m^2
Chamber Volume	$V_{reactor}$	0.04	m^3

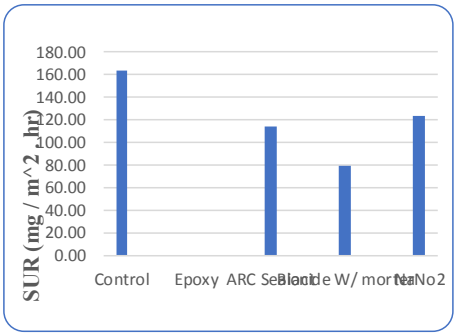

Volume calculation

	variables	inch	meter
Cores (2)	D	1.9	0.04826
	d	0.35	0.00889
	H	0.25	0.00635
	Volume	0.94384	0.000003
logger	D	2.25	0.05715
	H	5.5	0.13970
	Volume	21.88	0.00036
Fan + other	Volume	48.1358	0.00014
T. Chamber	L	17.25	0.43815
	W	9.85	0.25019
	H	13	0.33020
	Vol.	2208.86	0.03620
Net Vol.	$V_{reactor}$	2137.91	0.03570

$$r_{H2S} := \frac{-\Delta H2S}{\Delta t} \cdot P_{atm} \cdot \frac{MW_{Sulfur}}{R \cdot T} \cdot \frac{V_{reactor}}{S_{area}} = 79.707 \ \frac{mg}{m^2 \cdot hr}$$

Table A33, Concrete cores SUR readings as of January 2020

Samples: Wet Well Cores **Site visit** 1/21/2021 **H_2S test start:** 75 ppm
Location: Ellsworth-OH wet well **Test date** 1/27/2021 **Temperature (˚C)** 26.88
Background UR 4

	Control		Epoxy		ARC Sealant		Biocide W/ morter		NaNo2	
	D (in)	d (in)	D (in)	d (in)	D (in)	d (in)	D (in)	d (in)	D (in)	d (in)
Coupon #1	1.86	0.51	2.06	0.31	1.99	0.35	2.01	0.39	1.96	0.35
Coupon #2	1.96	0.38	2.08	0.32	1.98	0.37	1.99	0.31	2.05	0.3
Exposed Surface area	0.002189		0.003123		0.002677		0.002761		0.002866	
Change in H2S (PPM)	13		8		11		9		10	
SUR (mg/ m^2. hr)	**191.12**		**59.56**		**121.55**		**84.19**		**97.32**	

Equation Variables

Gas Constant	R	8.31	N-m/(mol-K)
Temperature	T	300.03	K
Atmospheric Pressure	P	101.33	kPa
Mol. Weight of Sulfer	$M.W_S$	32.07	g/mol
Exposed Surface area	Area	0.00	m^2
Chamber Volume	$V_{reactor}$	0.04	m^3

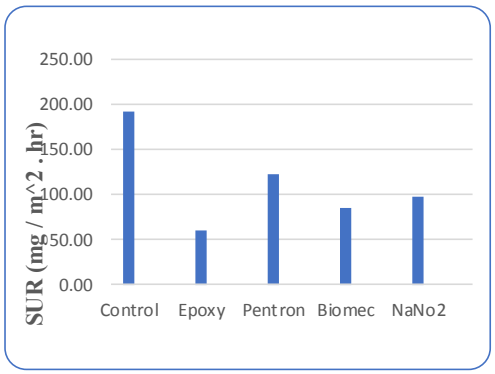

Volume calculation

	variables	inch	meter
Cores (2)	D	1.9	0.04826
	d	0.35	0.00889
	H	0.25	0.00635
	Volume	0.94384	0.000003
logger	D	2.25	0.05715
	H	5.5	0.13970
	Volume	21.88	0.00036
Fan + other	Volume	48.1358	0.00014
T. Chamber	L	17.25	0.43815
	W	9.85	0.25019
	H	13	0.33020
	Vol.	2208.86	0.03620
Net Vol.	$V_{reactor}$	2137.91	0.03570

$$r_{H2S} := \frac{-\Delta H2S}{\Delta t} \cdot P_{atm} \cdot \frac{MW_{Sulfur}}{R \cdot T} \cdot \frac{V_{reactor}}{S_{area}} = 79.707 \ \frac{mg}{m^2 \cdot hr}$$